Inflation and Dark Matter Primordial Black Holes

Dissertation

zur

Erlangung des Doktorgrades (Dr. rer. nat.)

der

Mathematisch-Naturwissenschaftlichen Fakultät

der

Rheinischen Friedrich-Wilhelms-Universität Bonn

vorgelegt von

Encieh Erfani

aus

Iran

Bonn, June 2012

Angefertigt mit Genehmigung der Mathematisch-Naturwissenschaftlichen Fakultät der Rheinischen Friedrich-Wilhelms-Universität Bonn

1. Gutachter: Prof. Dr. Manuel Drees

2. Gutachter: Prof. Dr. Hans Peter Nilles

Tag der promotion: 24.08.2012

Erscheinungsjahr: 2012

Abstract

In this thesis a broad range of single field models of inflation are analyzed in light of all relevant recent cosmological data, checking whether they can lead to the formation of long–lived Primordial Black Holes (PBHs) to serve as candidates for Dark Matter. To that end we calculate the spectral index of the power spectrum of primordial perturbations as well as its first and second derivatives. PBH formation is possible only if the spectral index increases significantly at small scales, *i.e.* large wave number k. Since current data indicate that the first derivative α_S of the spectral index $n_S(k_{\rm pivot})$ is negative at the pivot scale $k_{\rm pivot}$, PBH formation is only possible in the presence of a sizable and positive second derivative ("running of the running") β_S. Among the three small–field and five large–field inflation models we analyze, only one small–field model, the "running–mass" model, allows PBH formation, for a narrow range of parameters. We also note that none of the models we analyze can accord for a large and negative value of α_S, which is weakly preferred by current data. Similarly, proving conclusively that the second derivative of the spectral index is positive would exclude all the large–field models we investigated.

Acknowledgments

First of all, I appreciate Manuel Drees for his patience and support during the whole period of my PhD.

I thank former and present group members; among others, Nicolás Bernal for having never minded to answer my questions and being a really good officemate.

I take this apportunity to thank Prof. Dr. Hans-Peter Nilles, Prof. Dr. R. Izzard and Priv.-Doz. Dr. P. Friederichs for being the committee members.

I specially thank Nicolás and Ivonne Zavala for having read this thesis carefully.

Above all, I am grateful to my friends; among them, Sahar, Zeinab, Fahimeh, Fatemeh, Zhaleh, Nezhla, Sarah, Hanieh and Zahra. I specially thank Nana for being my best friend in Bonn.

Finally my greatest thank goes to my family for having constantly encouraging and supporting me. Thank you maman, baba and dadashi. I am proud to have you in my life.

Contents

1 Introduction

1.1 Theme of the thesis

According to the ΛCDM model, the energy density of the Universe is primarily composed of two mysterious forms: dark energy (Λ) and Cold Dark Matter (CDM), hence the name ΛCDM. The presence of Dark Matter (DM) has been firmly established by a host of observations, and its abundance was measured by the SPT+BAO+H_0+WMAP7+*Clusters* [1] with an unprecedented precision:

$$\Omega_{\mathrm{DM}} h^2 = 0.111 \pm 0.002\,. \tag{1.1}$$

Where SPT, BAO and WMAP7 refere to South Pole Telescope [2], Baryon Acoustic Oscillation [3] and seven years data of Wilkinson Microwave Anisotropy Probe [4], respectively. Here Ω_{DM} is the energy density of DM in units of the critical density, and h is the scaled Hubble parameter such that $H_0 = 100\,h\,\mathrm{km\,s^{-1}\,Mpc^{-1}}$ where $H_0 = 73.8 \pm 2.4\,\mathrm{km\,s^{-1}\,Mpc^{-1}}$ [5] is the current Hubble parameter.
However it is not known yet what DM is made of, and the question remains a big mystery in modern cosmology as well as particle physics.

Analyses of structure formation in the Universe indicate that most DM should be "cold" or "cool", *i.e.*, should have been non-relativistic at the onset of galaxy formation. Candidates for DM in eq. (1.1) must satisfy several conditions: they must be stable on cosmological time scales (otherwise they would have decayed by now), they must interact very weakly with electromagnetic radiation (otherwise they wouldn't qualify as *dark* matter), and they must have the right relic density. Candidates include axions, sterile neutrinos, Weakly Interacting Massive Particles (WIMPs) and **Primordial Black Holes**.

The existence of axions [6] was first postulated to solve the strong *CP* problem of QCD; they also occur naturally in superstring theories. They are pseudo Nambu-Goldstone

bosons associated with the spontaneous breaking of a new global "Peccei-Quinn" $U(1)$ symmetry at scale f_a. Although very light, axions would constitute CDM, since they were produced non-thermally.

"Sterile" $SU(2) \times U(1)_{\rm Y}$ singlet neutrinos with KeV masses [7] could be a candidate for DM. If they were produced non-thermally through mixing with standard neutrinos, they would eventually decay into a standard neutrino and a photon.

Weakly interacting massive particles are particles with mass roughly between 10 GeV and a few TeV, and with cross sections of approximately weak strength. Within standard cosmology, their present relic density can be calculated reliably if the WIMPs were in thermal and chemical equilibrium with the Standard Model (SM) particles after inflation. The currently best motivated WIMP candidate is the Lightest Supersymmetric Particle (LSP) in supersymmetric models [8] with exact R–parity (which guarantees the stability of the LSP).

If the DM is made of WIMPs, we may be able to observe collider (*e. g.* missing transverse energy $\not{E}_{\rm T}$ at Large Hadron Collider (LHC) [9]), direct (*e.g.* recoil energy at CoGeNT [10], XENON100 [11], DAMA/LIBRA [12], CDMS [13] experiments) and indirect (*e.g.* neutrinos, γ-rays, positrons, antiprotons and antinuclei from WIMPs annihilation at SuperKamiokande [14], ANTARES [15], IceCube [16], AMS-02 [17], Fermi/LAT [18] experiments) DM signatures.

Primordial Black Hole (PBH) is a DM candidate in the framework of SM. What makes the PBH particularly as a DM candidate is that it is naturally long–lived due to the gravitational suppressed evaporation rate and also it is not an elementary particle. In the early Universe, PBHs can form when the density perturbation becomes large. It has been known that a PBH of mass greater than 10^{15} g survives the Hawking evaporation [19] and therefore contributes to the DM density [20]. It is still not clear whether PBHs formed but, if they did, they could provide the unique probe of the early Universe, gravitational collapse, high energy physics and quantum gravity (see section 1.4.2). Indeed their study may place interesting constraints on the physics relevant to those areas even if they never existed.

There are several ways (see section 1.4.1) to realize large density fluctuations leading to PBH formation but the fluctuations which arise during the inflation are the most likely sources of PBH; on the other hand, upper limits on the number of PBHs place constraints on inflationary models.

In this thesis we focus on long–lived PBHs as candidate for DM that could be produced by high density fluctuations which arised during the (single field) inflation models.

1.2 Outline of the thesis

In the first chapter, we review the recent developments in the study of PBHs and their properties, with particular emphasis on their formation. Since one of the process of PBH's formation is associated with production of the scalar mode of perturbations during inflation, we review the inflation scenario in section 1.5, too. We summerize the current bounds on the observational parameters and we find the upper bound on the second derivative of the spectral index, *i.e.* "running of running of the spectral index".

In chapter 2 we investigate the formation of PBHs in the radiation dominated era after inflation. We present a brief review of the Press-Schechter formalism describing (long–lived) PBH formation. We show that for the formation of DM PBHs, the spectral index at the scale of the PBHs formation $n_S(k_{\rm PBH})$ should be "blue", *i.e.* $n_S(k_{\rm PBH}) > 1$.

In the third chapter, with the result of the latter chapter, we systematically analyze single field inflation models. We investigate a wide range of inflationary models (three small–field and five large–field), checking whether they can give rise to significant PBH formation given the constraints from observational data. In so doing, we also check whether these models can account for a sizably negative running of the spectral index, as (weakly) favored by current data. We focus on models where the cosmic expansion was driven by a single, self–interacting scalar inflaton field. Moreover, we only consider models with simple potentials, which have been suggested for reasons not related to PBH formation.

Chapter 4 is the summary and conclusion of this thesis.

1.3 Publications

Parts of this thesis have been published in scientific journals:

- *Dark Matter Primordial Black Holes and Inflation Models*
  Manuel Drees and Encieh Erfani, arXiv: 1205.4012, Contribution to Moriond Cosmology 2012 proceedings.

- *Running Spectral Index and Formation of Primordial Black Hole in Single Field Inflation Models*
  Manuel Drees and Encieh Erfani, JCAP 1201 (2012) 035 [arXiv: 1110.6052].

- *Running–Mass Inflation Model and Primordial Black Holes*
  Manuel Drees and Encieh Erfani, JCAP 1104 (2011) 005 [arXiv: 1102.2340].

1.4 Primordial Black Holes

Black Holes (BHs) are normally thought of as being produced by the collapse of stars. However, one would also expect there be a certain number if BHs with masses from 10^{-5} g upwards which were formed in the early stages of the Universe [20]. This is because the existence of galaxies implies that there must have been departures from homogeneity and isotropy at all times in the history of the Universe. These could have been very large in the early stages and even if they were small on average there would be occasional regions in which they were large. One would therefore expect at least a few regions to become sufficiently compressed for gravitational attraction to overcome pressure forces and the velocity of expansion and cause collapse to a BH. These BHs are known as *primordial* which was first put forward by Zel'dovich and Novikov [21] and then independently by Hawking [20]. So since Primordial Black Holes (PBHs) are not formed by the stellar collapse could have wide range of masses.

The standard picture of PBH formation from initial inhomogeneities prescribes that an overdense region with size R will overcome pressure and collapse to form a BH if its size is bigger that the associated Jeans length[1] [22, 23]

$$R_{\rm J} = c_{\rm s}\left(\frac{\pi}{G\rho}\right)^{1/2} = \sqrt{\frac{8w}{3}}\pi R_{\rm PH}\,, \tag{1.2}$$

here G is the gravitational constant, $\rho = \dfrac{3H^2}{8\pi\, G}$ is the energy density and $c_{\rm s}$ is the speed of sound which is given by

$$c_{\rm s}^2 = w = \frac{p}{\rho}\,, \tag{1.3}$$

where p is the pressure and for the case of the radiation domination, $w = 1/3$ and in the matter dominated era $w = 0$ [23]. We also assume that the particle horizon $R_{\rm PH}$ (see section 1.5.1) is of order of the Hubble radius $R_{\rm H} = 1/H$.

The size of the initial inhomogeneity must also be smaller than the separate universe scale not to overclose the Universe

$$R_{\rm PH} \simeq \frac{1}{H}\,, \tag{1.4}$$

consequently the mass of a PBH is close to the particle horizon mass.[2] This gives a simple formula for the mass of a PBH forming at time t [22]

$$M_{\rm PBH} \simeq M_{\rm PH} = \frac{4\pi}{3}R_{\rm PH}^3\,\rho = \frac{t}{2G} = 10^{15}\left(\frac{t}{10^{-23}\,{\rm s}}\right)\,{\rm g}\,. \tag{1.5}$$

[1] Throughout the thesis we use natural units, *i.e.* $c = \hbar = k_{\rm B} = 1$, where c is the speed of light, $\hbar$ is the reduced Planck constant and $k_{\rm B}$ is the Boltzmann constant.

[2] The PBH mass is not exactly the particle horizon mass. For more details see Appendix A.

PBHs could thus span an enormous mass range: those formed at the Planck time (10^{-43} s) would have the Planck mass (10^{-5} g), whereas those formed at 1 s would have a mass as large as $10^5\,M_\odot$,[3] comparable to the mass of the holes thought to reside in galactic nuclei. By contrast, BHs forming at the present epoch could never be smaller than about $1\,M_\odot$.

The realization that PBHs might be small prompted Hawking to study their quantum properties. This led to his famous discovery [24] that BHs radiate thermally with a temperature

$$T_{\rm BH} = \frac{\hbar\,c^3}{8\pi\,G\,M_{\rm BH}\,k_{\rm B}} \sim 10^{-7}\left(\frac{M_{\rm BH}}{M_\odot}\right)^{-1}\,{\rm K}\,. \tag{1.6}$$

A BH of mass M will emit particles like a black-body of temperature [19]

$$T \sim 10^{26}\left(\frac{M}{1\,{\rm g}}\right)^{-1}\,{\rm K} \sim \left(\frac{\rm M}{10^{13}\,{\rm g}}\right)^{-1}\,{\rm GeV}\,, \tag{1.7}$$

assuming that the hole has no charge or angular momentum. This is a reasonable assumption since charge and angular momentum will also be lost through quantum emission but on a shorter timescale than the mass [25].

Holes larger than 10^{17} g are only able to emit "massless" particles like photons, neutrinos and gravitons. Holes in the mass range $10^{15}\,{\rm g} \lesssim M \lesssim 10^{17}\,{\rm g}$ are also able to emit electrons, while those in the range $10^{14}\,{\rm g} \lesssim M \lesssim 10^{15}\,{\rm g}$ emit muons which subsequently decay into electrons and neutrinos. Once M falls below 10^{14} g, a BH can also begin to emit hadrons. However, hadrons are composite particles made up of quarks held together by gluons. For temperature exceeding the QCD confinement scale of $\Lambda_{\rm QCD} = 250 - 300$ MeV, one would therefore expect these fundamental particles to be emitted rather than composite particles. Only pions would be light enough to be emitted below $\Lambda_{\rm QCD}$. One can regard the BH as emitting quark and gluon jets which then fragment into hadrons over the QCD distance, $\Lambda_{\rm QCD}^{-1} \sim 10^{-13}$ cm [26]. These hadrons may then decay into stable elementary particles of the SM.

Due to the particle emission, BHs evaporate on a timescale [24]

$$\tau_{\rm BH} \sim \frac{\hbar\,c^4}{G^2 M_{\rm BH}^3} \sim 10^{64}\left(\frac{M_{\rm BH}}{M_\odot}\right)^3\,{\rm y}\,. \tag{1.8}$$

Only BHs smaller than 10^{15} g would have evaporated by the present epoch ($t \simeq 10^{10}$ y),[4] so eqs. (1.5) and (1.6) imply that this effect could be important only for BHs which formed at a temperature above 10^9 GeV and before 10^{-23} s. For comparison of the mass of BH and its lifetime see Table 1.1.

[3] $M_\odot = 1.989 \times 10^{33}$ g is the solar mass.

[4] If we consider the number of the emitted particle species, the critical mass M_* for which $\tau_{\rm BH}$ equals the age of the Universe is $\simeq 5.1 \times 10^{14}$ g [27].

$M_{\rm BH}$	$\tau_{\rm BH}$
A man	10^{-12} s
A building	1 s
10^{15} g	10^{10} y
The Earth	10^{49} y
The Sun	10^{66} y
The Galaxy	10^{99} y

Table 1.1: Comparison of the mass of BH and its lifetime.

Hawking's result [24] was a tremendous conceptual advance, since it linked three previously disparate areas of physics – quantum theory, general relativity and thermodynamics. Since PBHs with a mass of around 10^{15} g would be producing photons with energy of order 100 MeV at the present epoch, the observational limit on the γ-ray background intensity at 100 MeV immediately implied that their density could not exceed about 10^{-8} times the critical density [28]. This suggested that there was little chance of detecting their final emission phase at the present epoch [29]. It also meant that PBHs with an extended mass function could provide the DM only if the fraction of their mass around 10^{15} g were tiny. Nevertheless, it was soon realized that the γ-ray background limit does not preclude PBHs having important cosmological effects [30].

1.4.1 How PBHs form?

The high density of the early Universe is a necessary but not sufficient condition for PBH formation. One also needs density fluctuations, so that overdense regions can eventually stop expanding and recollapse [31]. Indeed one reason for studying PBH formation is that it impose important constriants on primordial inhomogeneities.

Various mechanisms for PBHs formation are as following:

- *Soft equation of state.* Some phase transitions can lead the equation of state to become soft ($w \ll 1$) for a while. For example, the pressure may be reduced if the Universe's mass is ever channelled into particles which are massive enough to be non-relativistic. In such cases, the effect of pressure in stopping collapse is unimportant and the probability of PBH formation just depends upon the fraction of regions which are sufficiently spherical to undergo collapse [32]. For a given spectrum of primordial fluctuations, this means that there may just be a narrow mass range – associated with the period of the soft equation of state – in which the

PBHs form. For example, PBHs can form at the QCD era [33, 34] and especially likely if the early Universe went through a dustlike phase at early times as a result of either being dominated by non-relativistic particles for a period [32] or undergoing slow reheating after inflation [35, 36].

- *Bubble collisions.* Bubbles of broken symmetry might arise at any spontaneously broken symmetry epoch and various authors suggested that PBHs could form as a result of bubble collisions [37]. However, this happens only if the bubble formation rate per Hubble volume is finely tuned: if it is much larger than the Hubble rate, the entire Universe undergoes the phase transition immediately and there is not time to form BHs; if it is much less than the Hubble rate, the bubbles are very rare and never collide. The holes should have a mass of the order of the horizon mass at the phase transition, so PBHs forming at the Grand Unification Theory (GUT) epoch would have a mass of 10^3 g, those forming at the ElectroWeak (EW) epoch would have a mass of 10^{28} g, and those forming at the QCD (quark-hadron) phase transition would have mass of around $1\,M_\odot$.

- *Collapse of cosmic loops.* Cosmic strings are topological defects formed at the phase transitions in the very early Universe. In the cosmic string scenario, one expects some strings to self-intersect and form cosmic loops. A typical loop will be larger than its Schwarzschild radius[5] by the factor $(G\mu)^{-1}$, where μ is the string mass per unit length. If strings play a role in generating Large Scale Structure (LSS), $G\mu$ must be of order 10^{-6}. However, as discussed by many authors [38], there is always a small probability that a cosmic loop will get into a configuration in which every dimension lies within its Schwarzschild radius. So the formation of PBHs from cosmic loops is subdominant with respect to the standard picture of collapse of overdensities. Note that the holes form with equal probability at every epoch, so they should have a extended mass spectrum.

- *Collapse of domain walls.* The collapse of sufficiently large closed domain walls produced at a second order phase transition in the vacuum state of a scalar field, such as might be associated with inflation, could lead to PBH formation [39].

- *Fluctuations by inflation.* Inflation has two important consequences for PBHs. On the one hand, any PBH formed before the end of inflation will be diluted to a negligible density. Inflation thus impose a lower limit on the PBH mass spectrum

[5]The Schwarzschild radius is the distance from the center of an object such that, if all the mass of the object were compressed within that sphere, the escape speed from the surface would equal the speed of light which is proportional to the mass, $r = 2G\,M$.

formed in radiation dominated era [40]

$$M_{\rm min} = M_{\rm P} \left(\frac{T_{\rm RH}}{T_{\rm P}} \right)^{-2} , \tag{1.9}$$

where $T_{\rm RH}$ is the reheat temperature and $T_{\rm P} \sim 10^{18}$ GeV is the Planck temperature. The Cosmic Microwave Background (CMB) quadrupole measurement implies $T_{\rm RH} \sim 10^{16}$ GeV, so $M_{\rm min}$ certainly exceeds 1 g. On the other hand, inflation will itself generate fluctuations and these may suffice to produce PBHs after reheating.[6]

The quantum fluctuation arising in various inflationary scenarios are of particular interest for PBHs formation. In some of these scenarios the fluctuations generated by inflation decrease with increasing scale and this means that the PBHs form shortly after reheating [36, 40, 42]. In others, PBH formation arises because the power spectrum of the fluctuations exhibits a peak on some scale [43] or a running of the spectral index [44, 45, 46].

1.4.2 Why PBHs are useful?

The study of PBHs provide a unique probe of four areas of physics: the early Universe, quantum gravity, gravitational collapse and high energy physics. One can probe the last two topics only if PBHs exist today but one can gain insight into the first two topics even if PBHs never formed.

- *PBHs as a probe of the early Universe* ($M \lesssim 10^{15}\,$g). These would have completely evaporated by now but many processes in the early Universe could have been motivated by them. For example, PBH evaporations occurring in the first second of the Big Bang could generate the entropy of the Universe [47], change the details of baryogenesis [48] and nucleosynthesis [49], provide a source of neutrinos [50], gravitinos [51] and supersymmetric particles [52]. PBHs evaporating at later times could also have important astrophysical effects, such as helping to reionize the Universe [53, 54].

- *PBHs as a probe of gravitational collapse* ($M \gtrsim 10^{15}\,$g). Roughly 25% of the total density of the Universe is now thought to be in the form of cold DM [1]. Recently there has been a lot of interest in whether PBHs could provide this, since

[6] Note that in the standrad scenario inflation ends by the decay of the inflaton into radiation. However, in the preheating scenario inflation ends more rapidly because of resonant coupling between the inflaton and another scalar field. This generate extra fluctuations which might also produce PBHs [41].

those larger than 10^{15} g would not have evaporated yet and would certainly be massive enough to be dynamically "cold". Since they formed at the time when the Universe was radiation dominated, they should be classified as non-baryonic and so could avoid the constraints on the baryonic density associated with cosmological nucleosynthesis. In many respects, they would be like (non-baryonic) WIMPs but they would be much more massive and so could also have the sort of dynamical, lensing and gravitational wave signatures associated with (baryonic) MAssive Compact Halo Objects (MACHOs). At one stage there seemed to evidence for MACHOs with $M \sim 0.5\,M_\odot$ from microlensing observations [55] and PBHs formed at the quark-hadron phase transition seemed one possible explanation for this [34]. The data now seems less clear but there are no constraints excluding PBHs in the sublunar range $10^{20}\,\mathrm{g} < M < 10^{26}$ g [56, 57, 58] or intermediate mass range $10^2\,M_\odot < M < 10^4\,M_\odot$ [59] from having an appreciable density. Large PBHs might also influence the development of LSS [60], seed the supermassive BHs thought to reside in galactic nuclei[7] [61] or generate background gravitational waves [62].

- *PBHs as a probe of high energy physics* ($M \sim 10^{15}\,\mathrm{g}$). These would be evaporating today could contribute to cosmic rays, whose energy distribution would then give significant information about the high energy physics involved in the final explosive phase of BH evaporation [63]. Also since they are dynamically cold, one would expect some of them to have clustered within the Galactic halo. Besides contributing to the cosmological γ-ray background, such PBHs could contribute to the Galactic γ-ray background [64] and the antiprotons or positrons in cosmic rays [30, 65]. They might also generate γ-ray bursts [66].

- *PBHs as a probe of quantum gravity* ($M \sim 10^{-5}\,\mathrm{g}$). Many new factors could come into play when a BH's mass gets down to the Planck regime, including the effects of extra dimensions and quantum-gravitational spacetime fluctuations. For example, it has been suggested that BH evaporation could cease at this point, in which case Planck relics could contribute to the DM [58, 67] but in this thesis we are not interested in such kind of relics. More radically, it is possible that quantum gravity effects could appear at the TeV scale and this leads to the intriguing possibility that small BHs could be generated in accelerators experiments [68] or cosmic ray events [69]. Although such BHs are not technically "primordial", this would have radical implications for PBHs themselves.

[7] Since no PBHs are likely to form after 1 s, corresponding to a maximum formation mass of $10^5\,M_\odot$, this requires a large amount of accretion [61].

1.4.3 Cosmological constraints on PBHs

Even if PBHs had none of the above effects, it is still interesting to study them because each one is associated with an interesting upper limit on the fraction of the Universe which can have gone into PBHs on some mass scale M. This fraction – being denoted by $\beta(M)$ – is epoch-dependent but its value at the formation epoch of the PBHs is of great cosmological interest. We will calculate this quantity in chapter 2.

The current density parameter $\Omega_{\rm PBH}$ (in units of the critical density) associated with unevaporated PBHs ($M > 10^{15}$ g) which form at redshift z or time t is roughly related to β by[8] [31]

$$\Omega_{\rm PBH} \simeq \beta\,\Omega_{\rm r}\,(1+z) \sim 10^{6}\,\beta\left(\frac{t}{1\,{\rm s}}\right)^{-1/2} \sim 10^{18}\,\beta\left(\frac{M}{10^{15}\,{\rm g}}\right)^{-1/2}\,, \tag{1.10}$$

where $\Omega_{\rm r}$ is the density parameter of the CMB and we have used eq. (1.5). The $(1+z)$ factor arises because the radiation density scales as $(1+z)^4$, whereas the PBH density scales as $(1+z)^3$. Any limit on $\Omega_{\rm PBH}$ therefore places constraints on β over all mass ranges. For example, the γ-ray limit implies $\beta(10^{15}\,{\rm g}) \lesssim 10^{-26}$ and this is one of the strongest constraints on β over all mass ranges. Another immediate constraints for PBHs with $M > 10^{15}$ g comes from requiring $\Omega_{\rm PBH}$ to be less than 0.20, the current upper limit on the DM density. There are also many constraints on $\beta(M)$ for PBHs which have already evaporated, although the parameter $\Omega_{\rm PBH}$ must then be interpreted since they no longer contribute to the cosmological density. The constraints on $\beta(M)$ was provided by some authors [27, 70, 71]. Here we review the most recent version of these constraints which have been summarized in Table 1.2 and figure 1.1 [27].[9]

The important qualitative point is that the initial mass fraction of PBHs are very tiny, $\beta(M) < \mathcal{O}(10^{-20})$ over almost every mass range [27], so any cosmological model which would entail an appreciable fraction of the Universe going into PBHs is immediately excluded. For example, this places strong constraints on the amplitude of the density inhomogeneities in the early Universe and on the deviations of such homogeneities from Gaussianity [72]. One can also infer indirect limits on the spectral index of the primordial density fluctuations [36, 44, 45, 70, 73] and constrain the reheating process which follows inflation [41].

Particles injected from evaporating PBHs have two components: the *primary* component, which is the direct Hawking emission, and the *secondary* component, which comes

[8] For more details see Appendix A.

[9] Constraints in Table 1.2 and figure 1.1 are giving by $\beta'(M)$ instead of $\beta(M)$ where $\beta'(M) \equiv \gamma^{1/2}\left(\frac{g_{*\rm i}}{106.75}\right)^{-1/4}\beta(M)$. Note that β' is not the derivative of β. For more details see Appendix A.

description	mass range	constraint
Evaporating PBHs		
LSP	$M < 10^9\,\mathrm{g}$	eq. (1.11)
Big Bang Nucleosynthesis (BBN)	$10^9\,\mathrm{g} < M_{\rm PBH} < 3\times10^{11}\,\mathrm{g}$	$\beta' < 3\times(10^{-23}-10^{-20})M^{1/2}$
Entropy generation by PBHs	$10^9\,\mathrm{g} < M_{\rm PBH} < 10^{13}\,\mathrm{g}$	$\beta' < 10^{10}M^{-5/2}$
CMB distortion	$10^{11}\,\mathrm{g} < M_{\rm PBH} < 10^{13}\,\mathrm{g}$	$\beta' < 10^{-16}\left(\frac{M}{10^{11}\,\mathrm{g}}\right)^{-1}$
Diffuse extragalactic γ-ray background	$M_* \simeq 5.1\times10^{14}\,\mathrm{g}$	$\beta' < 6\times10^{-26}$
Galactic γ-ray background	$M_* \simeq 5.1\times10^{14}\,\mathrm{g}$	$\beta' < 2\times10^{-26}$
Reionization and 21 cm absorption	$M_{\rm PBH} > 10^{14}\,\mathrm{g}$	$\beta' < 3\times10^{-29}\left(\frac{M}{10^{14}\,\mathrm{g}}\right)^{7/2}$
Non-evaporating PBHs		
Femtolensing of γ-ray bursts	$10^{-16}\,M_\odot < M_{\rm PBH} < 10^{-13}\,M_\odot$	$b(M) < 1$
MACHOs microlensing	$6\times10^{-8}\,M_\odot < M_{\rm PBH} < 30\,M_\odot$ $10^{-6}\,M_\odot < M_{\rm PBH} < 1\,M_\odot$ $10^{-3}\,M_\odot < M_{\rm PBH} < 0.1\,M_\odot$	$b(M) < 1$ $b(M) < 0.1$ $b(M) < 0.04$
Quasars microlensing	$10^{-3}\,M_\odot < M_{\rm PBH} < 60\,M_\odot$	$b(M) < 1$
Radio sources millilensing	$10^6\,M_\odot < M_{\rm PBH} < 10^8\,M_\odot$	$b(M) < 0.06$
Wide binary disruption (WB)	$400\,M_\odot < M_{\rm PBH} < 10^3\,M_\odot$ $10^3\,M_\odot < M_{\rm PBH} < 10^8\,M_\odot$	$b(M) < (M/400\,M_\odot)^{-1}$ $b(M) < 0.4$

Table 1.2: Summary of constraints on the initial PBH abundance.

from the decay of the hadrons produced by fragmentation of the primary quarks and gluons, and by the decay of gauge bosons.

The important point is that the Big Bang Nucleosynthesis (BBN) and γ-ray background limits are the most stringent ones over the entire mass range. There is just a small band in the range $10^{13}-10^{14}$ g where the CMB anisotropy effects dominates. 21 cm observations [54] could potentially provide a stronger constraint in some mass range around 10^{14} g, as indicated by the dotted line in figure 1.1, but such limits do not exist at present.

If PBHs of mass $M_* \simeq 5.1\times10^{14}$ g are clustered inside our own Galactic halo then there should also be a Galactic γ-ray background and since this would be anisotropic, it should be separable from the extragalactic background. Note that in this case, $\beta'(M_*) < 2\times10^{-26}$ is comparable to the extragalactic background constraint (see Table 1.2).

Evaporating PBH should also produce any unknown particles predicted in the theories beyond the SM. The number of PBHs is therefore limited by both the abundance of stable massive particles or the decay of long–lived ones. If LSPs are produced by the evaporation of the PBHs, in order not to exceed the observed CDM density at present, one obtains the upper bound [27]

$$\beta'(M) \lesssim 5\times10^{-19}\left(\frac{M}{10^9\,\mathrm{g}}\right)^{-1/2}\left(\frac{Y}{10^{-14}}\right)\left(\frac{x_\phi}{0.006}\right)^{-1} \qquad (M < 10^9\,\mathrm{g})\,, \tag{1.11}$$

where Y is the limit on the number density to entropy density ratio and x_ϕ is the fraction

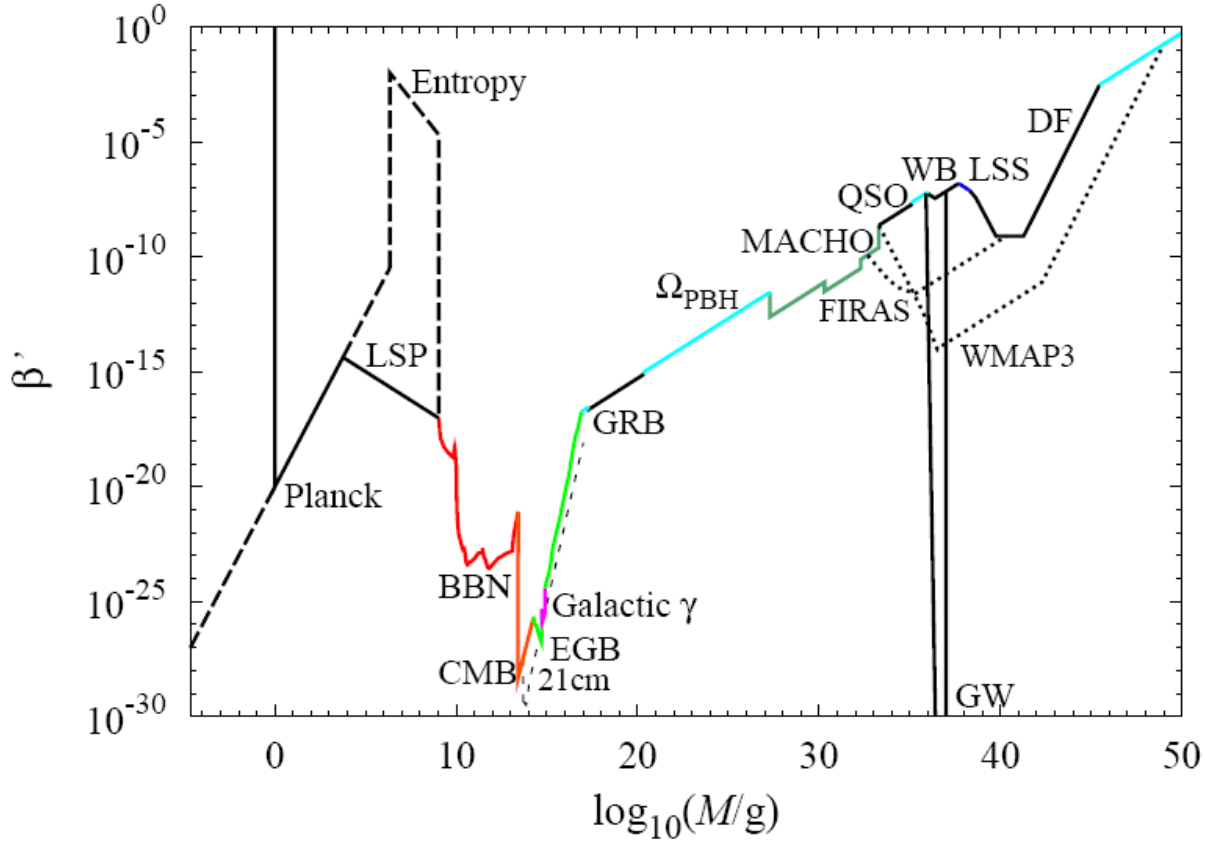

Figure 1.1: $\beta'(M)$ constraints diagram for the mass range $10^{-5} - 10^{50}$ g. (For more details see [27].)

of the luminosity going into massive particles, both being normalized to reasonable values.

In the case of PBHs which are too large to have evaporated by now, various constraints associated by assuming that PBHs cluster in the Galactic halo in the same way as other CDM particles. In this case, eq. (A.8) implies that the fraction of the halo in PBHs is related to $\beta'(M)$ by [27]

$$b(M) \equiv \frac{\Omega_{\rm PBH}}{\Omega_{\rm CDM}} \simeq 5\,\Omega_{\rm PBH} = 5 \times 10^8 \beta'(M) \left(\frac{M}{M_\odot}\right)^{-1/2}, \tag{1.12}$$

where we assume $\Omega_{\rm CDM} = 0.20$.

As mentioned before the mass of PBH formed after inflation exceeds 1 g (see the cut

in figure 1.1), but if PBH evaporations leave stable Planck-mass relics, these might also contribute to the DM. If the relics have a mass $\kappa M_{\rm P}$ then the requirement that they have less than the critical density implies that [36]

$$\beta' < 10^{-27}\kappa^{-1}\left(\frac{M}{M_{\rm P}}\right)^{3/2} . \tag{1.13}$$

This constriant is indicated by dotted line in figure 1.1.

All the limits considered here are brought together in a master $\beta'(M)$ diagram in figure 1.1. In particular, the constraints on $b(M)$ have been converted into limits on $\beta'(M)$ using eq. (1.12). The limits cover the entire mass range from $10^{-5} - 10^{50}$ g and involve a wide variety of physical effects. This reflects the fact that PBHs provide a unique probe of the early Universe, gravitational collapse, high energy physics and quantum gravity. In particular, they probe scales and epochs inaccessible by any type of cosmological observation.

Although none of the effects discussed in this section provide positive evidence for PBHs, figure 1.1 illustrates that even the non-detection of PBHs allows one to infer important constraints on the early Universe. In particular, the limits on $\beta(M)$ can be used to constrain all the PBH formation mechanism described in section 1.4.1.

Before proceeding to calculate $\beta(M)$, we will give a brief introduction about Inflation.

1.5 Inflation

1.5.1 Basics of the Big Bang Model

Observations show that the Universe is spatially isotropic and homogeneous on large scales ($\gg$10 Mpc) and the only metric compatible with these requirements reduce to the so called Friedmann-Robertson-Walker (FRW) metric[10] [23]

$$ds^2 = -dt^2 + a(t)^2\left[\frac{dr^2}{1-k\,r^2} + r^2\left(d\theta^2 + \sin^2\theta\, d\phi^2\right)\right] , \tag{1.14}$$

where $a(t)$ is the (cosmic) scale factor and $k = -1,\ 0,\ 1$ is the curvature signature. The coordinates r, θ and ϕ are referred as comoving coordinates. A particle at rest in these

[10]This section borrowed from [74].
We will use signature (-,+,+,+).

coordinates remains at rest, *i.e.* constant r, θ and ϕ. The physical separation between two points is $a(t)$ times the coordinate separation.

Under the hypothesis of homogeneity and isotropy, we can always write the energy-momentum tensor in the form

$$T_{\mu\nu} = \mathrm{diag}\left(\rho(t),\, p(t),\, p(t),\, p(t)\right)\,, \tag{1.15}$$

where ρ is the energy density of the system and p its pressure.

The evolution of scale factor is governed by the Friedmann equation

$$H^2 \equiv \left(\frac{\dot{a}}{a}\right)^2 = \frac{8\pi\, G}{3}\rho - \frac{k}{a^2}\,, \tag{1.16}$$

where ρ is the total energy density of the Universe and $H \equiv \dot{a}/a$ is the Hubble parameter. Differentiating eq. (1.16) and using the continuity[11] equation

$$\dot{\rho} + 3H\left(\rho + p\right) = 0\,, \tag{1.17}$$

we find the equation for the acceleration of the scale factor

$$\frac{\ddot{a}}{a} = -\frac{4\pi\, G}{3}\left(\rho + 3\, p\right)\,. \tag{1.18}$$

Combining eqs. (1.16) and (1.18) we find

$$\dot{H} = -4\pi\, G(\rho + p)\,. \tag{1.19}$$

Let's assume an equation of state for the cosmological matter of the form $p = w\rho$ with w constant; it follows from Friedmann equation that $\rho \propto a^{-3(1+w)}$ and $a(t) \sim t^{2/3(1+w)}$, so for $p = \rho/3$, relativistic matter, $\rho \propto a^{-4}$ and $a(t) \sim t^{1/2}$; for $p = 0$, non-relativistic matter, $\rho \propto a^{-3}$ and $a(t) \sim t^{2/3}$; and for $p = -\rho$, vacuum energy, $\rho =$ const. and $a(t) \sim \exp(Ht)$.

We can use the Friedmann equation to relate the curvature to the density and expansion rate

$$\Omega - 1 = \frac{k}{(aH)^2}\,, \quad \Omega = \frac{\rho}{\rho_c}\,, \tag{1.20}$$

and the critical density today $\rho_{\mathrm{c}} = 3H_0^2/8\pi\, G = 1.88\, h^2 \times 10^{-29}\,\mathrm{g\,cm^{-3}} \simeq 1.05\, h^2 \times 10^4\,\mathrm{eV\,cm^{-3}}$.

There is a one to one correspondence between Ω and the spatial curvature of the Universe: positively curved, $\Omega_0 > 1$; negatively curved, $\Omega_0 < 1$; and flat, $\Omega_0 = 1$. The curvature radius of the Universe is related to the Hubble radius and Ω by

$$R_{\mathrm{curv}} = \frac{H^{-1}}{|\Omega - 1|^{\frac{1}{2}}}\,. \tag{1.21}$$

[11] The continuity equation can be obtained from the energy-momentum conservation $D_\mu T^\mu_\nu = 0$.

Sometimes it is useful to write the metric in conformal time τ , which is defined through the following relation:

$$d\tau = \frac{dt}{a}\,. \tag{1.22}$$

The metric (1.14) then becomes

$$ds^2 = a(\tau)^2\left[-d\tau^2 + \frac{dr^2}{1-k\,r^2} + r^2(d\theta^2 + \sin^2\theta\, d\phi^2)\right]\,. \tag{1.23}$$

The reason why τ is called conformal is manifest form (1.23): the corresponding FRW line element is conformal to the Minkowski line element.

The concept of particle horizon

Photons travel on null paths characterized by $dr = dt/a(t)$; the particle horizon $R_{\rm PH}$ is defined as the physical distance that a photon could have traveled since the Big Bang until time t,

$$\begin{aligned} R_{\rm PH}(t) &= a(t)\int_0^t \frac{d\tilde{t}}{a(\tilde{t})} = \frac{t}{(1-n)} \\ &= n\,\frac{H^{-1}}{(1-n)} \sim H^{-1} \quad \text{for} \quad a(t)\propto t^n,\, n<1\,. \end{aligned} \tag{1.24}$$

Using the conformal time, the particle horizon becomes

$$R_{\rm PH}(\tau) = a(\tau)\int_{\tau_0}^{\tau} d\tau\,, \tag{1.25}$$

where τ_0 indicates the conformal time corresponding to $t = 0$. Note, in the standard cosmology the particle horizon is finite, and up to the numerical factors equals to the age of the Universe or the Hubble radius H^{-1}. For this reason, in the literature, people use horizon and Hubble radius interchangeably, but we will see that in inflationary models, the horizon and Hubble radius are not roughly equal as the horizon grows exponentially relative to the Hubble radius. In fact, at the end of inflation they differ by e^N, where N is the number of e–folds of inflation.

Let's compare a given physical length λ with the Hubble radius H^{-1}. We will say that, the physical length is within (outside) the Hubble radius if $\lambda < H^{-1}(\lambda > H^{-1})$. Since we can identify the length scale λ with its wavenumber k, $\lambda = 2\pi\, a/k$, we will have the following rule

$$\frac{k}{aH} \gg 1 \quad \Longrightarrow \quad \text{Scale } \lambda \text{ within the Hubble radius} \tag{1.26}$$

$$\frac{k}{aH} \ll 1 \quad \Longrightarrow \quad \text{Scale } \lambda \text{ outside the Hubble radius} \tag{1.27}$$

On scales smaller than the Hubble radius one can always use the local inertial frame in which spacetime can be well approximated by the Minkowski metric. On scales larger than the Hubble radius, due to the expansion of the Universe, the physical length exceeds the Hubble radius.

1.5.1.1 Puzzles of the Standard Big Bang Model

The Standard Big Bang Model (SBBM) is background Friedmann cosmological solution with small fluctuation around it together with the SM particles. This model has encountered remarkable successes, in particular with nucleosynthesis scenario and the prediction of the CMB. However, a few intriguing facts remains unexplained in the strict scenario of the SBBM:

- **The flatness (curvature) problem**

  We know that the Universe possesses a total density of material, $\Omega_{\rm tot} = \Omega_{\rm mat} + \Omega_\Lambda$, and the present observations show that it is close to the critical density; that means that the Universe is quite close to possessing the flat (Euclidean) geometry

  $$|\Omega_{\rm tot}(t) - 1| = \frac{|k|}{(aH)^2}\,. \tag{1.28}$$

  It evolves as

  $$|\Omega_{\rm i} - 1| = |\Omega_0 - 1|\,\frac{(Ha)_0^2}{(Ha)_{\rm i}^2} = |\Omega_0 - 1|\left(\frac{\dot a_0}{\dot a_{\rm i}}\right)^2\,. \tag{1.29}$$

  Let's consider the situation where we have a conventional energy density (matter or radiation dominated) where the normal matter is more important than the curvature or cosmological constant term. So we have

  $$\begin{array}{lcll} |\Omega_{\rm tot}(t) - 1| & \propto & t & \text{Radiation Domination (RD)} \\ |\Omega_{\rm tot}(t) - 1| & \propto & t^{2/3} & \text{Matter Domination (MD)} \end{array}$$

  In either case, the difference between $\Omega_{\rm tot}$ and 1 is an increasing function of time. That means that the flat geometry is an unstable situation for the Universe; so flatness observed today requires an extreme fine-tuning of Ω near 1 in the early Universe.

  In other words, let's assume the Universe always has only radiation in it. Using the equation above, we can ask how close to one the density parameter must have been at various early times, based on the constraint today ($t_0 \simeq 10^{17}$ s):

– At decoupling ($t \simeq 10^{13}\,\mathrm{s}$), we need $|\Omega_{\mathrm{tot}}(t) - 1| \leq 10^{-5}$.

– At matter–radiation equality ($t \simeq 10^{12}\,\mathrm{s}$), we need $|\Omega_{\mathrm{tot}}(t) - 1| \leq 10^{-6}$.

– At BBN ($t \simeq 1\,\mathrm{s}$), we need $|\Omega_{\mathrm{tot}}(t) - 1| \leq 10^{-18}$.

– At the scale of EW symmetry breaking ($t \simeq 10^{-12}\,\mathrm{s}$), we need $|\Omega_{\mathrm{tot}}(t) - 1\,| \leq 10^{-30}$.

– At Planck time ($t \simeq 10^{-34}\,\mathrm{s}$), we need $|\Omega_{\mathrm{tot}}(t) - 1| \leq 10^{-64}$.

In order to get the correct value of $|\Omega_0(t) - 1| \ll 1$ at present, the value of $|\Omega - 1|$ at early times have to be fine-tuned to values extremely close to zero. This is the reason why the flatness problem is also dubbed the "fine-tuning" problem.

- **Homogeneity, isotropy (horizon) problem**

The horizon problem is the most important problem with SBBM, and refers to communication between different regions of the Universe. The present homogeneous, isotropic Universe, is at least as large as the present horizon scale, $c\,t_0 \simeq 3 \times 10^{10}\,(\mathrm{cm/s}) \times 10^{17}\,(\mathrm{s}) \sim 10^{28}$ cm.[12] Initially the size of the Universe was smaller by the ratio of the corresponding scale factors, a_{i}/a_0

$$l_{\mathrm{i}} \sim c\,t_0 \frac{a_{\mathrm{i}}}{a_0}\,, \tag{1.30}$$

compare this scale to the size of a causal region $l_{\mathrm{c}} \sim c\,t_{\mathrm{i}}$

$$\frac{l_{\mathrm{i}}}{l_{\mathrm{c}}} \sim \frac{t_0}{t_{\mathrm{i}}} \frac{a_{\mathrm{i}}}{a_0}\,. \tag{1.31}$$

To estimate this ratio, let's assume $t_{\mathrm{i}} \sim t_{\mathrm{P}}$ ($\simeq 10^{-34}\,\mathrm{s}$), then its temperature is $T_{\mathrm{P}} \sim 10^{32}$ K. Hence

$$\frac{a_{\mathrm{i}}}{a_0} \sim \frac{T_0}{T_{\mathrm{P}}} \sim 10^{-32}\,, \tag{1.32}$$

and we obtain

$$\frac{l_{\mathrm{i}}}{l_{\mathrm{c}}} \sim \frac{10^{17}}{10^{-43}} 10^{-32} \sim 10^{28}\,. \tag{1.33}$$

[12] For clarity we use SI units in this section.

Thus, at the initial Planckian time, the size of our Universe exceeded the causality scale by 28 orders of magnitude and the Universe contained 10^{84} causality disconnected regions. If we assume that the scale factor grows as some power of time, we can use an estimate $a/t \sim \dot{a}$ and write (1.31) as

$$\frac{l_{\rm i}}{l_{\rm c}} \sim \frac{\dot{a}_{\rm i}}{\dot{a}_0}\,. \tag{1.34}$$

So, the size of our Universe was initially larger than that of a causal path by the ratio of the corresponding expansion rate. Since the expansion is decelerating, we conclude that the homogeneity scale is always larger than the scale of causality.

Let's explain the problem in another way. The most straightforward manifestation of the problem is the CMB sky map. One of the most important properties of the CMB is that it is very nearly isotropic. Indeed, the uniform flux of relic photons which come to us from different directions across the sky in fact were emitted at the moment of recombination when the size of the particle horizon was about $180\,h^{-1}$ Mpc. At present the size of the horizon is about $12000\,h^{-1}$ Mpc, and embraces as many as $(12000/180)^3 \sim 10^6$ Hubble patches at recombination. So, the question is; how 10^6 physically disconnected regions could be in thermal equilibrium without being able to "talk" to each other? The horizon problem is well represented by figure 1.2 where the green-solid line indicates the horizon scale and the dashed line any generic physical length scale λ. Suppose, indeed that λ indicates the distance between two photons we detect today. Since the dashed line is above the green-solid line at the time of emission (last-scattering), the two photons could not talk to each other.

1.5.2 Inflation scenario

We have seen so far that the same ratio $\dot{a}_{\rm i}/\dot{a}_0$, enters both horizon and flatness problems. Since the expansion is decelerating, then $\dot{a}_{\rm i}/\dot{a}_0$ is necessarily larger than unity. Therefore, the conclusion $\dot{a}_{\rm i}/\dot{a}_0 \gg 1$ can be avoided only if we assume that during some period of evolution of the Universe the expansion accelerates.

A period of accelerated expansion, which is called "*inflation*" is proposed by Alan Guth [75] in 1981, is a necessary condition for solving the problems of the SBBM. So the old picture of a decelerated Friedmann Universe is modified by inserting a stage of cosmic acceleration. It is obvious that if we do not want to spoil the successful predictions of the standard Friedmann model, inflation should begin and end sufficiently early, and also possesses a smooth exit into the decelerated Friedmann stage because otherwise the

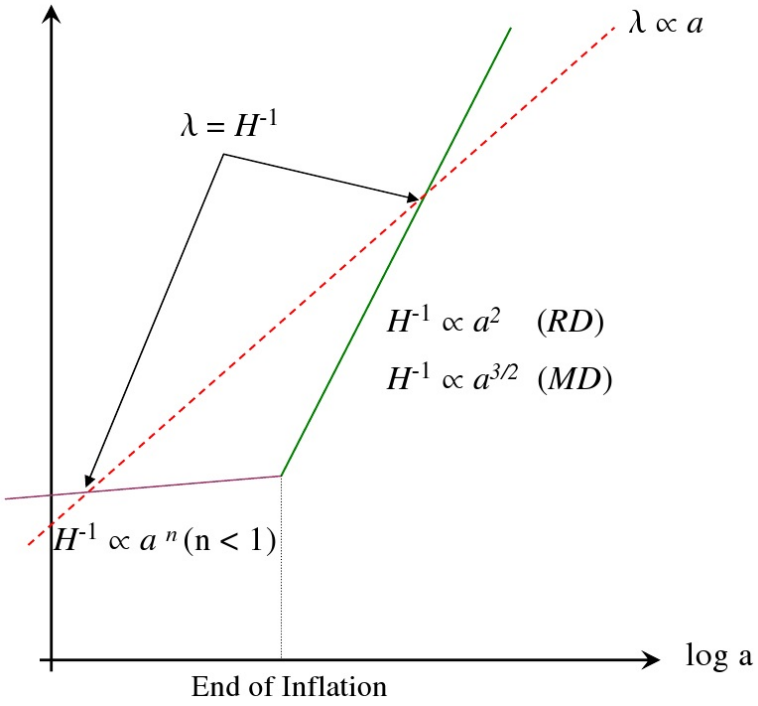

Figure 1.2: Behavior of a given scale λ (dashed line) and the Hubble radius H^{-1} with (purple-solid line) and without (green-solid line) inflation period.

homogeneity of the Universe would be destroyed.

How can inflation solve the problems of the SBBM?

- **Flatness problem**

  During inflation, the initial expansion rate is much smaller than the rate of expansion today, that is $\dot{a}_{\rm i}/\dot{a}_0 \ll 1$. Rewriting eq. (1.29) as

  $$\Omega_0 = 1 + (\Omega_{\rm i} - 1)\left(\frac{\dot{a}_{\rm i}}{\dot{a}_0}\right)^2 , \tag{1.35}$$

  we see that if $|\Omega_{\rm i} - 1| \sim \mathcal{O}(1)$ then $\Omega_0 = 1$ to very high accuracy. It is worth noting that, it contrast to a decelerating Universe where $\Omega(t) \to 1$ as $t \to 0$, in an accelerating Universe $\Omega(t) \to 1$ as $t \to \infty$; that is, $\Omega = 1$ is its future attractor.

- **Horizon problem**

During inflation, physical length scales go out of the Hubble radius H^{-1}, since the particle horizon is dominated by early times and it can be very large if inflation lasts sufficiently. In this case, the length scale λ which are within the Hubble radius today $\lambda < H^{-1}$ and were outside the Hubble radius for some period, $\lambda > H^{-1}$, had a chance to be within the Hubble radius at some primordial epoch, $\lambda < H^{-1}$, again (see figure 1.2).

So the broad definition of inflation is that it corresponds to a phase of acceleration of the Universe,

$$\ddot{a} > 0\,. \tag{1.36}$$

The question is that how we can get an inflation phase in the early Universe.

The acceleration equation (1.18) tells us that one can get acceleration only if the strong energy condition, $\rho + 3p > 0$, is violated, that is if, $p < -\rho/3$. One particular example of "matter" which violates the energy condition is a positive cosmological constant, for which $p = -\rho$. A period of the Universe during which $p = -\rho$ is called *de Sitter* stage. By using eqs. (1.16) and (1.17), we find that during the de Sitter phase

$$\begin{aligned} \rho &= \text{const.} \\ H_{\rm I} &= \text{const.}\,, \end{aligned}$$

where H_I indicates the value of the Hubble rate during the inflation. Also, solving eq. (1.16) gives

$$a = a_{\rm i}\, e^{H_{\rm I}(t-t_{\rm i})}\,, \tag{1.37}$$

where $t_{\rm i}$ denotes the time at which inflation starts. But, the exact de Sitter solution does not possesses a smooth exit into the Friedmann stage, since it leads to exponential inflation forever. Therefore, in realistic inflationary models, it can be utilized only as a zero order approximation. But in reality the Hubble parameter is not constant during the inflation (quasi de Sitter Universe). Another possibility which violates the strong energy dominance condition is a scalar field, which we will discuss in details.

1.5.2.1 Inflaton

In this section, we would like to show that by means of a simple scalar field, that we call it the *inflaton*, we can attain the required condition $p < -\rho/3$ for the inflation.

The dynamics of a scalar filed coupled to gravity is governed by the action

$$S = \int d^4x\,\sqrt{-g}\,\mathcal{L} = \int d^4x\,\sqrt{-g}\left[-\frac{1}{2}\partial_\mu\phi\,\partial^\mu\phi - V(\phi)\right]\,, \tag{1.38}$$

where $\sqrt{-g} = a^3$ for FRW metric (1.14). From the Euler-Lagrange equation we obtain

$$\ddot{\phi} + 3H\dot{\phi} + V'(\phi) = 0\,, \tag{1.39}$$

where $V'(\phi) = dV(\phi)/d\phi$. This equation has to be supplemented by Friedmann equation, $H^2 = \dfrac{8\pi\, G}{3}\left(\dfrac{1}{2}\dot{\phi}^2 + V(\phi)\right)$ where we have ignored the curvature; since as we discussed inflation flattens the Universe. Note, in particular, the appearance of the friction term $3H\dot{\phi}$: a scalar field rolling down its potential suffers a friction term due to the expansion of the Universe.

By using the definition $T^{\mu\nu} = \dfrac{2}{\sqrt{-g}}\dfrac{\delta S_{\rm mat}}{\delta g_{\mu\nu}}$ we can write the energy-momentum tensor of scalar field

$$T_{\mu\nu} = \partial_\mu\phi\,\partial_\nu\phi - \mathcal{L}\, g_{\mu\nu} = \partial_\mu\phi\,\partial_\nu\phi + g_{\mu\nu}\left(\frac{1}{2}g^{\alpha\beta}\partial_\alpha\phi\,\partial_\beta\phi + V(\phi)\right)\,. \tag{1.40}$$

The corresponding energy density ρ_ϕ and pressure p_ϕ are

$$\begin{aligned} T_{00} &= \rho_\phi = \frac{\dot{\phi}^2}{2} + V(\phi)\,, \\ T_{0i} &= 0\,, \\ T_{ii} &= p_\phi = \frac{\dot{\phi}^2}{2} - V(\phi)\,. \end{aligned} \tag{1.41}$$

Notice that, in FRW Universe we can neglect the gradient term and we can split the inflation field in

$$\phi = \phi_0(t) + \delta\phi(\mathbf{x},\, t)\,, \tag{1.42}$$

where ϕ_0 is the expectation value of the inflaton field on the initial isotropic and homogeneous Universe, while $\delta\phi(\mathbf{x}, t)$ represents the fluctuations around ϕ_0. So the energy-momentum tensor for unperturbed part becomes

$$\begin{aligned} T_{00} &= \rho_\phi = \frac{\dot{\phi_0}^2}{2} + V(\phi)\,, \\ T_{ii} &= p_\phi = \frac{\dot{\phi_0}^2}{2} - V(\phi)\,. \end{aligned} \tag{1.43}$$

Inflation can occur if the evolution of the field is sufficiently gradual that the potential energy dominates the kinetic energy $V(\phi) \gg \dot{\phi}^2 \Rightarrow p_\phi \simeq -\rho_\phi$; so the inflation is driven by the vacuum energy of the inflaton field and the second derivation of ϕ is small enough to allow this state of affairs to be maintained for a sufficient period.

1.5.2.2 Slow–roll conditions

If we require that $V(\phi) \gg \dot{\phi}^2$, the scalar field is slowly rolling down its potential. This is the reason why such a period is called *slow–roll*. The Friedmann equation (1.16) becomes

$$H^2 \simeq \frac{8\pi G}{3} V(\phi)\,. \tag{1.44}$$

The new equation of motion becomes

$$3H\dot{\phi} \simeq -V'(\phi)\,, \tag{1.45}$$

which gives $\dot{\phi}$ as a function of $V(\phi)$. Using eq. (1.45), slow–roll condition then requires

$$\dot{\phi}^2 \ll V(\phi) \quad \Rightarrow \quad \frac{V'^2}{V} \ll H^2\,, \tag{1.46}$$

and

$$\ddot{\phi} \ll 3H\,\dot{\phi} \quad \Rightarrow \quad V'' \ll H^2\,. \tag{1.47}$$

Satisfying these conditions require the smallness of the two dimensionless quantities known as slow–roll parameters

$$\begin{aligned} \epsilon &\equiv -\frac{\dot{H}}{H^2} = \frac{2}{M_{\rm P}^2}\frac{\dot{\phi}^2}{H^2} = \frac{M_{\rm P}^2}{2}\left(\frac{V'}{V}\right)^2\,, \\ \eta &\equiv M_{\rm P}^2\left(\frac{V''}{V}\right) = \frac{1}{3}\frac{V''}{H^2}\,. \end{aligned} \tag{1.48}$$

Note that $\epsilon \geq 0$, while η can have either sign.

The parameter ϵ quantifies how much the Hubble rate H changes with time during inflation. Note that, since

$$\frac{\ddot{a}}{a} = \dot{H} + H^2 = (1-\epsilon)H^2\,, \tag{1.49}$$

inflation can be attained if $\epsilon < 1$. As soon as this condition fails, inflation ends and inflaton evolves toward its minimum and it starts oscillating and then it decays to the SM particles and through these processes the energy in the inflaton potential converts into radiation through the process known as reheating and the temperature of the Universe increases up to a reheating temperature ($T_{\rm RH}$).

The inflaton field ϕ is supposed to be on a range of the potential which satisfies the flatness conditions

$$\begin{aligned} \epsilon &\ll 1\,, \\ |\eta| &\ll 1\,. \end{aligned} \tag{1.50}$$

Slow–roll parameters are in general scale–dependent, *i.e.* they have to be evaluated at the value of ϕ that the inflaton field had when the scale k crossed out of the horizon. Their derivates are given by [76]

$$\begin{aligned}\frac{d\epsilon}{d\ln k} &= -2\epsilon\eta + 4\epsilon^2\,,\\ \frac{d\eta}{d\ln k} &= 2\epsilon\eta - \xi^2\,,\\ \frac{d\xi^2}{d\ln k} &= 4\epsilon\xi^2 - \eta\xi^2 - \sigma^3\,,\end{aligned} \tag{1.51}$$

where

$$\begin{aligned}\xi^2 &\equiv M_{\rm P}^4\frac{V'V'''}{V^2}\,,\\ \sigma^3 &\equiv M_{\rm P}^6\frac{V'^2V''''}{V^3} = 2M_{\rm P}^4\,\epsilon\,\frac{V''''}{V}\,.\end{aligned} \tag{1.52}$$

The square in ξ^2 and cube in σ^3 are to indicate that they are second and third–order in the slow–roll expansion, respectively.[13] These parameters must be less than one for the slow–roll expansion to be valid.

1.5.2.3 Number of e–folds

When working with a specific inflationary model, it is important to be able to relate the cosmological scales at the time t_* when observable CMB scale first crossed the Hubble radius during inflation to the epoch $t_{\rm end}$ when inflation ended. For this reason, one usually introduce the *number of e–foldings*, denoted N, and simply defined as

$$N = \ln\frac{a_{\rm end}}{a_*}\,. \tag{1.53}$$

In the slow–roll approximation it is possible to express N as a function of the scalar field.

$$\begin{aligned}N \equiv \ln\frac{a_{\rm end}}{a_*} &= \int_{t_*}^{t_{\rm end}} H\,dt\\ &\simeq H\int_{\phi_*}^{\phi_{\rm end}}\frac{d\phi}{\dot\phi}\\ &\simeq \frac{1}{M_{\rm P}^2}\int_{\phi_{\rm end}}^{\phi_*}\frac{V}{V'}d\phi\,,\end{aligned} \tag{1.54}$$

[13] The powers on ξ^2 and σ^3 are purely by convention; in particular, ξ^2 could be negative.

where $\phi_{\rm end}$ is defined by $\max\left[\epsilon(\phi_{\rm end}), |\eta(\phi_{\rm end})|\right] = 1$. Note that inflation might end through dynamics of other fields coupled to the inflaton, as in hybrid inflation [77].

Assuming radiation dominated Universe, let us discuss the link between N and the present cosmological scales. During the radiation phase, the comoving Hubble radius $(aH)^{-1}$ increases like a. Since the comoving Hubble radius roughly scales like a^{-1} during inflation, the minimum amount of inflation is simply given by the number of e–folds between the end of inflation (start of radiation era) and today

$$N \equiv \ln\left(\frac{a_{\rm f}}{a_{\rm i}}\right) = \ln\left(\frac{T_0}{T_{\rm RH}}\right) \sim \ln\frac{T_0}{10^{16}\,{\rm GeV}} \sim \ln 10^{29} \sim 60\,, \tag{1.55}$$

where T_0 ($\sim 10^{-13}$GeV) is the present-day temperature of the CMB radiation. *i.e.* around 60 e–folds, for a temperature $T \sim 10^{16}$ GeV at the beginning of the radiation era.

From eq. (1.55) it is clear that the observationally required value of N depends logarithmically on the reheating temperature and the value of $N \simeq 60$ corresponds to a GUT scale reheating.[14] Assuming instantaneous change from inflation to relativistic matter domination, a reasonable range of values of the number of e–folds between t_* and $t_{\rm end}$ is taken to be $N = 54 \pm 7$ [78]. Requiring baryogenesis to take place at or above the EW scale implies that $N \gtrsim 30$.[15]

1.5.2.4 Inflation and the cosmological perturbations

A crucial element of inflationary scenarios is the production of density perturbation, which may be the origin of CMB temperature anisotropies, the formation and the evolution of the structure in the Universe that we observe today. The scales of these inhomogeneities were generated during inflation and stretched over astronomical scales because of the rapid expansion of the Universe during the (quasi) de Sitter epoch.
Any perturbation in the inflaton field means a perturbation of the energy-momentum tensor and its perturbation implies, through Einstein's equation, a perturbation of the metric.

$$\delta\phi \quad \Rightarrow \quad \delta T_{\mu\nu} \quad \Rightarrow \quad \delta g_{\mu\nu}\,.$$

This logic chain makes us conclude that the perturbations of the inflaton field and the metric are tightly coupled to each other and have to be studied together.

[14] Instantaneous reheating gives the minimum number of e–folds as one looks backwards to the time of perturbation production, while a prolonged period of reheating gives a larger number of e–folds.

[15] Arbitrarily many e–folds of inflation might have occurred at $t < t_*$, as in "eternal" inflation [79]. N of eq. (1.55) is a lower bound on the total number of e–folds of inflation.

Fluctuations of a massless scalar field during inflation

Let us study the fluctuations of a massless scalar field, which is *not* the inflaton field, and see how perturbations evolve as a function of time and compute their spectrum. We will consider an exact de Sitter epoch during which the Hubble rate is constant. As we discussed before, we can write the scalar field χ as

$$\chi = \chi_0(t) + \delta\chi(\mathbf{x},\, t)\,. \tag{1.56}$$

Expanding the scalar field χ in Fourier modes

$$\delta\chi(\mathbf{x},\, t) = \int \frac{d^3\mathbf{k}}{(2\pi)^{3/2}} e^{i\mathbf{k}.\mathbf{x}} \delta\chi_{\mathbf{k}}(t)\,, \tag{1.57}$$

we can write the equation for fluctuations as

$$\delta\ddot{\chi}_{\mathbf{k}} + 3H\delta\dot{\chi}_{\mathbf{k}} + \frac{k^2}{a^2}\delta\chi_{\mathbf{k}} = 0\,. \tag{1.58}$$

For studying the evolution of the fluctuations, let's perform the following redefinition and work in conformal time

$$\delta\chi_{\mathbf{k}} = \frac{\delta\sigma_{\mathbf{k}}}{a}\,. \tag{1.59}$$

Since we suppose a pure de Sitter expansion ($a \sim e^{Ht}$); the corresponding conformal factor reads

$$a(\tau) = -\frac{1}{H\tau} \qquad (\tau < 0)\,. \tag{1.60}$$

Rewrite eq. (1.58) in conformal time

$$\delta\sigma''_{\mathbf{k}} + \left(k^2 - \frac{a''}{a}\right)\delta\sigma_{\mathbf{k}} = 0\,. \tag{1.61}$$

The above equation has an exact solution

$$\delta\sigma_{\mathbf{k}} = \frac{e^{-ik\tau}}{\sqrt{2k}}\left(1 + \frac{i}{k\tau}\right)\,. \tag{1.62}$$

Let's study this solution in the two extreme regimes:

- On subhorizon scales ($k \gg aH \Rightarrow k^2 \gg a''/a$), the solution is a plane wave

$$\delta\sigma_{\mathbf{k}} = \frac{e^{-ik\tau}}{\sqrt{2k}}\,. \tag{1.63}$$

  So we find that the fluctuations with wavelength within the horizon oscillate exactly like in flat spacetime. This is not surprise, since as we mentioned before, in the subhorizon scale, the Minkowski spacetime is a good approximation, and we used this reality for finding the normalization factor of perturbed field.

- On superhorizon scales ($k \ll aH \Rightarrow k^2 \ll a''/a$), the solution is

$$|\delta\sigma_{\mathbf{k}}| \simeq \frac{H}{\sqrt{2k^3}}\,. \tag{1.64}$$

So on superhorizon scales the fluctuation of χ field is constant.

The comoving curvature perturbation

The intrinsic spatial curvature ${}^{(3)}R$ on hypersurfaces of constant conformal time τ is given by

$${}^{(3)}R = \frac{4}{a^2}\nabla^2\psi\,, \tag{1.65}$$

where the quantity ψ is usually referred to as the *curvature perturbation*. The curvature potential ψ is not gauge invariant, but is defined only on hypersurfaces of constant conformal time. Under a transformation on constant time hypersurfaces $\tau \to \tau + \delta\tau$

$$\psi \to \psi + \mathcal{H}\,\delta\tau\,, \tag{1.66}$$

where $\mathcal{H} \equiv a'/a$ and prime represents the derivative with respect to the conformal time.

We now consider the comoving hypersurfaces, on which $\delta\phi_{\rm com} = 0$. Since $\delta\phi \to \delta\phi - \phi'\,\delta\tau$ for a transformation on constant time hypersurfaces, this means that

$$\delta\phi \;\to\; \delta\phi_{\rm com} = \delta\phi - \phi'\,\delta\tau = 0 \;\to\; \delta\tau = \frac{\delta\phi}{\phi'}\,, \tag{1.67}$$

that is, $\delta\tau = \dfrac{\delta\phi}{\phi'}$ is the time-displacement needed to go from a generic hypersurface with generic $\delta\phi$ to the comoving hypersurface where $\delta\phi_{\rm com} = 0$. At the same time the curvature perturbation ψ transforms into

$$\psi \;\to\; \psi_{\rm com} = \psi + \mathcal{H}\,\delta\tau = \psi + \mathcal{H}\frac{\delta\phi}{\phi'}\,. \tag{1.68}$$

The quantity

$$\mathcal{R}_c \equiv \psi + \mathcal{H}\frac{\delta\phi}{\phi'}\,, \tag{1.69}$$

is the *comoving curvature perturbation* and is gauge invariant. The meaning of $\mathcal{R}_c$ is that it represents the gravitational potential on comoving hypersurfaces where $\delta\phi = 0$,

$$\mathcal{R}_c = \psi\,|_{\delta\phi=0}\,. \tag{1.70}$$

According to the observations, $\mathcal{R}_c$ is conserved on superhorizon scales.

Since we know that fluctuations are frozen in on superhorizon scales, we can infer that on superhorizon scales, the gravitational potential ψ is nearly constant; therefore we can relate the fluctuation of the gravitational potential ψ to the fluctuation of the inflaton field $\delta\phi$ on superhorizon scales in Fourier space

$$\psi_{\mathbf{k}} \simeq \epsilon\, H\, \frac{\delta\phi_{\mathbf{k}}}{\dot{\phi}}\,. \tag{1.71}$$

Now, let's assume the gauge-invariant comoving curvature perturbation $\mathcal{R}_c$

$$\mathcal{R}_c(k) = \psi_{\mathbf{k}} + H\,\frac{\delta\phi_{\mathbf{k}}}{\dot{\phi}} = H\,(1+\epsilon)\frac{\delta\phi_{\mathbf{k}}}{\dot{\phi}} \simeq H\,\frac{\delta\phi_{\mathbf{k}}}{\dot{\phi}}\,. \tag{1.72}$$

Then the power spectrum[16] of the comoving curvature $\mathcal{R}_c$ on superhorizon scales reads

$$\mathcal{P}_{\mathcal{R}_c}(k) = \frac{k^3}{2\pi^2}\frac{H^2}{\dot{\phi}^2_{\mathbf{k}}}\,|\delta\phi_{\mathbf{k}}|^2\,. \tag{1.73}$$

If we suppose that inflaton field is massless, by using eq. (1.64) we can compute the power spectrum of the primordial comoving curvature perturbation on superhorizon scales

$$\mathcal{P}_{\mathcal{R}_c}(k) = \left(\frac{H}{2\pi}\right)^2\left(\frac{H}{\dot{\phi}_{\mathbf{k}}}\right)^2\,, \tag{1.74}$$

where the right-hand side simply can be evaluated at the epoch of horizon exit $k = aH$. Using the slow–roll formula (1.45), and the critical density relation (1.44), this becomes

$$\mathcal{P}_{\mathcal{R}_c}(k) = \frac{1}{12\pi^2\,M_{\rm P}^6}\frac{V^3}{V'^2} = \frac{1}{24\pi^2\,M_{\rm P}^4}\frac{V}{\epsilon}\,. \tag{1.75}$$

It is worth to mention that on comoving hypersurfaces there is a simple relation between the density perturbation and the curvature perturbation [80]

$$\delta(k,t) = \frac{2(1+w)}{5+3w}\left(\frac{k}{aH}\right)^2\mathcal{R}_c(k)\,, \tag{1.76}$$

where $\delta(k,t)$ is the density perturbation on comoving hypersurfaces.

The density and curvature perturbation power spectra are therefore related by

$$\mathcal{P}_\delta(k,t) = \frac{4(1+w)^2}{(5+3w)^2}\left(\frac{k}{aH}\right)^4\mathcal{P}_{\mathcal{R}_c}(k)\,. \tag{1.77}$$

[16]For the definition of the power spectrum, see Appendix B.

Now we discuss the scale dependence of the spectrum. No matter what its form, we can define an "effective spectral index" $n(k)$ of the comoving curvature perturbation as

$$n(k) - 1 \equiv \frac{d \ln \mathcal{P}_{\mathcal{R}_c}}{d \ln k} \,. \tag{1.78}$$

Over an interval of k, where $n(k)$ is constant, the simplest assumption for the power spectrum is a scale-free power-law

$$\mathcal{P}_{\mathcal{R}_c}(k) = \mathcal{P}_{\mathcal{R}_c}(k_0) \left(\frac{k}{k_0}\right)^{n(k)-1} \,, \tag{1.79}$$

where k_0 is a suitably chosen normalization scale.

However, if the primordial perturbations are produced by inflation then the power spectrum is not expected to be an exact power law over all scales. We parameterize the scale dependence of n as[17] [81]

$$n(k) = n_S(k_0) + \frac{1}{2!}\,\alpha_S(k_0)\,\ln\left(\frac{k}{k_0}\right) + \frac{1}{3!}\,\beta_S(k_0)\,\ln^2\left(\frac{k}{k_0}\right) + \ldots \,. \tag{1.80}$$

The parameters α_S and β_S denote the running of the effective spectral index n_S and the running of the running, respectively

$$n_S(k_0) \equiv \left.\frac{d \ln \mathcal{P}_{\mathcal{R}_c}}{d \ln k}\right|_{k=k_0} \,, \tag{1.81}$$

$$\alpha_S(k_0) \equiv \left.\frac{d n_S}{d \ln k}\right|_{k=k_0} \,, \tag{1.82}$$

$$\beta_S(k_0) \equiv \left.\frac{d^2 n_S}{d \ln^2 k}\right|_{k=k_0} \,. \tag{1.83}$$

Using eqs. (1.51) and (1.75), we find the spectral parameters [76, 81, 82]

$$\begin{aligned} n_S &= 1 - 6\epsilon + 2\eta \,, \\ \alpha_S &= -24\epsilon^2 + 16\epsilon\eta - 2\xi^2 \,, \\ \beta_S &= -192\epsilon^3 + 192\epsilon^2\eta - 32\epsilon\eta^2 - 24\epsilon\xi^2 + 2\eta\xi^2 + 2\sigma^3 \,. \end{aligned} \tag{1.84}$$

In most (small–field) inflation models, eqs. (1.48) and (1.52) imply two strong inequalities between (combinations of) slow–roll parameters (hierarchy)

$$\begin{aligned} |\epsilon| &\ll |\eta| \,, \\ |\epsilon\eta| &\ll |\xi^2| \,. \end{aligned} \tag{1.85}$$

[17] In [81], this Taylor expansion has been done up to the second term. It will become clear in the next chapter why we extend the expansion. However, it is worth to mention that, this expansion is valid provided $\ln(k/k_0)$ is small for the relevant k values. This is the case for cosmological observations, but not for the wide range of scales probed by PBH constraints.

The first relation means that $n_S - 1$ is essentially determined by η. Similarly, both relations together imply that α_S is basically fixed by ξ^2, while only the last two terms in the expression for β_S are relevant; these two terms are generically of similar order of magnitude.

Along with these, another crucial inflationary observable is the influence of gravitational waves, relative to density perturbations, on large–angle microwave background anisotropies, given by [80]

$$r \equiv \frac{C_2(\text{grav})}{C_2(\text{dens})} \simeq 14\epsilon\,. \tag{1.86}$$

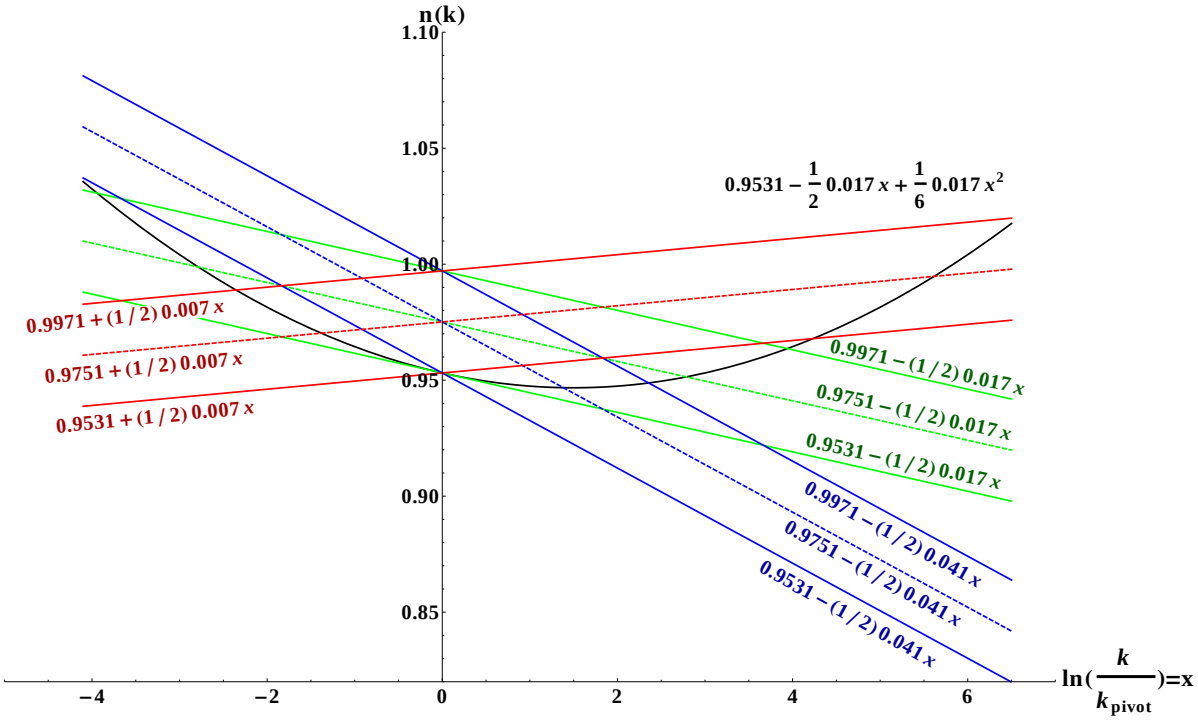

Figure 1.3: Parabola function of eq. (1.80) in $k \in [2.4 \times 10^{-4}, 10]\,\text{Mpc}^{-1}$ (black-solid line) where $k_{\text{pivot}} = 0.015\,\text{Mpc}^{-1}$.

Observational bounds on $\mathcal{P}_{\mathcal{R}_c}$, r, n_S and α_S at the pivot $k_{\text{pivot}} = 0.015\,\text{Mpc}^{-1}$, where

n_S and α_S are essentially uncorrelated,[18] are reported in [1] as follows[19]

$$\begin{aligned} n_S(k_{\rm pivot}) &= 0.9751 \pm 0.0110\,, \\ \alpha_S(k_{\rm pivot}) &= -0.017 \pm 0.012\,, \\ \mathcal{P}_{\mathcal{R}_c}(k_0) &= (2.33 \pm 0.092) \times 10^{-9}\,, \\ r &< 0.17\,(95\%\,{\rm CL})\,. \end{aligned} \tag{1.87}$$

By requiring $n_S \in [0.9531,\, 0.9971]$ and $\alpha_S \in [-0.041,\, 0.007]$ for all $k \in [2.4 \times 10^{-4},\, 10]$ Mpc^{-1} (*i. e.* down to the Lyman–α range), we find from eq. (1.80) that values of β_S up to 0.017 are allowed (Figure 1.3). The ranges of n_S and α_S are simply in $2\,\sigma$ range of (1.87), and the range of k encompasses all cosmologically relevant scales. Here we used the error bars derived from the analysis of the"SPT+WMAP7+BAO+H_0+*Clusters*" data set [1].[20]

Combining eqs. (1.84) and (1.86) gives [84]

$$\begin{aligned} \alpha_S &\simeq 6\left(\frac{r}{7}\right)^2 + 4\left(\frac{r}{7}\right)(n_S - 1) - 2\xi^2\,, \\ \beta_S &\simeq -15\left(\frac{r}{7}\right)^3 - 15\left(\frac{r}{7}\right)^2 (n_S - 1) - 2\left(\frac{r}{7}\right)(n_S - 1)^2 \\ &+ \frac{\alpha_S}{2}\left[9\left(\frac{r}{7}\right) - (n_S - 1)\right] + 2\sigma^3\,. \end{aligned} \tag{1.88}$$

In the left frame of figure 1.4 we show contours of $\alpha_S + 2\xi^2$ in the (n_S, r) plane, while contours of $\beta_S - 2\sigma^3$ in the $(n_S,\, \alpha_S)$ plane are shown in the right frame, assuming a negligible tensor–to–scalar ratio. We see that the observational constraints on n_S and r imply that $\alpha_S + 2\xi^2$ is very small, roughly $-9 \times 10^{-4} \leq \alpha_S + 2\xi^2 \leq 2.2 \times 10^{-3}$ if n_S and r are within their current $2\,\sigma$ intervals. Any significant running must therefore be due to

[18] The "pivot scale" is where the errors on n_S and α_S are essentially uncorrelated; at k–values above (below) this scale, n_S and α_S are correlated (anticorrelated) (Fore more details, see figure 1 in [83].). Note that this scale is different for different data sets.

[19] The amplitude of the primordial scalar fluctuations is reported at the "COBE" scale $k_0 = 0.002\,{\rm Mpc}^{-1}$.

[20] We ignore possible tensor modes, which is appropriate for small–field inflation models (see chapter 3). Allowing a sizable contribution from tensor modes changes the mean value of α_S [4], but unfortunately the pivot scale where the spectral index and its running are uncorrelated is not reported in running+tensor model. In the SPT data [1], the inflation parameters are not reported in running+tensor model. So although in the large–field inflation models, tensor modes are not negligible (see chapter 3) we will assume that the upper bound of β_S is the same as in small–field models. Note that the precise value of the upper bound on β_S derived here is not important for our analysis, since it is in any case well above the lower bound needed for successful PBH formation (see chapter 2). Note also that, this upper bound on β_S is lower than the bound found from the "WMAP+H_0+BAO" data set [44], since the older data set [4] allowed somewhat larger values of α_S.

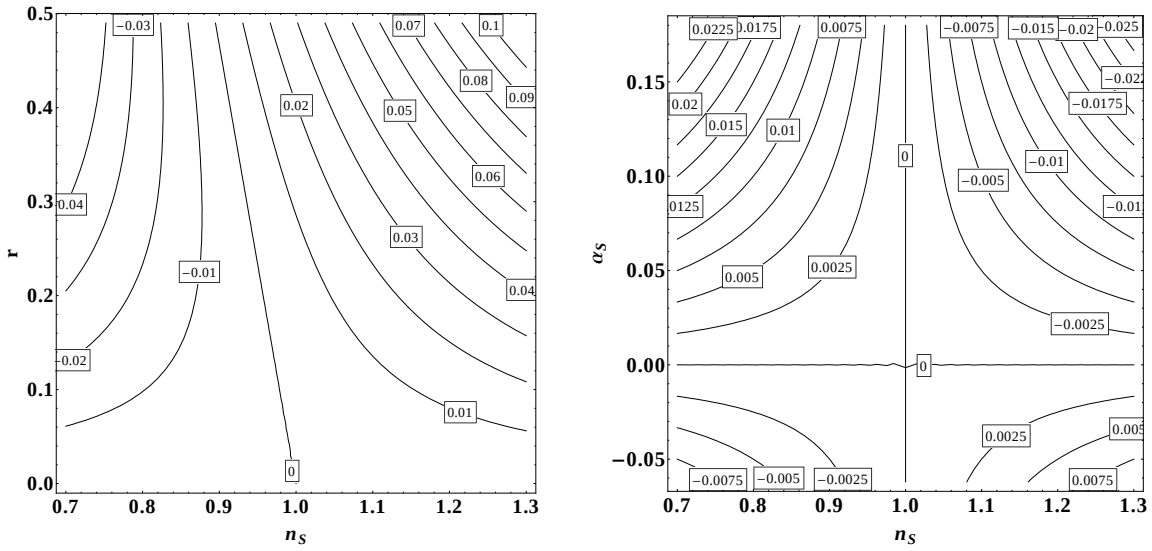

Figure 1.4: Contours of $\alpha_S + 2\xi^2$ (left) and of $\beta_S - 2\sigma^3$ (right); the right frame assumes negligible tensor modes, $r = 0$.

ξ^2. Similarly, $-5 \times 10^{-4} \leq \beta_S - 2\sigma^3 \leq -4 \times 10^{-5}$ if $r = 0$ and n_S and α_S are within their $1\,\sigma$ intervals. Even using $2\,\sigma$ intervals and allowing $r \leq 0.17$, this range only expands to $-0.0053 \leq \beta_S - 2\sigma^3 \leq 0.001$, so that significant positive running of the running can only be due to σ^3.

2 Primordial Black Holes Formation

In this chapter we investigate the DM PBHs formation by using the Press-Schechter formalism [85] in the radiation dominated era after inflation.

2.1 Press-Schechter formalism

The traditional treatment of PBH formation is based on the Press-Schechter formalism used widely in LSS studies. Press-Schechter theory simply asserts that if we smooth the *linear* theory density field on some mass range M, then the fraction of space in which the smoothed density field exceeds some threshold $\delta_{\rm th}$ is in collapsed objects of mass greater than M. This is illustrated in figure 2.1.

Here the density field is smoothed on a scale $R(M)$. In the case at hand, $R(M)$ is given by the mass enclosed inside radius R when R crossed the horizon. The probability of PBH formation is then estimated by simply integrating the probability distribution $P(\delta; R)$ over the range of perturbations δ which allow PBH formation: $\delta_{\rm th} < \delta < \delta_{\rm cut}$, where the upper limit arises since very large perturbations would correspond to separate closed 'baby' universes [22, 31]. We will show that in practice $P(\delta; R)$ is such a rapidly decreasing function of δ above $\delta_{\rm th}$ that the upper cutoff is not important. The threshold density is taken as $\delta_{\rm th} > w$, where $w = p/\rho$ is the equation of state parameter describing the epoch during which PBH formation is supposed to have occurred [31]. Here we take $w = 1/3$, characteristic for the radiation dominated epoch which should have started soon after the end of inflaton. However the correct value of the threshold $\delta_{\rm th}$ is quite uncertain. Niemeyer and Jedamzik [86] carried out numerical simulations of the collapse of the isolated regions and found the threshold for PBH formation to be 0.7. We will show that PBHs abundance is sensitive to the value of $\delta_{\rm th}$.

The fraction of the energy density of the Universe in which the density fluctuation exceeds the threshold for PBH formation when smoothed on scale $R(M)$, $\delta(M) > \delta_{\rm th}$, which will hence end up in PBHs with mass $\geq \gamma M$ is given as in Press–Schechter theory

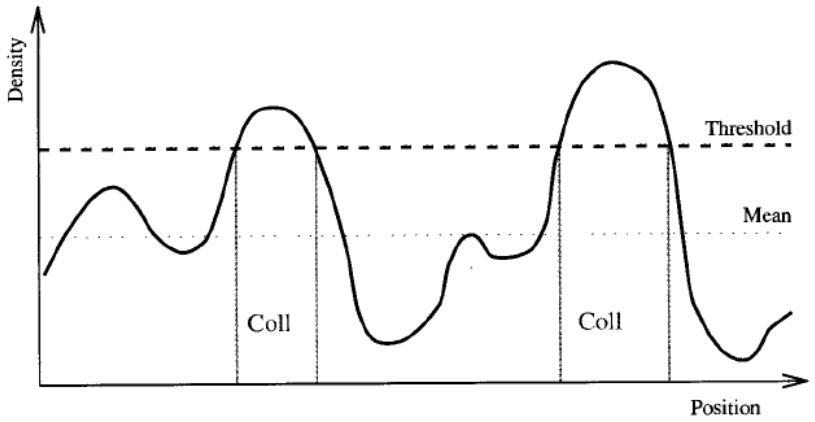

Figure 2.1: Schematic of Presse-Schechter theory applied to the density field smoothed on some scale. The volume in regions above the threshold, indicated by "Coll" for collapsed, is identified with objects of the smoothing mass and above [80].

by[1]

$$f(\geq M) = 2\gamma \int_{\delta_{\rm th}}^{\infty} P(\delta;\, M(R)) d\delta \,. \tag{2.1}$$

Here $P(\delta;\, M(R))$ is the probability distribution function (PDF) of the linear density field δ smoothed on a scale R, and γ is the fraction of the total energy within a sphere of radius R that ends up inside the PBH. A simple analytical calculation suggests that it is around $\gamma \simeq 0.2$ during the radiation era [31].

For Gaussian fluctuations, the probability distribution of the smoothed density field is given by[2]

$$P(\delta;\, R) = \frac{1}{\sqrt{2\pi}\,\sigma_\delta(R)} \exp\left(-\frac{\delta^2}{2\sigma_\delta^2(R)}\right) . \tag{2.2}$$

[1] $f(\geq M)$ is $\beta(M)$ which has been defined in chapter 1. We rename it here not to get confused with β_S which is the running of the running of the spectral index.
We follow ref. [87] in including a factor of two on the right–hand side. The reason is that since (2.1) does not take into account those regions that are underdense on a scale $M_{\rm PH}$, but nevertheless overdense on some larger scale. In the Press-Schechter formalism this seems to be taken care of in some models by multiplying (2.1) with a factor 2. Fortunately, in most cases (as well as in PBH formation) $f(M)$ is a very rapidly falling function of mass, so this effect can be neglected.
Moreover, we set $\delta_{\rm cut}$ to infinity.

[2] This PDF is often written as $P(\delta(R))$. However, we think it is more transparent to consider P to be the PDF of δ, which is just an integration variable in eq. (2.1). Eq. (2.2) shows that the functional form of $P(\delta)$ depends on the parameter R, which in turn depends on the horizon mass M.

This PDF is thus uniquely determined by the variance $\sigma_\delta(R)$ of δ, which is given by

$$\sigma_\delta^2(R) = \int_0^\infty W^2(kR)\,\mathcal{P}_\delta(k)\frac{dk}{k}\,. \tag{2.3}$$

In order to compute the variance, we therefore have to know the power spectrum of δ, $\mathcal{P}_\delta(k) \equiv k^3/(2\pi^2)\,\langle|\delta_k|^2\rangle$, as well as the volume–normalized Fourier transform of the window function used to smooth δ, $W(kR)$.

It is not obvious what the correct smoothing function $W(kR)$ is; a top–hat function has often been used in the past, but we prefer to use a Gaussian window function[3],

$$W(kR) = \exp\left(-\frac{k^2R^2}{2}\right)\,. \tag{2.4}$$

The mass fraction of the Universe that will collapse into PBHs can now be computed by inserting eqs. (1.77) and (2.4) into eq. (2.3) to determine the variance as function of R. This has to be used in eq. (2.2), which finally has to be inserted into eq. (2.1). Since we assume a Gaussian $P(\delta)$ in eq. (2.2), the integral in eq. (2.1) simply gives an error function.

In order to complete this calculation one needs to relate the mass M to the comoving smoothing scale R. It is straightforward to show that (see Appendix A.)

$$\frac{R}{1\,\mathrm{Mpc}} = 5.54\times10^{-24}\,\gamma^{-\frac{1}{2}}\left(\frac{M_{\mathrm{PBH}}}{1\,\mathrm{g}}\right)^{1/2}\left(\frac{g_*}{3.36}\right)^{1/6}\,, \tag{2.5}$$

where g_* is the number of the relativistic degrees of freedom.

Note that $M_{\mathrm{PBH}} \propto R^2$, not $\propto R^3$ as one might naively have expected. Recall that M_{PBH} is related to the horizon mass at the time when the comoving scale R again crossed into the horizon, *i.e.* $R = (aH)^{-1}$. Larger scales re–enter later, when the energy density was lower; this weakens the dependence of M_{PBH} on R. Moreover, the lightest BHs to form are those corresponding to a comoving scale that re–enters the horizon immediately after inflation.[4]

The Gaussian window function in eq. (2.3) strongly suppresses contributions with $k > 1/R$. At the same time, the factor k^4 in eq. (1.77) suppresses contributions to the integral in eq. (2.3) from small k. As a result, this integral is dominated by a limited range of $k-$values near $1/R$. Over this limited range one can to good approximation assume a power–law primordial power spectrum with *fixed* power n_S[5]

[3] Bringmann *et al.* [88] argued that a top–hat window function predicts a larger PBH abundance.

[4] In fact, PBH formation might also occur on scales that never leave the horizon, *i.e.* subhorizon scales [89]. We do not consider this contribution here.

[5] "Fixed" here means that n_S does not depend on k; however, n_S does depend on R, since a large range of values of R has to be considered for PBH formation of different masses.

$\mathcal{P}_{\mathcal{R}_c}(k) = \mathcal{P}_{\mathcal{R}_c}(k_R)(k/k_R)^{n_S(R)-1}$, with $k_R = 1/R$. With this ansatz, the variance of the primordial density field at horizon crossing is given by

$$\sigma_\delta^2(R) = \frac{2(1+w)^2}{(5+3w)^2}\mathcal{P}_{\mathcal{R}_c}(k_R)\,\Gamma\left[\frac{n_S(R)+3}{2}\right], \tag{2.6}$$

for $n_S(R) > -3$.

As mentioned in previous chapter, the power $\mathcal{P}_{\mathcal{R}_c}$ is known accurately at CMB scales (Eqs. (1.87)). In order to relate this to the scales relevant for PBH formation, we parameterize the power spectrum as

$$\mathcal{P}_{\mathcal{R}_c}(k_R) = \mathcal{P}_{\mathcal{R}_c}(k_0)(k_R/k_0)^{n(R)-1}\,. \tag{2.7}$$

It is important to distinguish between $n_S(R)$ and $n(R)$ at this point. $n_S(R)$ describes the *slope* of the power spectrum at scales $k \sim k_R = 1/R$, whereas $n(R)$ fixes the *normalization* of the spectrum at $k_R \gg k_0$. The two powers are identical if the spectral index is strictly constant, *i.e.* if neither n_S nor n depend on R. However, in this case CMB data imply [1] that $n = n_S$ is close to unity. Eqs. (2.6) and (2.7) then give a very small variance, leading to essentially no PBH formation.

Significant PBH formation can only occur in scenarios with running spectral index. In latter chapter we parameterize the scale dependence of n as:

$$n(R) \quad = \quad n_S(k_0) - \frac{1}{2!}\,\alpha_S\,\ln(k_0R) + \frac{1}{3!}\,\beta_S\,\ln^2(k_0R) + \dots\,, \tag{2.8}$$

recall that we are interested in $R \ll 1/k_0$, *i.e.* $\ln(k_0R) < 0$.

Eq. (2.8) illustrates the difference between $n(R)$ and $n_S(R)$. The latter has an expansion similar to eq. (2.8), but with the usual Taylor–expansion coefficients, 1 in front of α_S and 1/2 in front of β_S. One therefore has

$$n_S(R) \quad = \quad n(R) - \frac{1}{2}\,\alpha_S\,\ln(k_0R) + \frac{1}{3}\,\beta_S\,\ln^2(k_0R) + \dots\,. \tag{2.9}$$

Setting $n_S(k_0) = 1$ for simplicity, eq. (2.9) implies $n_S(R) = 2n(R) - 1$ for $\beta_S = 0$, and $n_S(R) = 3n(R) - 2$ for $\alpha_S = 0$. We will compute the variance $\sigma(R)$, and hence the PBH fraction f, for these two relations; they represent extreme cases if neither α_S nor β_S is negative.

The result of this calculation is shown in figure 2.2. Here we have fixed $\gamma = 0.2$, and show results for two choices of the threshold $\delta_{\rm th}$ and three choices of $n(R)$. We see that scenarios where $n(R) = 1.3$ (or smaller) are safe in the SM, because there is no model–independent limit on f for $M_{\rm PBH} < 10^{10}$ g [71]. As noted earlier, PBHs contributing to DM today must have $M_{\rm PBH} \gtrsim 10^{15}$ g; at this mass, they saturate the DM relic density if $f \simeq 5 \times 10^{-19}$ [27].[6] Figure 2.2 shows that this requires $n(R) \simeq 1.37\,(1.41)$ for

[6]Note that f describes the fraction of the energy density in PBHs at the time of their formation. Since they behave like matter at all times, their fractional contribution to the energy density increases during the radiation dominated epoch, and stays essentially constant during the subsequent matter dominated epoch.

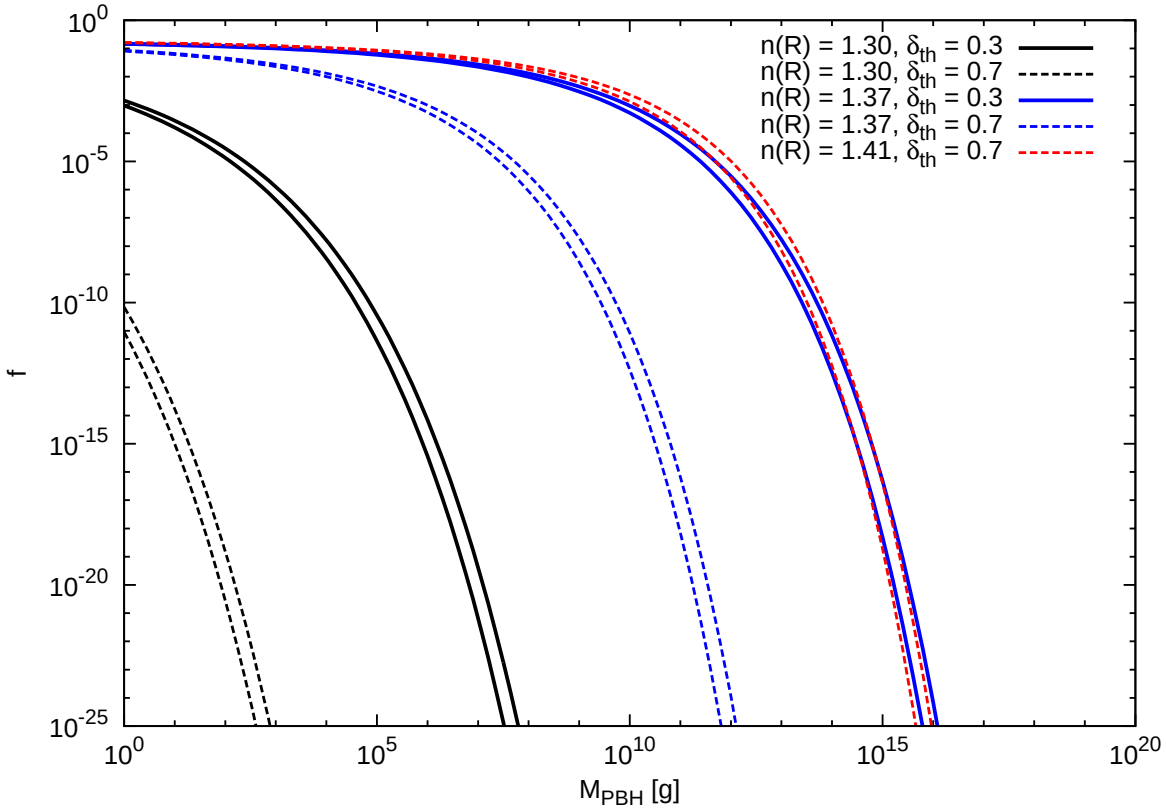

Figure 2.2: Fraction of the energy density of the Universe collapsing into PBHs as a function of the PBH mass, for three different values of $n(R)$ and two different choices of the threshold $\delta_{\rm th} = 0.3\,(0.7)$ for the solid (dashed) curves. On the upper [lower] of two curves with equal pattern and color we have assumed $n_S(R) = 2n(R) - 1$ [$n_S(R) = 3n(R) - 2$].

$\delta_{\rm th} = 0.3\,(0.7)$. The dependence on n_S is much milder. Therefore in order to get long–lived PBHs the amplitude of the perturbations at PBH scales must therefore exceed that at CMB scales by a factor 10^3–10^4. Current data favor a negative or at best slightly positive value of α_S at the CMB pivot scale, as well as a spectral index at the pivot scale somewhat below 1; so the first two terms in eq. (2.8) can thus not lead to PBH formation.

Figure 2.2 also illustrates a serious problem that all scenarios that aim to explain the required CDM density in terms of post–inflationary PBH formation face. We just saw that this can happen only if the spectral index n increases significantly between the scales probed by the CMB and other cosmological observations and the scale $R \simeq 10^{-9}$ pc relevant for the formation of 10^{15} g PBHs. However, n must then *decrease* rapidly when going to slightly smaller length scales, since otherwise one would *overproduce*

lighter PBHs. For example, successful BBN requires $f(10^{13}\,\mathrm{g}) \leq 2 \times 10^{-20}$ [71], about 12 orders of magnitude below that predicted by keeping $n(R)$ fixed at the value required for having 10^{15} g PBHs as CDM candidates.

Another problem is that the expansion of $n(R)$ in eq. (2.8) will generally only be accurate if $|\ln(k_0 R)|$ is not too large. This is the case for cosmological observations, which probe scales $\gtrsim 1$ Mpc. The expansion becomes questionable for the scales probed by PBH formation. For example, fixing $k_0 = 0.002$ Mpc^{-1}, eq. (2.5) gives $|\ln(k_0 R)| = 41.1$ for $M_{\mathrm{PBH}} = 10^{15}$ g. Fortunately within the framework of a given inflationary scenario this second problem can be solved by computing $n(R)$ and $n_S(R)$ exactly, rather than using the expansion (2.8).

On the other hand, eq. (2.8) shows that for $\alpha_S = 0$ we only need $\beta_S(k_0) \simeq 0.0015$ in order to generate sufficiently large density perturbations to allow formation of 10^{15} g PBHs. Even if we set $\alpha_S(k_0)$ equal to its central value, $\alpha_S(k_0) = -0.017$, we only need $\beta_S(k_0) \simeq 0.0028$. Including the running of the running of the spectral index thus easily allows to accommodate DM PBH formation in scenarios that reproduce all current cosmological observations at large scales.

Of course, this kind of model–independent analysis does not show whether simple, reasonably well–motivated inflationary models exist that can generate a sufficiently large β_S. In the next chapter we study different models of inflation and check whether they can lead to PBHs formation. As a by–product, we also check whether these models can accommodate a sizably negative value of α_S, as indicated by current data.

2.2 Summary

In this chapter we have investigated the formation of PBHs in the radiation dominated era just after inflation. Since PBHs behave like matter, their contribution to the energy density increases with time during the radiation dominated epoch. For this reason, the PBHs formed considerably before the end of radiation dominated era are the most relevant to cosmology. We have focused in this chapter on these kind of PBHs and we also considered the standard case of PBHs formation, which applies to scales which have left the horizon at the end of inflation. We only considered Gaussian and spherically symmetric perturbations and we assumed that the mass of the PBH formed is proportional to the mass of the horizon mass at horizon entry. We reviewed the Press–Schechter type formalism for PBH formation and we found that for the formation of long–lived PBHs with mass larger than 10^{15} g as candidate for DM, the spectral index at scale k_{PBH} should be at least 1.37, even for the lower value of 1/3 for the threshold δ_{th}. This value is higher that the value 1.25 found in [70] because here we have assumed that the mass of the collapsed region to form PBH is only 20% of the entire energy density inside the

particle horizon. We have also shown that PBHs abundance is sensitive to the value of $\delta_{\rm th}$. We also investigated that including the running of the running of the spectral index thus easily allows to accommodate DM PBH formation.

3 Inflation Models

Most models of inflation predict an approximately scale–free spectrum with a spectral index n_S (as well as n) close to the scale–invariant (Harrison–Zel'dovich) case $n_S = n = 1$. As shown in latter chapter, a significant number of long–lived PBHs can only be produced for $n > 1$ (a "blue spectrum"), since these values lead to more power on small scales. Observational limits (both from Hawking radiation and the fact that PBHs must not overclose the Universe) strongly constrain n_S [70, 73]. This, therefore, yields a constraint on inflationary models that is independent of the cosmological constraints from the CMB and LSS. However, we will see in this chapter that in most simple models of inflation constraints on model parameters derived from the latter are far more stringent than the PBH constraint, to the point of making the formation of long–lived PBHs impossible.

In this chapter we study the possibility of PBH formation in two different categories of inflation models: small–field models and large–field models. Hybrid models [77] are not studied here because in these models, PBH formation can occur by different mechanisms. (For analyses of PBH formation in multi-field or multi-stage inflation models which include hybrid models, see [90, 91].) As noted above, the spectral index will have to increase at very small scales (very large k) in order to allow PBH formation, but we will also check whether the models we analyze are compatible with a sizably negative value of α_S at scales probed by the CMB and LSS data, as indicated by eqs. (1.87).

3.1 Small–field models

Small–field models are defined as those for which the variation in the inflaton field is less than the reduced Planck mass. Typically, the first slow–roll parameter ϵ and hence the amplitude of gravitational waves generated in such models is small and the spectral index and its running provide the key observational discriminators.

3.1.1 Hilltop/inflection point inflation

A popular ansatz for the small field inflaton potential is given by [92]

$$V(\phi) = V_0 \left[1 - \left(\frac{\phi}{\mu}\right)^p\right] , \tag{3.1}$$

where V_0, μ and p are positive constants.[1] This potential is equivalent to the potential $V(\phi) = \Lambda^4 - \lambda\, M_{\rm P}^{4-n}\dfrac{\phi^n}{n}$ in the literature [93] which can be specialized to several distinct models: *e.g.* hilltop ($n = 2$ or $n = 4$) and inflection point ($n = 3$). We consider the case that the dominant term is the leading one, V_0. When p is an integer greater than 2, such a potential may be generated by the self–coupling of the inflaton at tree–level.

For $p > 0$, the hierarchies (1.85) hold among slow–roll parameters. So the spectral parameters are given by

$$\begin{aligned} n_S - 1 &\simeq -2p(p-1)\left(\frac{M_{\rm P}}{\mu}\right)^2\left(\frac{\phi}{\mu}\right)^{p-2} , \\ \alpha_S &\simeq -2p^2(p-1)(p-2)\left(\frac{M_{\rm P}}{\mu}\right)^4\left(\frac{\phi}{\mu}\right)^{2(p-2)} , \\ \beta_S &\simeq -4p^3(p-1)(p-2)^2\left(\frac{M_{\rm P}}{\mu}\right)^6\left(\frac{\phi}{\mu}\right)^{3(p-2)} . \end{aligned} \tag{3.2}$$

Inflation ends at $\phi_{\rm end} \lesssim \mu$, and in order to have a small field model we take $\mu \lesssim M_{\rm P}$. Then

$$N = -\frac{p-1}{p-2} + \frac{1}{p(p-2)}\left(\frac{\mu}{M_{\rm P}}\right)^2\left(\frac{\mu}{\phi}\right)^{p-2} . \tag{3.3}$$

For $p > 2$, the first term in eq. (3.3) can be neglected. We then find, independently of μ:

$$\begin{aligned} n_S - 1 &\simeq -\frac{p-1}{p-2}\frac{2}{N} , \\ \alpha_S &\simeq -\frac{p-1}{p-2}\frac{2}{N^2} = \frac{1}{N}(n_S - 1) , \\ \beta_S &\simeq -\frac{p-1}{p-2}\frac{4}{N^3} = \frac{2}{N^2}(n_S - 1) . \end{aligned} \tag{3.4}$$

In figure 3.1 the spectral index, its running and its running of running are shown as functions of the number of e–folds before the end of inflation, for $p = 4$.

[1] This potential is unbounded from below for $\phi \to \infty$. There must be additional terms that prevent this. Here we follow the usual assumption that these terms do not affect the dynamics of inflation.

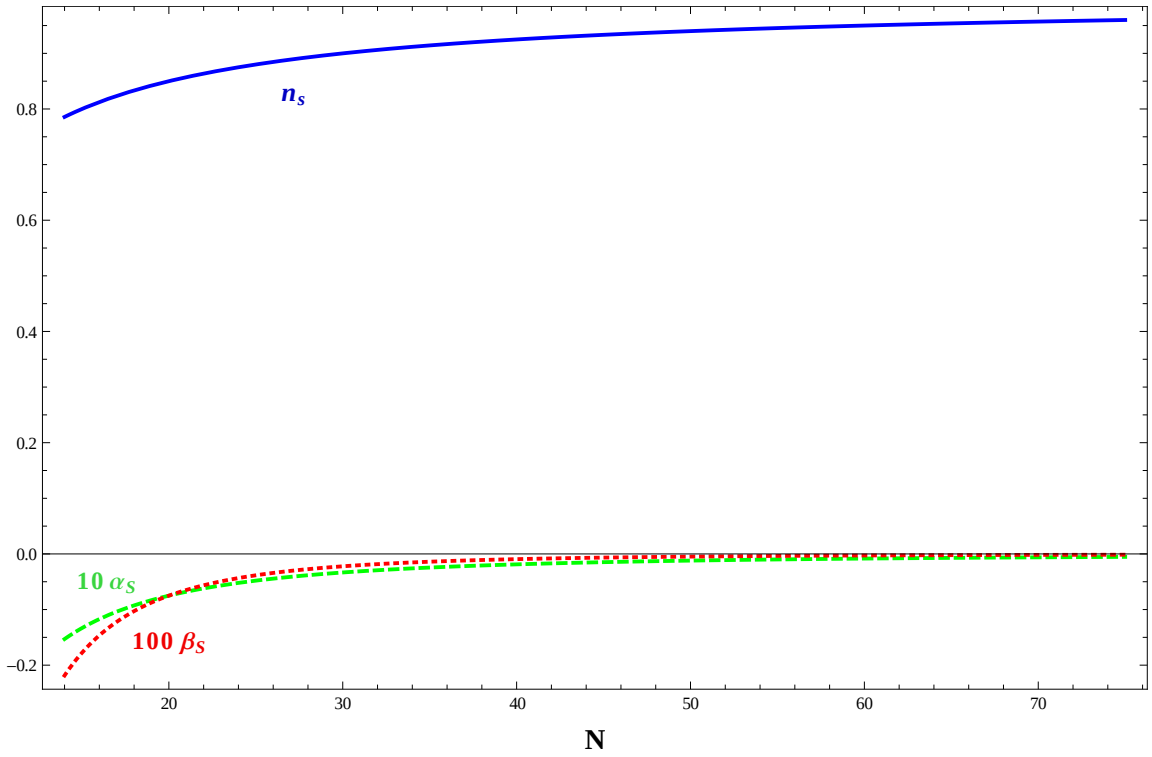

Figure 3.1: Illustrating the dependence according to eqs. (3.4) of n_S (solid curve), $10\,\alpha_S$ (dashed curve) and $100\,\beta_S$ (dotted curve), on the number of e–folds before the end of inflation, for the fixed value of $p = 4$.

It is clear that in this model both $n_S - 1$ and α_S are negative, but it is not possible to reproduce the observed central value of α_S, which would require $\alpha_S \sim \mathcal{O}(n_S - 1)$ (see figure 3.1). Moreover, the value of β_S is also negative. So the conclusion is that this model cannot produce sufficient high density fluctuations at small scales to produce PBHs.

In the case at hand, the power spectrum can be calculated exactly as function of N. Again neglecting the first term in eq. (3.3) we have from eq. (1.75)

$$\mathcal{P}_{\mathcal{R}_c}(N) = \frac{1}{12\pi^2}\frac{V_0\,\mu^2}{p^2\,M_{\rm P}^6}\left[N\,p(p-2)\frac{M_{\rm P}^2}{\mu^2}\right]^{\frac{2p-2}{p-2}} . \tag{3.5}$$

Note that the exponent is positive for $p > 2$. This implies less power at smaller N, *i.e.* at smaller length scales.

3.1.2 Running–mass inflation

This model,[2] proposed by Stewart [94], exploits the observation that in field theory the parameters of the Lagrangian are scale dependent. This is true in particular for the mass of the scalar inflaton, which can thus be considered to be a "running" parameter.[3] The running of the mass parameter can be exploited to solve the "η–problem"[4]of inflation in supergravity [92]. This problem arises because the vacuum energy driving inflation also breaks supersymmetry (SUSY). In "generic" supergravity models the vacuum energy therefore gives a large (gravity–mediated) contribution to the inflaton mass, yielding $|\eta| \sim 1$. However, this argument applies to the scale where SUSY breaking is felt, which should be close to the (reduced) Planck scale $M_{\rm P} = 2.4 \times 10^{18}$ GeV. In the running–mass model, renormalization group (RG) running of the inflaton mass reduces the inflaton mass, and hence $|\eta|$, at scales where inflation actually happens. There are four types of model, depending on the sign of the squared inflaton mass at the Planck scale, and on whether or not that sign change between $M_{\rm P}$ and the scales characteristic for inflation [95].

The simplest running–mass model is based on the inflationary potential

$$V_\phi = V_0 + \frac{1}{2} m_\phi^2(\phi)\phi^2 \,, \tag{3.6}$$

where ϕ is a real scalar; in SUSY it could be the real or imaginary part of the scalar component of a chiral superfield. The natural size of $|m_\phi^2(M_{\rm P})|$ in supergravity is of order $V_0/M_{\rm P}^2$. Even for this large value of m_ϕ^2, which gives $|\eta| \sim \mathcal{O}(1)$, the potential will be dominated by the constant term for $\phi^2 \ll M_{\rm P}^2$; as mentioned above, running is supposed to reduce $|m_\phi^2|$ even more at lower ϕ^2.

The potential (3.6) would lead to eternal inflation. One possibility to end inflation is to implement the idea of hybrid inflation [77]. To that end, one introduces a real scalar "waterfall field" ψ, and adds to the potential the terms[5]

$$V_\psi = \frac{\lambda}{4}\phi^2\psi^2 - \sqrt{\frac{V_0\,\kappa}{6}}\psi^2 + \frac{\kappa}{24}\psi^4 \,. \tag{3.7}$$

Here λ and κ are real couplings, and the coefficient of the ψ^2 term has been chosen such that $V_{\rm inf} = V_\phi + V_\psi$ has a minimum with $\langle V \rangle = 0$ if $\phi = 0$, $\psi \neq 0$. As long as

[2]The possibility of PBHs formation in the running–mass inflation model has been studied in detail in [44] for "WMAP7+BAO+H_0" data set [4] where $n_S = 0.964 \pm 0.012$ and $\alpha_S = -0.022 \pm 0.020$ at $k_0 = 0.0155\,{\rm Mpc}^{-1}$.

[3]Note that the physical, or pole, mass of the inflaton is not "running"; however, at the quantum level the physical mass differs from the parameter m_ϕ appearing in eq. (3.6) even if $\phi = 0$.

[4]The supergravity theory gives $|\eta| \gtrsim 1$, in violation of the flatness condition $|\eta| \ll 1$. This is called the η–problem [80].

[5]The parameters of this potential will in general also be scale dependent; however, this is immaterial for our argument.

$\phi^2 > \sqrt{\frac{8V_0\,\kappa}{3\lambda^2}}$, ψ remains frozen at the origin. Once ϕ^2 falls below this critical value, ψ quickly approaches its final vacuum expectation value, given by $\langle\psi\rangle^2 = \sqrt{\frac{24V_0}{\kappa}}$, while ϕ quickly goes to zero, thereby "shutting off" inflation. However, in this thesis we focus on the inflationary period itself; the evolution of perturbations at length scales that left the horizon a few e–folds before the end of inflation should not be affected by the details of how inflation is brought to an end.[6]

During inflation, the potential is thus simply given by eq. (3.6). Here $m_\phi^2(\phi)$ is obtained by integrating an RG equation of the form

$$\frac{dm_\phi^2}{d\ln\phi} = \beta_m\,, \tag{3.8}$$

where β_m is the β–function of the inflaton mass parameter. If m_ϕ^2 is a pure SUSY–breaking term, to one loop β_m can be schematically written as [94, 96]

$$\beta_m = -\frac{2C}{\pi}\alpha\,\widetilde{m}^2 + \frac{D}{16\pi^2}|\lambda_Y|^2\,m_s^2\,, \tag{3.9}$$

where the first term arises from the gauge interaction with coupling α and the second term from the Yukawa interaction λ_Y. C and D are positive numbers of order one, which depend on the representations of the fields coupling to ϕ, $\widetilde{m}$ is a gaugino mass parameter, while m_s^2 is the scalar SUSY breaking mass–squared of the scalar particles interacting with the inflaton via Yukawa interaction λ_Y.

For successful inflation the running of m_ϕ^2 must be sufficiently strong to generate a local extremum of the potential V_ϕ for some nonvanishing field value, which we call ϕ_*. The inflaton potential will obviously be flat near ϕ_*, so that inflation usually occurs at field values not very far from ϕ_*. We therefore expand $m_\phi^2(\phi)$ around $\phi = \phi_*$. The potential we work with thus reads

$$V = V_0 + \frac{1}{2}m_\phi^2(\phi_*)\,\phi^2 + \frac{1}{2}\,c\,\phi^2\,\ln\left(\frac{\phi}{\phi_*}\right) + \frac{1}{4}\,g\,\phi^2\,\ln^2\left(\frac{\phi}{\phi_*}\right)\,. \tag{3.10}$$

Here $c \equiv \left.\frac{dm_\phi^2}{d\ln\phi}\right|_{\phi=\phi_*}$ is given by the β–function of eq. (3.9), and $g \equiv \left.\frac{d^2m_\phi^2}{d(\ln\phi)^2}\right|_{\phi=\phi_*}$ is given by the scale dependence of the parameters appearing in eq. (3.9). In contrast to earlier analyses of this model [95, 96, 97, 98], we include the $\ln^2(\phi/\phi_*)$ term in the potential. This is a two–loop correction, but it can be computed by "iterating" the one–loop correction.[7] Since the coefficient g of this term is of fourth order in couplings,

[6] It has recently been pointed out that the waterfall phase might contribute to PBH formation [90].

[7] There are also "genuine" two–loop corrections, which can not be obtained from a one–loop calculation, but they only affect the term linear in $\ln(\phi/\phi_*)$. They are thus formally included in our coefficient c.

one will naturally expect $|g| \ll |c|$. However, this need not be true if $|c|$ "happens" to be suppressed by a cancellation in eq. (3.9). Including the second correction to $m_\phi^2(\phi)$ seems natural given that we also expanded the running of the spectral index to second (quadratic) order.

Recall that we had defined ϕ_* to be a local extremum of V_ϕ, *i.e.* $V'(\phi_*) = 0$. This implies [95] $m_*^2 \equiv m_\phi^2(\phi_*) = -\frac{1}{2}c$; this relation is not affected by the two–loop correction $\propto g$.

Combining eqs. (3.10), (1.48) and (1.52) we see that we need $V_0 \gg c\phi^2 L,\, g\phi^2 L^2$, where we have introduced the short–hand notation

$$L \equiv \ln \frac{\phi}{\phi_*} \,. \tag{3.11}$$

In other words, the inflaton potential has to be dominated by the constant term, as noted earlier.

By having the potential in hand and noting that the hierarchies (1.85) among slow–roll parameters hold in this model and replacing the factor of V appearing in the denominators of eqs. (1.48) and (1.52), we find the spectral parameters

$$\begin{aligned}
n_S - 1 &= 2\frac{c\,M_\mathrm{P}^2}{V_0}\left[L + 1 + \frac{g}{2c}\left(L^2 + 3L + 1\right)\right] , \\
\alpha_S &= -2\left(\frac{c\,M_\mathrm{P}^2}{V_0}\right)^2 L\left[1 + \frac{g}{2c}\left(2L + 3\right)\right]\left[1 + \frac{g}{2c}\left(L + 1\right)\right] , \\
\beta_S &= 2\left(\frac{c\,M_\mathrm{P}^2}{V_0}\right)^3 L\left[1 + \frac{g}{2c}\left(L + 1\right)\right]\left[1 + \frac{g}{2c}\left(3L + 2\right) + \frac{g^2}{2c^2}\left(3L^2 + 5L + \frac{3}{2}\right)\right] ,
\end{aligned} \tag{3.12}$$

where L has been defined in eq. (3.11). Clearly the spectral index is not scale–invariant unless c and g are very close to zero. Note that V_0 appears in eqs. (3.12) only in the dimensionless combination $c\,M_\mathrm{P}^2/V_0$, while ϕ only appears via L, *i.e.* only the ratio ϕ/ϕ_* appears in these equations.

Applying our potential (3.10) to eq. (1.75), replacing V by V_0 in the numerator, we see that $\mathcal{P}_{\mathcal{R}_c}$ not only depends on $c\,M_\mathrm{P}^2/V_0$ and L, but also on the ratio $V_0/(M_\mathrm{P}^2\,\phi^2)$. We can thus always find parameters that give the correct normalization of the power spectrum, for all possible combinations of the spectral parameters.

We want to find out whether the potential (3.10) can accommodate sufficient running of n_S to allow PBH formation. There are strong observational constraints on n_S and α_S. It is therefore preferable to use these physical quantities directly as inputs, rather than the model parameters $c\,M_\mathrm{P}^2/V_0$, L and g/c. To this end we rewrite the first eq. (3.12) as

$$\frac{c\,M_\mathrm{P}^2}{V_0} = \frac{n_S - 1}{2(L+1) + \dfrac{g}{c}\left(L^2 + 3L + 1\right)} \,. \tag{3.13}$$

Inserting this into the second eq. (3.12) gives

$$\alpha_S = -\frac{(n_S-1)^2}{2}\, L\, \frac{\left[1+\frac{g}{2c}\,(2L+3)\right]\left[1+\frac{g}{2c}\,(L+1)\right]}{\left[L+1+\frac{g}{2c}\,(L^2+3L+1)\right]^2}\,. \tag{3.14}$$

We thus see that the running of the spectral index is "generically" of order $(n_S-1)^2$; similarly, the running of the running can easily be seen to be $\propto (n_S-1)^3$. This is true in nearly all inflationary scenarios that have a scale–dependent spectral index.

Eq. (3.14) can be solved for g/c. Bringing the denominator to the left–hand side leads to a quadratic equation, which has two solutions. They can be written as

$$\frac{g}{2c} = -\frac{(L+1)\,(L^2+3L+1) + r_S\,L\,(1.5L+2) \pm L\sqrt{r_S\left[(L+1)^2+1\right] + r_S^2\,(0.5L+1)^2}}{(L^2+3L+1)^2 + r_S\,L\,(2L+3)\,(L+1)}\,, \tag{3.15}$$

where we have introduced the quantity

$$r_S \equiv \frac{(n_S-1)^2}{2\alpha_S}\,. \tag{3.16}$$

Since g and c are real quantities, eq. (3.15) only makes sense if the argument of the square root is non–negative. Note that the coefficients multiplying r_S and r_S^2 inside the square root are both non–negative. This means that the model can in principle accommodate any non–negative value of r_S. However, small negative values of r_S cannot be realized. It is easy to see that the constraint on r_S is weakest for $L = 0$. The argument of the square root is then positive if $2r_S + r_S^2 > 0$, which implies either $r_S > 0$ or $r_S < -2$. Recalling the definition (3.16) we are thus led to the conclusion

$$\alpha_S \geq -\frac{(n_S-1)^2}{4}\,, \tag{3.17}$$

this bound should hold on all scales, as long as the potential is described by eq. (3.10). Note that it is identical to the bound found in ref. [97], *i.e.* it is not affected by adding the term $\propto L^2$ to the inflaton potential. This is somewhat disappointing, since recent data indicate that α_S is negative at CMB scales. Even the generalized version of the running mass model therefore cannot reproduce the current $1\,\sigma$ range of α_S.

However, at the $2\,\sigma$ level significantly positive α_S values are still allowed. Let us therefore continue with our analysis, and search for combinations of parameters within the current $2\,\sigma$ range that might lead to significant PBH formation. Using eqs. (3.13) and (3.15) we can use $n_S(k_0)-1$, $\alpha_S(k_0)$ and $L_0 \equiv \ln(\phi_0/\phi_*)$ as input parameters in the last eq. (3.12) to evaluate $\beta_S(k_0)$. This can then be inserted into eq. (2.8) to see how large the density perturbations at potential PBH scales are.

In general requiring the correct normalization of the power spectrum at CMB scales does not impose any constraint on the spectral parameters. However, any inflation model also has to satisfy several consistency conditions. To begin with, the running–mass model should provide a sufficient amount of inflation. In the slow–roll approximation, the number of e–folds of inflation following from the potential (3.10) is given by

$$\begin{aligned}\Delta N(L) &= -\frac{2}{\tilde{c}}\int_{L_0}^{L}\frac{d\,L'}{L'\left[1+\dfrac{g}{2c}\,(L'+1)\right]} \\ &= -\frac{2}{\tilde{c}\left(1+\dfrac{g}{2c}\right)}\left[\ln\frac{L}{L_0}-\ln\frac{1+\dfrac{g}{2c}(L+1)}{1+\dfrac{g}{2c}(L_0+1)}\right], \end{aligned} \tag{3.18}$$

where we have introduced the dimensionless quantity

$$\tilde{c}\equiv\frac{2c\,M_{\rm P}^2}{V_0}\,, \tag{3.19}$$

recall that it can be traded for $n_S(k_0)-1$ using eq. (3.13). Moreover, $L\equiv\ln(\phi/\phi_*)$ can be related to the scale k through

$$k(L)=k_0\,{\rm e}^{\Delta N(L)}\,. \tag{3.20}$$

This can be inverted to give

$$L(k)=L_0\,\frac{E(k)\left(1+\dfrac{g}{2c}\right)}{1+\dfrac{g}{2c}\left[L_0\left(1-E(k)\right)+1\right]}\,, \tag{3.21}$$

where we have introduced

$$E(k)=\left(\frac{k}{k_0}\right)^{-\frac{\tilde{c}}{2}\left(1+\frac{g}{2c}\right)}\,. \tag{3.22}$$

The problem is that the denominator in eq. (3.21) vanishes for some finite value of k. This defines an extremal value of ΔN

$$\Delta N_{\rm ex}=-\frac{2}{\tilde{c}\left(1+\dfrac{g}{2c}\right)}\ln\left[1+\frac{1}{L_0}\left(1+\frac{2c}{g}\right)\right]. \tag{3.23}$$

A negative value of $\Delta N_{\rm ex}$ is generally not problematic, since only a few e–folds of inflation have to have occurred before our pivot scale k_0 crossed out of the horizon. However, a small positive value of $\Delta N_{\rm ex}$ would imply insufficient amount of inflation after the scale k_0 crossed the horizon. In our numerical work we therefore exclude scenarios with

$-5 < \Delta N_{\rm ex} < 50$, *i.e.* we (rather conservatively) demand that at least 50 e–folds of inflation can occur after k_0 crossed out of the horizon.

A second consistency condition we impose is that $|L|$ should not become too large. Specifically, we require $|L(k)| < 20$ for all scales between k_0 and the PBH scale. For (much) larger values of $|L|$ our potential (3.10) may no longer be appropriate, *i.e.* higher powers of L may need to be included.

Note that eq. (3.21) allows to compute the effective spectral index $n_S(k)$ *exactly*

$$n_S(k) - 1 = [n_S(k_0) - 1] \, \frac{L(k) + 1 + \dfrac{g}{2c} \left[L(k)^2 + 3L(k) + 1\right]}{L_0 + 1 + \dfrac{g}{2c} \left(L_0^2 + 3L_0 + 1\right)} \, . \tag{3.24}$$

This in turn allows an *exact* (numerical) calculation of the spectral index $n(k)$

$$n(k) - 1 = \frac{1}{\ln \dfrac{k}{k_0}} \int_0^{\ln \frac{k}{k_0}} [n_S(k') - 1] \, d \, \ln k' \, . \tag{3.25}$$

In our numerical scans of parameter space we noticed that frequently the exact value for $n(k)$ at PBH scales differs significantly from the values predicted by the expansion of eq. (2.8); similar statements apply to $n_S(k)$. This is not very surprising, given that $|\ln(k_0 R)| = 39.1$ for our value of the pivot scale and $M_{\rm PBH} = 10^{15}$ g. In fact, we noticed that even if $\alpha_S(k_0)$ and $\beta_S(k_0)$ are both positive, $n_S(k)$ may not grow monotonically with increasing k. In some cases $n_S(k)$ computed according to eq. (3.24) even becomes quite large at values of k some 5 or 10 e–folds below the PBH scale. This is problematic, since our calculation is based on the slow–roll approximation, which no longer works if $n_S - 1$ becomes too large. We therefore demanded $n_S(k) < 2$ for all scales up to the PBH scale; the first eq. (1.84) shows that this corresponds to $\eta < 0.5$. This last requirement turns out to be the most constraining one when looking for combinations of parameters that give large $n(k_{\rm PBH})$.

Numerical Results

We are now ready to present some numerical results. We begin in figure 3.2, which shows a scatter plot of the spectral parameters $\alpha_S(k_0)$ and $\beta_S(k_0)$, which has been obtained by randomly choosing model parameters $\tilde{c}$ [defined in eq. (3.19)], g/c and L_0 in the ranges[8] $|\tilde{c}| \leq 1$, $|g| M_{\rm P}^2 / V_0 \leq 1$, $|L_0| \leq 20$. We require that $n_S(k_0)$ and $\alpha_S(k_0)$ lie within their $2\,\sigma$ ranges, and impose the consistency conditions discussed above. The plot shows a very strong correlation between β_S and α_S: if the latter is negative or small, the former

[8] We actually only find acceptable solutions for $|\tilde{c}| < 0.8$.

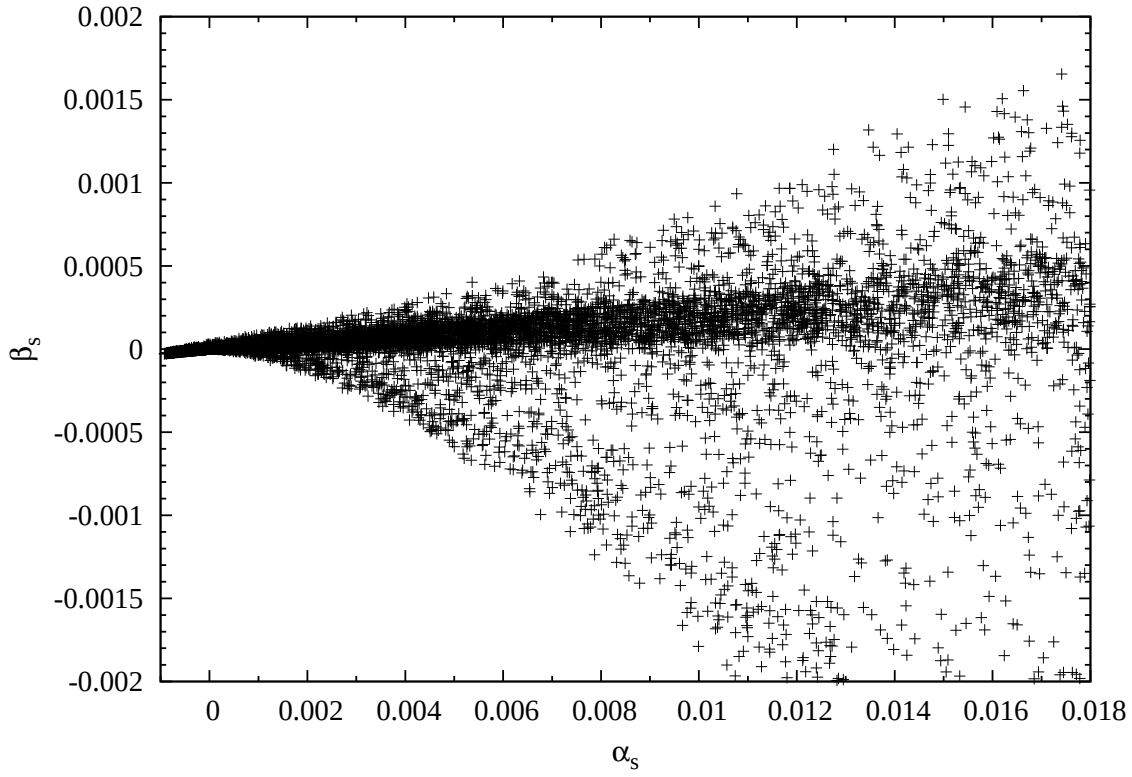

Figure 3.2: Scatter plot of $\beta_S(k_0)$ vs. $\alpha_S(k_0)$. Here the model parameters $\tilde{c} \equiv 2c\,M_{\rm P}^2/V_0$, g/c and L_0 are scanned randomly, with flat probability distribution functions.

is also small in magnitude. Moreover, there are few points at large α_S, and even there most allowed combinations of parameters lead to very small β_S. The accumulation of points at small α_S can be understood from our earlier result (3.14), which showed that α_S is naturally of order $(n_S - 1)^2 < 0.004$ within $2\,\sigma$. Moreover, β_S is naturally of order $\alpha_S^{3/2}$. On the other hand, for α_S values close to the upper end of the current $2\,\sigma$ range, we do find some scenarios where β_S is sufficiently large to allow the formation of 10^{15} g PBHs.

We also explored the correlation between $n_S(k_0)$ and $\alpha_S(k_0)$. Here the only notable feature is the lower bound (3.17) on $\alpha_S(k_0)$; values of $\alpha_S(k_0)$ up to (and well beyond) its observational upper bound can be realized in this model for any value of $n_S(k_0)$ within the presently allowed range. Similarly, we do not find any correlation between $n_S(k_0)$ and $\beta_S(k_0)$. This lack of correlation can be explained through the denominator in eq. (3.14), which also appears (to the third power) in the expression for β_S once eq. (3.13) has been used to trade c for $n_S - 1$: this denominator can be made small through a cancellation, allowing sizable α_S even if n_S is very close to 1. Since the same denominator appears

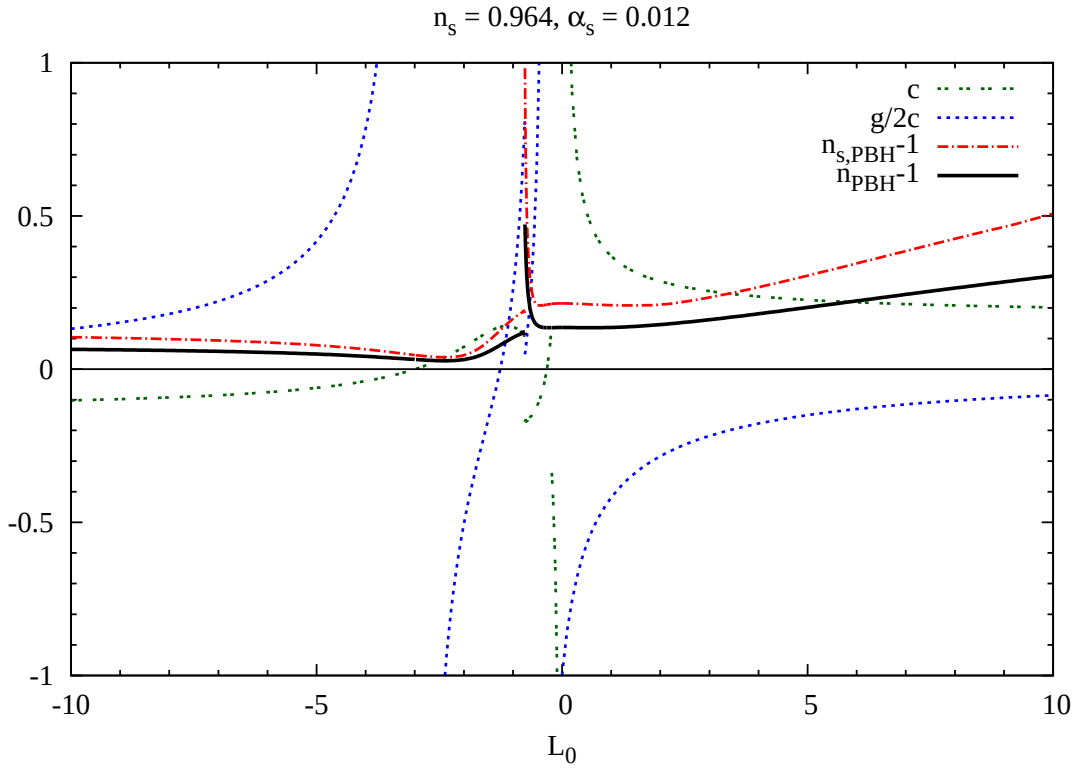

Figure 3.3: The potential parameters c (in units of $V_0/(2M_{\rm P}^2)$; double–dotted [green] curve), $g/(2c)$ (dotted, blue), the effective spectral index $n_S - 1$ at the PBH scale (dot–dashed, red) and the spectral index $n-1$ at the PBH scale (solid, black) are shown as functions of $L_0 = \ln(\phi_0/\phi_*)$, for $n_S(k_0) = 0.964$ and $\alpha_S(k_0) = 0.012$. If both solutions in eq. (3.15) for g/c are acceptable, we have taken the one giving larger n at the PBH scale.

(albeit with different power) in the expressions for α_S and β_S, it does not destroy the correlation between these two quantities discussed in the previous paragraph.

Figure 3.3 indicates that large values of n at the PBH scale can be achieved only if α_S at the CMB scale is positive and not too small. In that figure we therefore explore the dependence of the potential parameters, and of the spectral parameters at the PBH scale on L_0, for $n_S(k_0) = 0.964$, $\alpha_S(k_0) = 0.012$. Note that varying L_0 also changes the parameters c and g (or g/c), see eqs. (3.13) and (3.15). The latter in general has two solutions; however, for most values of L_0, only one of them leads to sufficient inflation while keeping $|L| < 20$; if both solutions are allowed, we take the one giving a larger spectral index at the PBH scale, taken to be $1.5 \times 10^{15}\,{\rm Mpc}^{-1}$ corresponding to $M_{\rm PBH} = 10^{15}$ g. Note that n_S and n at the PBH scale are calculated exactly, using eqs. (1.84) and (3.25). We find that the expansion (2.8) is frequently very unreliable,

e.g. giving the wrong sign for $n-1$ at the PBH scale for $L_0 < -1$.

Figure 3.3 shows that $\tilde{c}$ is usually well below 1, as expected from the fact that $n_S - 1 \propto \tilde{c}$, see the first eq. (3.12). Moreover, in most of the parameter space eq. (3.15) implies $|g| < |c|$; recall that this is also expected, since g is a two–loop term. We find $|g| > |c|$ only if $|c|$ is small. In particular, the poles in $g/(2c)$ shown in figure 3.3 occur only where c vanishes; note that the spectral parameters remain smooth across these "poles".

There are a couple of real discontinuities in figure 3.3, where the curves switch between the two solutions of eq. (3.15). The first occurs at $L_0 \simeq -0.756$. For smaller values of L_0, the solution giving the smaller $|g/c|$ violates our slow–roll condition $|n_S - 1| < 1$ at scales close to the PBH scale. For larger L_0 this condition is satisfied. Just above the discontinuity, where n_S is close to 2 at the PBH scale, we find the largest spectral index at the PBH scale, which is close to 0.47. Recall from figure 3.3 that this will generate sufficiently large density perturbations to allow the formation of PBHs with $M_{\rm PBH} = 10^{15}$ g. However, the formation of PBHs with this mass is possible only for a narrow range of L_0, roughly $-0.756 \leq L_0 \leq -0.739$.

At $L_0 = -0.31$, c goes through zero, giving a pole in g/c as discussed above. Then, at $L_0 = -0.214$, the second discontinuity occurs. Here the curves switch between the two solutions of eq. (3.15) simply because the second solution gives a larger spectral index at the PBH scale. Right at the discontinuity both solutions give the same spectral index, *i.e.* the curve depicting $n_{\rm PBH}$ remains continuous; however, $\tilde{c}$ jumps from about 0.132 to -0.339. The effective spectral index n_S at the PBH scale also shows a small discontinuity. Recall from our discussion of eq. (2.9) that n_S will generally be larger than n at the PBH scale, but the difference between the two depends on the model parameters.

For very small values of $|L_0|$, $\tilde{c}$ becomes very large; this region of parameter space is therefore somewhat pathological. For sizably positive L_0, n at the PBH scale increases slowly with increasing L_0, while $|\tilde{c}|$ and $|g/c|$ both decrease. However, the spectral index at the PBH scale remains below the critical value for the formation of long–lived PBHs.

Note that L always maintains its sign during inflation, since $L = 0$ corresponds to a stationary point of the potential, which the (classical) inflaton trajectory cannot cross. For most of the parameter space shown in figure 3.3, $|L|$ decreases during inflation. If $L_0 < 0$ decreasing $|L|$ corresponds to $V'(\phi_0) < 0$, *i.e.* the inflaton rolls towards a minimum of the potential at $\phi = \phi_*$. For $L_0 > 0$ we instead have $V'(\phi_0) > 0$, *i.e.* the inflaton rolls away from a maximum of the potential.

In fact, this latter situation also describes the branch of figure 3.3 giving the largest spectral index at the PBH scale; since here $L_0 < 0$, $|L|$ increases during inflation on this branch. This is illustrated in figures 3.4, which show the (rescaled) inflaton potential as well as the effective spectral index as function of either the inflaton field (left frame) or of the scale k (right frame). Note that all quantities shown here are dimensionless, and are determined uniquely by the dimensionless parameters $\tilde{c}$ defined in eq. (3.19), g/c and L_0. This leaves two dimensionful quantities undetermined, *e.g.* V_0 and ϕ_*; one combination of these quantities can be fixed via the normalization of the CMB power

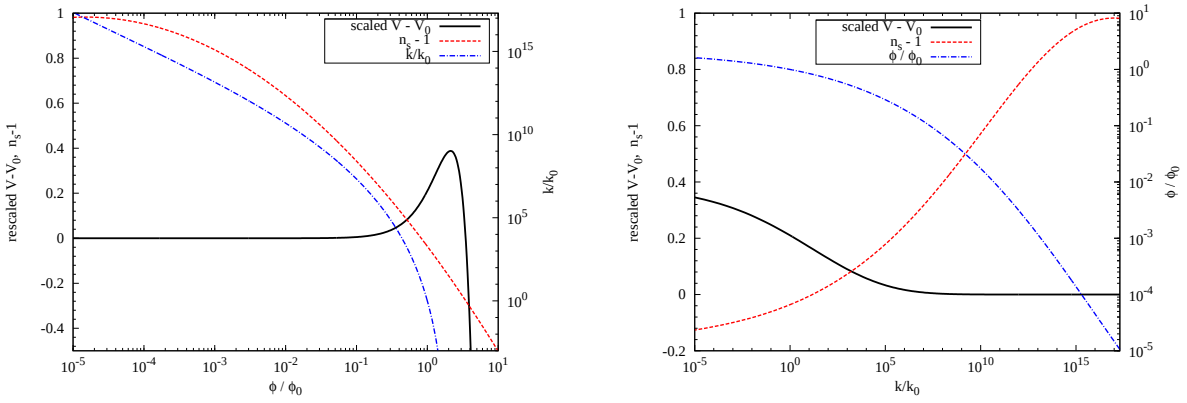

Figure 3.4: Evolution of the rescaled inflaton potential, $4M_P^2(V - V_0)/(V_0\phi_0^2)$ (solid, black), and of the effective spectral index n_S (dashed, red), as a function of the inflaton field ϕ/ϕ_0 (left frame) or of the ratio of scales k/k_0 (right frame). In the left frame the dot–dashed (blue) curve shows k/k_0, whereas in the right frame it depicts ϕ/ϕ_0; this curve in both cases refers to the scale to the right. We took $\tilde{c} = -0.1711$, $g/c = 0.09648$, $L_0 = -0.756$; these parameters maximize the spectral index at the PBH scale for $n_S(k_0) = 0.964$, $\alpha_S(k_0) = 0.012$ (see figure 3.3).

spectrum, leaving one parameter undetermined (and irrelevant for our discussion).

The left frame shows that the (inverse) scale k first increases quickly as ϕ rolls down from its initial value ϕ_0. This means that ϕ initially moves rather slowly, as can also be seen in the right frame. Since $\alpha_S > 0$, the effective spectral index increases with increasing k. The right frame shows that this evolution is quite nonlinear, although for $k/k_0 \lesssim 10^{10}$, $n_S(k)$ is to good approximation a parabolic function of $\ln(k/k_0)$. However, for even smaller scales, *i.e.* larger k, the rate of growth of n_S decreases again, such that $n_S - 1$ reaches a value very close to 1 at the scale $k = 1.6 \times 10^{16}\, k_0$ relevant for the formation of PBHs with $M_{\rm PBH} = 10^{15}$ g. Recall that we only allow solutions where $n_S(k) < 2$ for the entire range of k considered; figures 3.4 therefore illustrate our earlier statement that this constraint limits the size of the spectral index at PBH scales.

The left frame of figure 3.4 shows that the inflaton potential as written becomes unbounded from below for $\phi \to +\infty$. This can be cured by introducing a quartic (or higher) term in the inflaton potential; the coefficient of this term should be chosen sufficiently small not to affect the discussion at the values of ϕ of interest to us. Note also that this pathology of our inflaton potential is not visible in the right frame, since assuming $\phi = \phi_0 < \phi_*$ at $k = k_0$, the inflaton field can never have been larger than ϕ_*: as noted above, it cannot have moved across the maximum of the potential.

Figure 3.2 indicated a strong dependence of the maximal spectral index at PBH scales on $\alpha_S(k_0)$. This is confirmed by figure 3.5, which shows the maximal possible $n(k_{\rm PBH})$

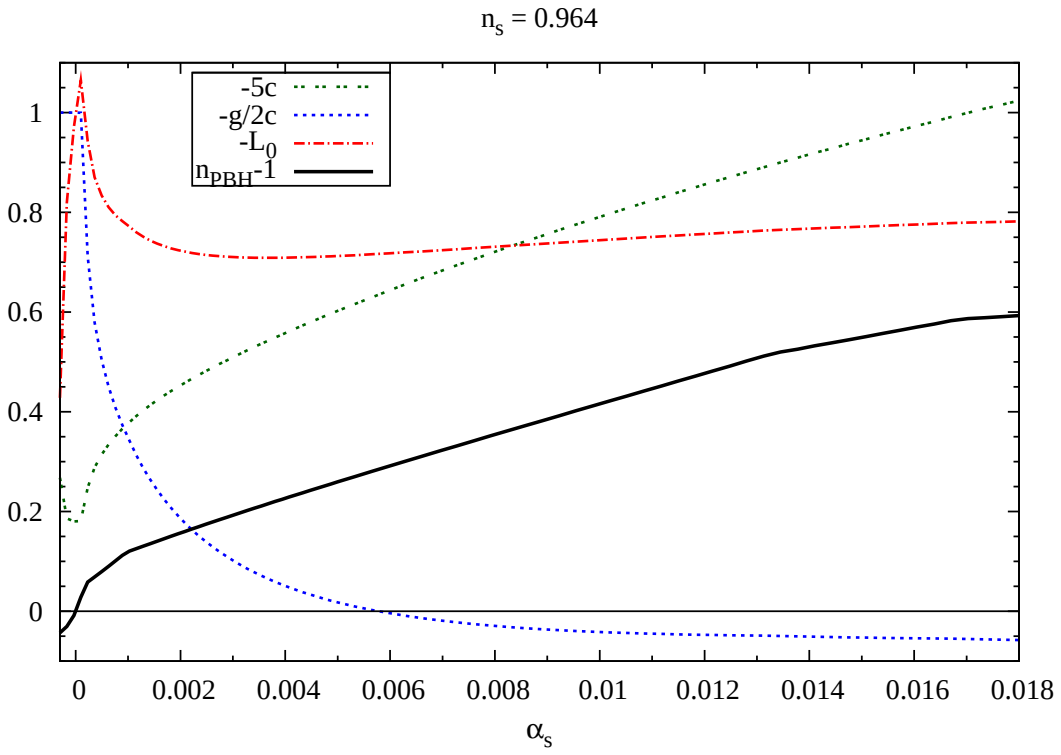

Figure 3.5: The solid (black) curve shows the maximal spectral index at the PBH scale $k_{\rm PBH} = 1.6 \times 10^{19} k_0$ that is consistent with the constraints we impose, as function of $\alpha_S(k_0)$. The other curves show the corresponding model parameters: $\tilde{c}$ (double-dotted, green), multiplied with -5 for ease of presentation; $-g/(2c)$ (dotted, blue); and $-L_0$ (dot–dashed, red). $n_S(k_0)$ is fixed at 0.964, but the bound on $n_{\rm PBH}$ is almost independent of this choice.

consistent with our constraints as function of $\alpha_S(k_0)$, as well as the corresponding values of the parameters $\tilde{c}$, g/c and L_0. We saw in the discussion of eq. (3.15) that $\alpha_S < 0$ is only allowed for a narrow range of L_0. In this very constrained corner of parameter space, $n(k_{\rm PBH})$ remains less than 1, although the effective spectral index $n_S(k_{\rm PBH})$ can exceed 1 for $\alpha_S(k_0) > -1.7 \times 10^{-4}$; recall that for the given choice $n_S(k_0) = 0.964$, solutions only exist if $\alpha_S(k_0) > -3.24 \times 10^{-4}$, see eq. (3.17).

For $\alpha_S(k_0) \leq 1.5 \times 10^{-4}$ the optimal set of parameters lies well inside the region of parameter space delineated by our constraints. $n_S(k_{\rm PBH})$ therefore grows very fast with increasing $\alpha_S(k_0)$. For these very small values of $\alpha_S(k_0)$, the largest spectral index at PBH scales is always found for $g = -2c$, which implies that the second derivative of the inflaton potential also vanishes at $\phi = \phi_*$, *i.e.* ϕ_* corresponds to a saddle point, rather than an extremum, of the potential.

For slightly larger values of $\alpha_S(k_0)$ the choice $g = -2c$ allows less than 50 e–folds of

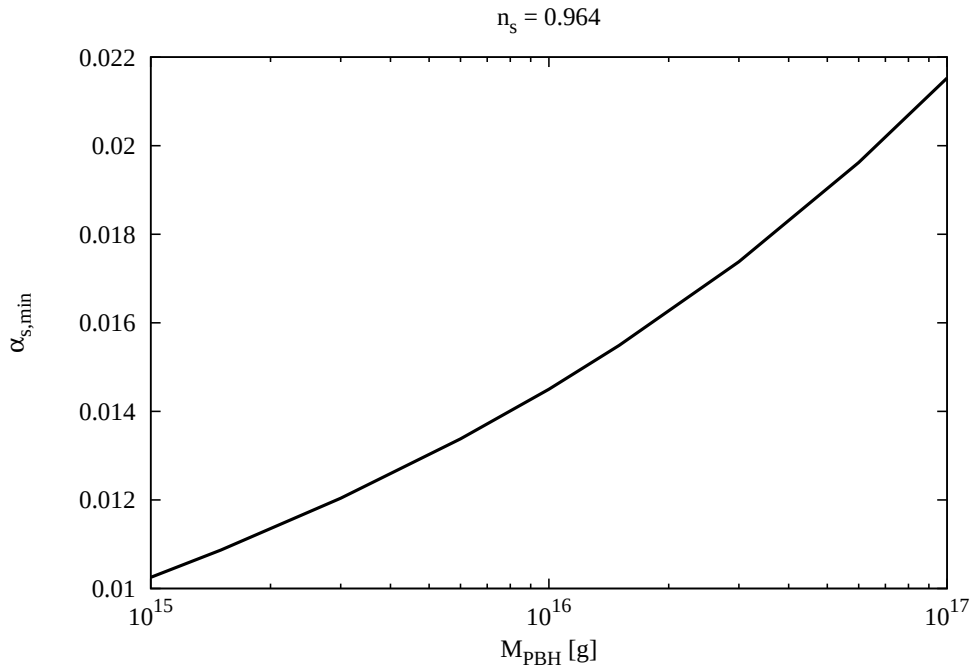

Figure 3.6: The minimal value of $\alpha_S(k_0)$ that allows the formation of primordial black holes of a given mass as a result of density perturbations produced during the slow–roll phase of inflation.

inflation after k_0 exited the horizon. Requiring at least 50 e–folds of inflation therefore leads to a kink in the curve for $n(k_{\rm PBH})$. The optimal allowed parameter set now has considerable smaller $|g/c|$, but larger $|\tilde{c}|$.

The curve for the maximal $n(k_{\rm PBH})$ shows a second kink at $\alpha_S(k_0) = 0.001$. To the right of this point the most important constraint is our requirement that $|n_S - 1| < 1$ at all scales up to $k_{\rm PBH}$, as discussed in connection with figures 3.3 and 3.4. Note that for $\alpha_S(k_0) > 0.014$, the optimal parameter choice leads to n_S reaching its maximum at some intermediate k close to, but smaller than, $k_{\rm PBH}$. This leads to a further flattening of the increase of $n(k_{\rm PBH})$.

We nevertheless see that for values of $\alpha_S(k_0)$ close to the upper end of the $2\,\sigma$ range of the spectral index at the scale relevant for the formation of 10^{15} g PBHs can be well above the minimum for PBH formation found in chapter 2. Figure 2.2 then implies that the formation of considerably heavier PBHs might be possible in running–mass inflation. However, larger PBH masses correspond to smaller $k_{\rm PBH}$, see eq. (2.5). This in turn allows for less running of the spectral index. In order to check whether even heavier PBHs might be formed during the slow–roll phase of running mass inflation, one therefore has to re–optimize the parameters for different choices of $k_{\rm PBH}$.

The result of such an analysis is shown in figure 3.6. We see that in the given model,

the formation of PBHs that are sufficiently massive, and hence long–lived, to be CDM candidates could only have been triggered during the slow–roll phase of inflation if $\alpha_S(k_0)$ is more than one standard deviation above its central value. If $\alpha_S(k_0)$ is at the upper end of its present $2\,\sigma$ range, PBHs with mass up to 5×10^{16} g could have formed as result of density perturbations created at the end of slow–roll inflation. These results are again insensitive to the value of $n_S(k_0)$.

Summary

In running–mass inflation model, we included a term quadratic in the logarithm of the field, *i.e.* we included the "running of the running" of the inflaton mass along with the "running of the running" of the spectral index. We showed that this model can accommodate a sizably positive second derivative of the spectral index at PBH scales. However, this is only possible if the first derivative is also positive and sizable. In fact, like most inflationary scenarios with a smooth potential [99] the model does not permit large negative running of the spectral index at CMB scales. Moreover, we saw that a quadratic (in $\ln k$) extrapolation of the spectral index to PBH scales is not reliable, and therefore computed the spectral index exactly. Imposing several consistency conditions, we found that density perturbations that are sufficiently large to trigger PBH formation only occur for a very narrow region of parameter space. Among other things, the signs of the parameters of the inflaton potential must be chosen such that the potential has a local maximum, and the initial value of the field must be slightly (by typically less than one e–fold) below this maximum.

We emphasize that one major challenge of this model is that for parameters allowing PBH formation the spectral index keep increasing at yet smaller scales. Parameters that lead to the formation of many PBHs with mass around 10^{15} g, which could form the DM in the Universe, would predict the over–production of unstable PBHs, in conflict with data *e.g.* from the non–observation of BH evaporation and (for yet smaller masses) BBN. This problem seems quite generic for this mechanism. One way to solve it might be to abruptly cut off inflation just after the scales relevant for the formation of the desired PBHs leave the horizon, which could *e.g.* be achieved by triggering the waterfall field in hybrid inflation. However, this is somewhat in conflict with the use of the slow–roll formalism of structure formation, which is usually assumed to require a few more e–folds of inflation after the scales of interest left the horizon. Moreover, a sharp end of inflation means that the visible Universe only inflated by about 45 e–folds; this solves the Big Bang problems only if the reheat temperature was rather low.

We can therefore not state with confidence that formation of PBHs as DM candidates is possible in running–mass inflation; all we can say is that certain necessary conditions can be satisfied. Even that is possible only for a very limited range of parameters. This

also means that constraints from the over–production of PBHs only rule out a small fraction of the otherwise allowed parameter space of this model.

3.1.3 Inverse power law inflation

A generic feature of models in nonperturbative gauge dynamics in SUSY [100] is the presence of scalar potentials of the form $\frac{\Lambda_3^{p+4}}{\phi^p}$, where the index p and the scale Λ_3 depend on the underlying gauge group. Like models of hybrid inflation [77], these models are characterized by a potential dominated by the constant term V_0 and require coupling to another sector to end inflation when ϕ reaches the critical value ϕ_c. Unlike standard hybrid inflation models, models of this type postulate a field far from the minimum of the potential.

We take the potential to be described by a single degree of freedom ϕ, of the general form

$$V(\phi) = V_0 + \frac{\Lambda_3^{p+4}}{\phi^p} + \dots , \tag{3.26}$$

where the dots represent nonrenormalizable terms suppressed by powers of the Planck mass, which are not relevant for the present discussion, but will prevent ϕ from "running away" to infinity. In the limit $\phi \ll \langle\phi\rangle$, the term $\sim \phi^{-p}$ dominates the dynamics

$$\begin{aligned} V(\phi) &\simeq V_0 + \frac{\Lambda_3^{p+4}}{\phi^p}, \qquad \phi \ll \langle\phi\rangle \\ &= V_0 \left[1 + \alpha \left(\frac{M_{\rm P}}{\phi}\right)^p\right] , \end{aligned} \tag{3.27}$$

where $\alpha \equiv \frac{\Lambda_3^{p+4}}{M_{\rm P}^p V_0}$. We assume that the constant V_0 dominates the potential, or $\alpha \left(\frac{M_{\rm P}}{\phi}\right)^p \ll 1$. In this case also hierarchies (1.85) hold among the slow–roll parameters which leads to the following spectral parameters

$$\begin{aligned} n_S - 1 &\simeq 2\,p(p+1)\,\alpha \left(\frac{M_{\rm P}}{\phi}\right)^{p+2} , \\ \alpha_S &\simeq -2\,p^2(p+1)(p+2)\,\alpha^2 \left(\frac{M_{\rm P}}{\phi}\right)^{2(p+2)} , \\ \beta_S &\simeq 4\,p^3(p+1)(p+2)^2\,\alpha^3 \left(\frac{M_{\rm P}}{\phi}\right)^{3(p+2)} . \end{aligned} \tag{3.28}$$

The number of the e–folds N is given by

$$N \simeq \frac{1}{p(p+2)\,\alpha}\left[\left(\frac{\phi_c}{M_{\rm P}}\right)^{p+2} - \left(\frac{\phi}{M_{\rm P}}\right)^{p+2}\right], \tag{3.29}$$

where ϕ_c is the critical value at which inflation ends. The value of ϕ_c is in general determined by a coupling of the field to some other sector of the theory which we have here left unspecified. Note that from eq. (3.29), for $\phi \ll \phi_c$ the number of e–folds approaches a constant, which we call $N_{\rm tot}$,

$$N_{\rm tot} \equiv \frac{1}{p(p+2)\,\alpha}\left(\frac{\phi_c}{M_{\rm P}}\right)^{p+2}. \tag{3.30}$$

This puts an upper limit on the total amount of expansion that takes place during the inflationary phase, although that upper bound can in principle be very large. Using eqs. (3.28)–(3.30), we can rewrite the cosmological parameters as functions of the number of e–folds before the end of inflation

$$\begin{aligned}
n_S - 1 &\simeq \frac{p+1}{p+2}\frac{2}{N_{\rm tot}\left(1-\dfrac{N}{N_{\rm tot}}\right)}, \\
\alpha_S &\simeq -\frac{p+1}{p+2}\frac{2}{N_{\rm tot}^2\left(1-\dfrac{N}{N_{\rm tot}}\right)^2} = -\frac{p+2}{p+1}\frac{(n_S-1)^2}{2}, \\
\beta_S &\simeq \frac{p+1}{p+2}\frac{4}{N_{\rm tot}^3\left(1-\dfrac{N}{N_{\rm tot}}\right)^3} = \left(\frac{p+2}{p+1}\right)^2\frac{(n_S-1)^3}{2}.
\end{aligned} \tag{3.31}$$

This model thus predicts $n_S > 1$, which is currently disfavored at more than 2 standard deviation. Moreover, figure 3.7 shows that the spectrum becomes scale–invariant towards the end of inflation, *i.e.* it becomes less blue at smaller length scales, as also indicated by the negative value of α_S. In combination with the constraint that $|n_S - 1| \ll 1$ at CMB scale, this implies that this model cannot accommodate PBH formation.

This can also be seen by directly computing the power spectrum as a function on N

$$\mathcal{P}_{\mathcal{R}_c}(N) = \frac{V_0}{12\pi^2\,M_{\rm P}^4}\frac{1}{\alpha^2 p^2}\left[\alpha\,p(p+2)(N_{\rm tot}-N)\right]^{\frac{2p+2}{p+2}}, \tag{3.32}$$

where we have used (3.29). The power does increase with decreasing N, but only by a small amount. For example, the ratio of the power at the end of inflation ($N = 0$) to that at the COBE scale is

$$q \equiv \frac{\mathcal{P}_{\mathcal{R}_c}(N=0)}{\mathcal{P}_{\mathcal{R}_c}(N_{\rm COBE})} = \left(\frac{N_{\rm tot}-N_{\rm COBE}}{N_{\rm tot}}\right)^{-\frac{2p+2}{p+2}}. \tag{3.33}$$

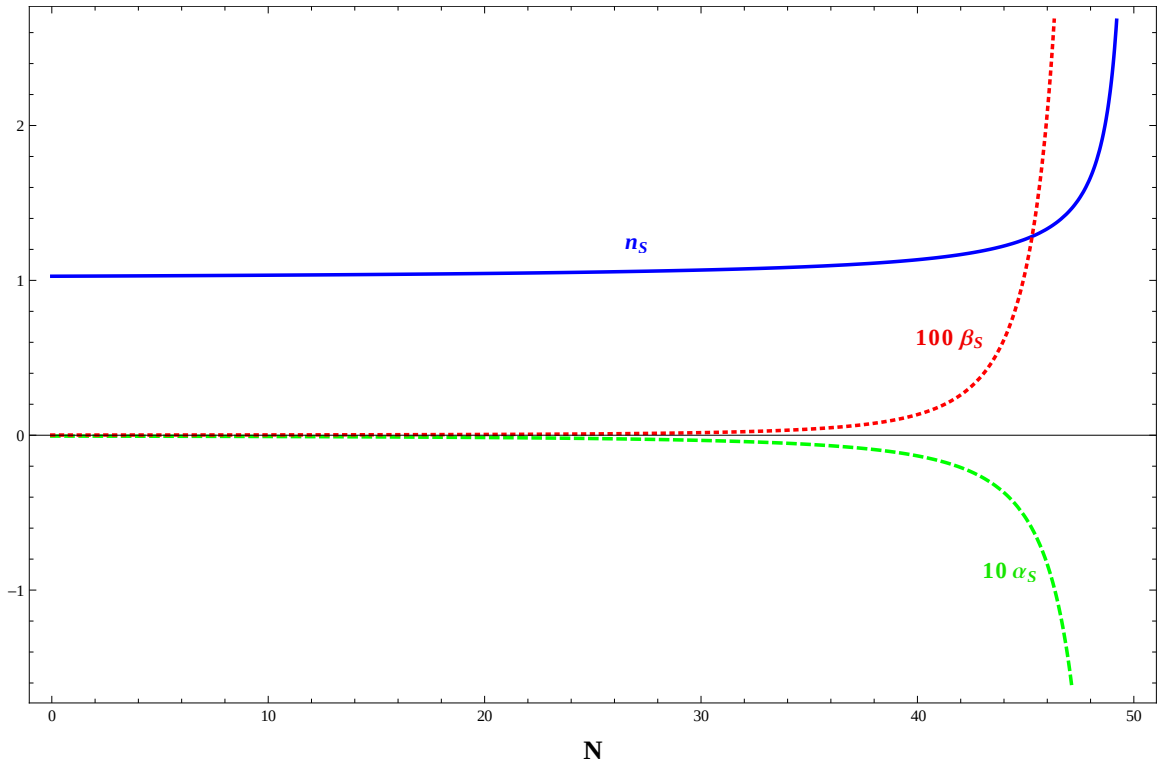

Figure 3.7: Spectral parameters as a function of the number of e–folds $N \propto \ln(k)$ for $p = 1$. Note especially the rapid approach to scale–invariance at short wavelengths (small N).

On the other hand, the first eq. (3.31) gives

$$n_S(N_{\rm COBE}) - 1 \simeq \frac{p+1}{p+2} \frac{2}{N_{\rm COBE}\left(\dfrac{N_{\rm tot}}{N_{\rm COBE}} - 1\right)} \,. \tag{3.34}$$

Eq. (3.33) can be rewritten as

$$\frac{1}{\dfrac{N_{\rm tot}}{N_{\rm COBE}} - 1} = q^{\frac{p+2}{2p+2}} - 1 \,. \tag{3.35}$$

Inserting this into eq. (3.34) finally yields

$$q^{\frac{p+2}{2p+2}} = 1 + \frac{p+2}{2(p+1)} N_{\rm COBE} \left[n_S(N_{\rm COBE}) - 1\right] \simeq 2 \,. \tag{3.36}$$

The power can therefore only increase by small amount in the course of inflation; in contrast, PBH formation would require an increase by a factor 10^7 or so.

3.2 Large–field models

Large–field models are characterized by the condition $|\Delta\phi| \gtrsim M_{\rm P}$. Note that a super–Planckian field variation is a necessary condition for the generation of an observable tensor-to-scalar ratio [101]. On the other hand, such large field models raise issues of stability in the presence of "quantum gravity" corrections, which are suppressed by inverse powers of $M_{\rm P}$. These corrections should not be important for small–field models, but need not be small for large–field models.

3.2.1 Power–law (a. k. a. chaotic) inflation

The polynomial potential $V(\phi) = \Lambda^4 \left(\frac{\phi}{\mu}\right)^p$ is equivalent to $V(\phi) = \frac{\lambda}{M_{\rm P}^{p-4}}\phi^p$ in the literature [102]. In this model, the hierarchies (1.85) do not hold. We find

$$\begin{aligned} n_S - 1 &= -p(p+2)\left(\frac{M_{\rm P}}{\phi}\right)^2 , \\ \alpha_S &= -2p^2(p+2)\left(\frac{M_{\rm P}}{\phi}\right)^4 , \\ \beta_S &= -8p^3(p+2)\left(\frac{M_{\rm P}}{\phi}\right)^6 , \\ r &= 7p^2\left(\frac{M_{\rm P}}{\phi}\right)^2 . \end{aligned} \tag{3.37}$$

Note that these quantities are independent of the normalization of the potential (described by Λ^4/μ^p or, equivalently, by λ), but do depend on its shape (described by p) as well as on the field value.

Inflation ends at $\phi_{\rm end} = \frac{pM_{\rm P}}{\sqrt{2}}$ where $\epsilon = 1$. Then, it is straightforward to rewrite the inflation parameters as functions of the number of e–folds, N

$$\begin{aligned} n_S - 1 &= -\frac{2(p+2)}{4N+p} , \\ \alpha_S &= -\frac{8(p+2)}{(4N+p)^2} = -\frac{2}{p+2}(n_S-1)^2 , \\ \beta_S &= -\frac{64(p+2)}{(4N+p)^3} = \frac{8}{(p+2)^2}(n_S-1)^3 , \\ r &= \frac{14p}{4N+p} = -\frac{7p}{p+2}(n_S-1) . \end{aligned} \tag{3.38}$$

Evidently the spectrum is "red" in this model, $n_S - 1$, α_S and β_S all being negative. However, this model also cannot accommodate the current central values, according to which both $|n_S - 1|$ and $|\alpha_S|$ are of order 10^{-2}. Moreover, $N_{\rm pivot} \leq 50$ implies $n_S - 1 \leq 0.040\,(0.059)$ for $p = 2\,(4)$, *i. e.* $n_S - 1$ comes out somewhat below the current central value in this model.

Computing the power directly from eq. (1.75), we find

$$\mathcal{P}_{\mathcal{R}_c}(N) = \frac{1}{12\pi^2}\left(\frac{\Lambda^2}{\mu\, M_{\rm P}}\right)^2 \left[2p\left(N + \frac{p}{4}\right)\right]^{\frac{p+2}{2}} . \tag{3.39}$$

This decreases quickly towards the end of inflation ($N \to 0$), again showing that PBH formation is not possible in this model.

3.2.2 Generalized exponential inflation

We now turn to the generalized exponential potential [81]

$$V(\phi) = \Lambda^4 e^{(\phi/\mu)^p} , \tag{3.40}$$

where p is a positive dimensionless constant and μ is a constant with dimension of mass. In this model the hierarchies (1.85) among the slow–roll parameters again do not hold and the values of the spectral parameters depend on the field value ϕ

$$\begin{aligned}
n_S - 1 &= p\left(\frac{M_{\rm P}}{\mu}\right)^2 \left[2(p-1)\left(\frac{\phi}{\mu}\right)^{p-2} - p\left(\frac{\phi}{\mu}\right)^{2p-2}\right] , \\
\alpha_S &= 2p^2(p-1)\left(\frac{M_{\rm P}}{\mu}\right)^4 \left[p\left(\frac{\phi}{\mu}\right)^{3p-4} - (p-2)\left(\frac{\phi}{\mu}\right)^{2p-4}\right] , \\
\beta_S &= 2p^3(p-1)\left(\frac{M_{\rm P}}{\mu}\right)^6 \left[-p(3p-4)\left(\frac{\phi}{\mu}\right)^{4p-6} + 2(p-2)^2\left(\frac{\phi}{\mu}\right)^{3p-6}\right] , \\
r &= 7p^2\left(\frac{M_{\rm P}}{\mu}\right)^2 \left(\frac{\phi}{\mu}\right)^{2p-2} .
\end{aligned} \tag{3.41}$$

We allow p to be a positive real (not necessarily integer) number. If p is not integer, ϕ has to be non-negative to get a real potential. In any case the field ϕ will roll from larger to smaller values during inflation.

For $p > 2$, both terms in the first eq. (3.41), or equivalently both ϵ and η, decrease with decreasing ϕ. The requirements $|\eta| < 1$, $\epsilon < 1$ then yield an upper bound on ϕ,

but inflation will never stop once ϕ is below this upper bound. This would require an additional mechanism to end inflation; we therefore only consider $p < 2$ here.

For $p < 2$, the requirement $|\eta| < 1$ gives a lower bound on ϕ, which is approximately given by

$$\phi_{\min} \simeq \mu \left[\frac{p\,|p-1|\,M_{\mathrm{P}}^2}{\mu^2} \right]^{\frac{1}{2-p}} \qquad (p < 2)\,. \tag{3.42}$$

This bound vanishes for $p = 1$. Eqs. (3.41) show that this choice leads to a constant spectral index n_S and vanishing α_S and β_S. This means that inflation does not end for $p = 1$. Moreover, $\alpha_S = 0$ is (mildly) in conflict with present data, and a constant n_S in the allowed range will not lead to PBH formation.

If $p > 1$, the requirement $\epsilon < 1$ implies an upper bound on ϕ

$$\phi_{\max} \simeq \mu \left(\frac{\mu}{pM_{\mathrm{P}}} \right)^{\frac{1}{p-1}} \qquad (p > 1)\,. \tag{3.43}$$

The number of e–folds that occur after the inflaton field had a value ϕ is given by

$$N(\phi) = \frac{1}{p(2-p)} \left(\frac{\mu}{M_{\mathrm{P}}} \right)^2 \left[\left(\frac{\phi}{\mu} \right)^{2-p} - \left(\frac{\phi_{\min}}{\mu} \right)^{2-p} \right], \tag{3.44}$$

where $\phi_{\min}$ is given by (3.42), and for $p > 1$, ϕ has to satisfy $\phi < \phi_{\max}$, with $\phi_{\max}$ given by eq. (3.43).

For $p < 1$, n_S is always less than 1, in accord with observation. The running of the spectral index, given by α_S, is also negative, but we find $\alpha_S > -(n_S - 1)^2$ for all allowed combinations of parameters that allow at least 30 e–folds of inflation after the pivot scale. This model can therefore not accommodate a sizable and negative value of α_S, either.

For $1 < p < 2$, $n_S - 1$ can have either sign, while α_S is always positive, in contrast to the bound of current data. Quite large and positive α_S are in principle possible, if parameters are chosen such that the two contributions to $n_S - 1$ in eq. (3.41) cancel approximately. However, such large values of α_S are definitely in conflict with observation. Moreover, if $\alpha_S > 0.004$, β_S turns negative, limiting the growth of power at small scales. This is illustrated in figure 3.8, which shows a scatter plot of allowed values of α_S and β_S assuming that n_S lies in its currently allowed $2\,\sigma$ range and 45 e–folds of inflation occurred after the pivot scale.

Using the exact expression (1.75) we numerically find $n \leq 1.15$ at scales relevant for the formation of 10^{15} g PBHs; we saw in chapter 2 that $n > 1.37$ is required for the formation of such PBHs. This model therefore cannot accommodate PBH formation, either.

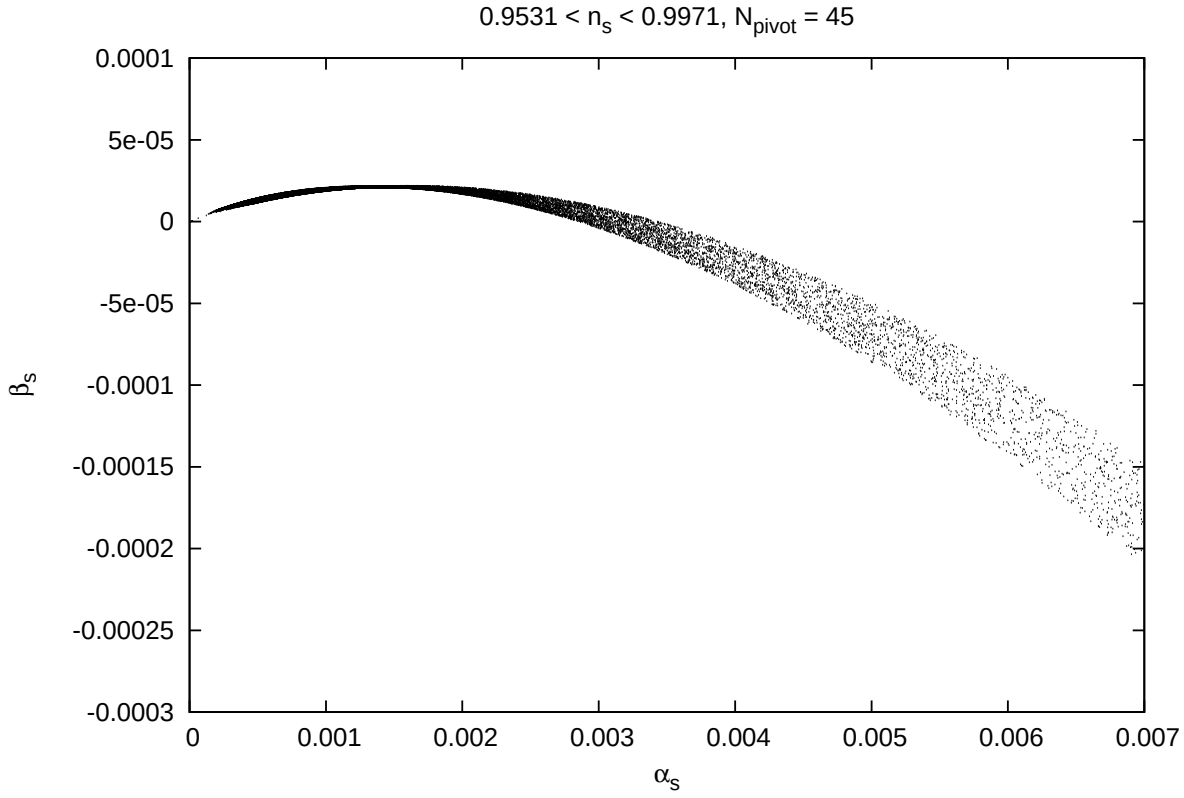

Figure 3.8: Scatter plot of allowed values of α_S and β_S assuming that n_S lies in its currently allowed $2\,\sigma$ range and 45 e–folds of inflation occurred after the pivot scale for potential (3.40).

3.2.3 Inflation with negative exponential and Higgs inflation

Another potential that has been proposed is [92]

$$V(\phi) = V_0 \left(1 - e^{-q\,\phi/M_{\rm P}}\right) . \tag{3.45}$$

For $q > 0$ the inflaton field ϕ rolls towards smaller field values during inflation.[9] The potential is sufficiently flat only for $q\phi > M_{\rm P}$, where the hierarchies (1.85) between

[9] If negative values of ϕ are allowed, the potential (3.45) becomes unbounded for $\phi \to -\infty$. In this case additional terms have to be added to the potential, which we again assume to be unimportant during the slow–roll phase.

slow–roll parameters hold. The inflationary parameters are

$$\begin{aligned} n_S - 1 &\simeq -2q^2 e^{-q\,\phi/M_{\rm P}}\,, \\ \alpha_S &\simeq -2q^4 e^{-2q\,\phi/M_{\rm P}} = -\frac{1}{2}(n_S-1)^2\,, \\ \beta_S &\simeq -4q^6 e^{-3q\,\phi/M_{\rm P}} = \frac{1}{2}(n_S-1)^3\,, \\ r &\simeq 7q^2 e^{-2q\,\phi/M_{\rm P}}\,, \end{aligned} \tag{3.46}$$

where we have approximated the denominators of eqs. (1.48) and (1.52) by V_0; this is appropriate for the phase of slow–roll where $n_S \simeq 1$, unless $q^2 \ll 1$. Inflation ends at $\phi_{\rm end} = 2M_{\rm P}\dfrac{\ln q}{q}$. N e–folds before the end of inflation the spectral parameters are given by

$$\begin{aligned} n_S - 1 &\simeq -\frac{2}{N+1}\,, \\ \alpha_S &\simeq -\frac{2}{(N+1)^2}\,, \\ \beta_S &\simeq -\frac{4}{(N+1)^3}\,, \\ r &\simeq \frac{7}{q^2}\frac{1}{(N+1)^2}\,. \end{aligned} \tag{3.47}$$

Note that the q–dependence cancels when the spectral parameters are expressed in terms of N.

In this model $n_S - 1$ and α_S are manifestly negative, in agreement with current data. However, while $n_S - 1$ also has approximately the right magnitude, $|\alpha_S|$ at the pivot scale is much smaller than the experimental central value. Moreover, since α_S and β_S are both negative, PBH formation is not possible in this model; this can also be seen from the exact expression (1.75), which shows that the power always decreases with decreasing N.

Higgs inflation

A very similar potential describes the Higgs inflation model [103] where the Higgs boson of the SM plays the role of the inflaton. Starting point of this model is the non–minimal coupling of the Higgs field to gravity. The relevant part of the action in the Jordan frame is

$$S_{\rm J} = \int d^4x\,\sqrt{-g}\left\{-\frac{M^2+\xi h^2}{2}R + \frac{\partial_\mu h\,\partial^\mu h}{2} - \frac{\lambda}{4}(h^2-v^2)^2\right\}\,, \tag{3.48}$$

where M is some mass parameter[10], R is the scalar curvature, h is the Higgs field in the unitary gauge and ξ determines the coupling of the Higgs to gravity.[11] By making a conformal transformation from the Jordan frame to the Einstein frame one can get rid of the non–minimal coupling

$$\hat{g}_{\mu\nu} = \Omega^2 g_{\mu\nu}\,, \qquad \Omega^2 = 1 + \frac{\xi h^2}{M_{\rm P}^2}\,. \tag{3.49}$$

This transformation induces a non–canonical kinetic energy term for h. It is therefore convenient to redefine h in terms of the scalar field ϕ which casts the kinetic term into the canonical form [103]

$$\frac{d\phi}{dh} = \sqrt{\frac{\Omega^2 + 6\,\xi^2\,h^2/M_{\rm P}^2}{\Omega^4}}\,. \tag{3.50}$$

In terms of this new field, the potential is

$$V(\phi) = \frac{1}{\Omega(\phi)^4}\frac{\lambda}{4}\left[h(\phi)^2 - v^2\right]^2\,. \tag{3.51}$$

For small field value, $h^2 \ll M_{\rm P}^2/\xi$, one has $h \simeq \phi$ and $\Omega^2 \simeq 1$; the two frames are indistinguishable so the potential for the field ϕ is the same as that for the initial Higgs field. However, for large values, $h \gg M_{\rm P}/\sqrt{\xi}$, one has $\Omega^2 \simeq \xi h^2/M_{\rm P}^2$, and [103]

$$h \simeq \frac{M_{\rm P}}{\sqrt{\xi}}\exp\left(\frac{\phi}{\sqrt{6}\,M_{\rm P}}\right)\,. \tag{3.52}$$

Substituting this into eq. (3.51) we obtain the expression for the potential

$$V(\phi) = \frac{\lambda M_{\rm P}^4}{4\xi^2}\left[1 - \exp\left(-\frac{2\phi}{\sqrt{6}\,M_{\rm P}}\right)\right]^2\,. \tag{3.53}$$

The full effective potential in the Einstein frame is presented in figure 3.9. It is the flatness of the potential at $\phi \gg M_{\rm P}$ which makes the successful inflation possible.

Recall that this expression holds only for $h \gg M_{\rm P}/\sqrt{\xi}$, which implies that the exponential term in eq. (3.53) is small. The square of this term is then even smaller, and can be neglected during inflation. The potential therefore effectively almost reduces to the form (3.45), with $q = 2/\sqrt{6}$, except that the exponential term is multiplied with 2 (due to the square in eq. (3.53)). This also increases $n_S - 1$ by a factor of 2

$$n_S - 1 \simeq -\frac{8}{3}\frac{M_{\rm P}^2}{\xi h^2}\,. \tag{3.54}$$

[10] In the range of ξ of interest to us, $M \simeq M_{\rm P}$ [103].

[11] Higgs inflation requires $\xi \gg 1$. This leads to a breakdown of tree–level unitarity at scales well below the Planck scale [104], but according to ref. [105] this does not invalidate the scenario, since the relevant energy scale during inflation always remains in the unitary regime.

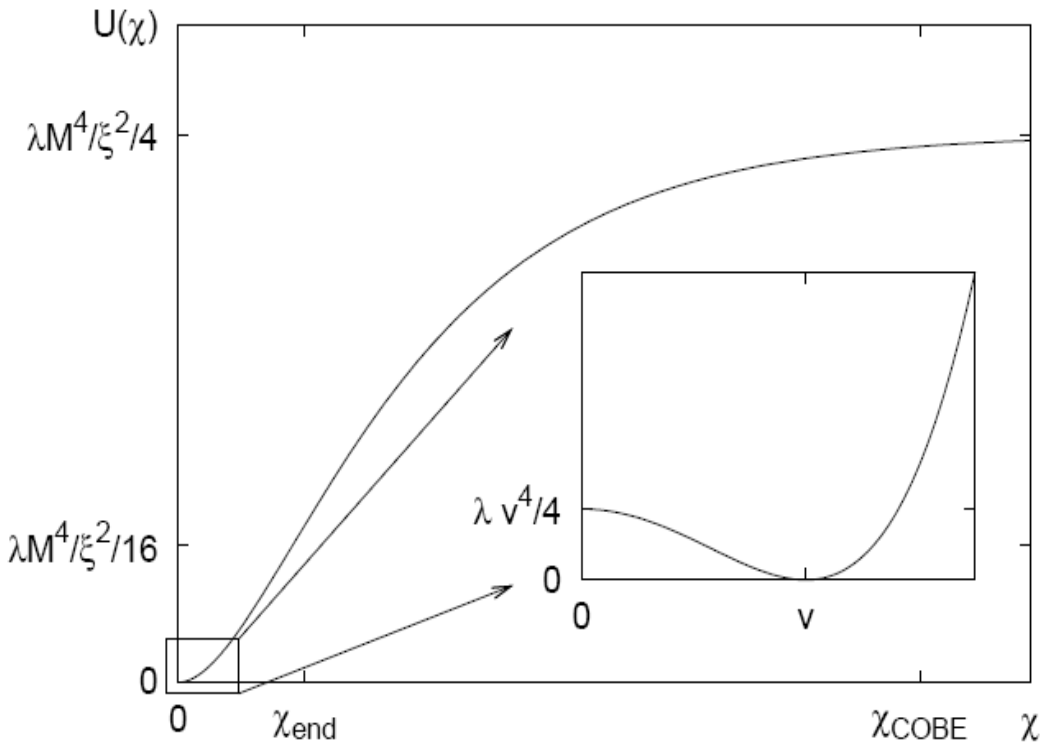

Figure 3.9: Effective potential in the Einstein frame where χ is the inflaton field, ϕ [103].

However, this factor of 2 cancels if $n_S - 1$ is expressed in terms of the number of e–folds of inflation that occur after the field had the value ϕ, *i.e.* the first eq. (3.47) remains valid in Higgs inflation. Moreover, α_S and β_S are as in eqs. (3.46) when expressed in terms of $n_S - 1$ or N. For most practical purposes (of inflation), Higgs inflation can therefore be understood as a particle physics implementation of negative exponential inflation.

3.2.4 Natural inflation

One way to obtain a very flat potential is to consider the natural inflation [106] where a Pseudo Nambu–Goldstone Boson (PNGB) is used as inflaton.[12] In this model, the

[12]Natural inflation can be either a large– or small–field inflation model, depending on the value of f. Here we assume $f > M_{\rm P}$.

inflaton field has a particular form of the potential which results from explicit breaking of a shift symmetry

$$V(\phi) = \Lambda^4 \left[1 \pm \cos\left(a\,\frac{\phi}{f}\right)\right] . \tag{3.55}$$

We will take the positive sign in eq. (3.55) and assume that initially $\phi \ll f/a$. For appropriately chosen values of the mass scales, *e.g.* $f/a \sim M_{\rm P}$ and $\Lambda \sim M_{\rm GUT} \sim 10^{16}$ GeV, the PNGB field ϕ can drive inflation. We set $a = 1$ for simplicity and treat f as a free parameter. The Slow–roll parameters are then given by

$$\begin{aligned}
\epsilon &= \frac{1}{2}\left(\frac{M_{\rm P}}{f}\right)^2 \left[\frac{\sin(\phi/f)}{1+\cos(\phi/f)}\right]^2 \simeq \frac{1}{8}\left(\frac{M_{\rm P}}{f}\right)^2 \left(\frac{\phi}{f}\right)^2 , \\
\eta &= -\left(\frac{M_{\rm P}}{f}\right)^2 \left[\frac{\cos(\phi/f)}{1+\cos(\phi/f)}\right] \simeq -\frac{1}{2}\left(\frac{M_{\rm P}}{f}\right)^2 , \\
\xi^2 &= -\left(\frac{M_{\rm P}}{f}\right)^4 \left[\frac{\sin(\phi/f)}{1+\cos(\phi/f)}\right]^2 \simeq -\frac{1}{4}\left(\frac{M_{\rm P}}{f}\right)^4 \left(\frac{\phi}{f}\right)^2 , \\
\sigma^3 &= \left(\frac{M_{\rm P}}{f}\right)^6 \frac{\cos(\phi/f)\,\sin^2(\phi/f)}{[1+\cos(\phi/f)]^3} \simeq \frac{1}{8}\left(\frac{M_{\rm P}}{f}\right)^6 \left(\frac{\phi}{f}\right)^2 ,
\end{aligned} \tag{3.56}$$

where the approximate equalities hold for $\phi \ll f$. It is clear that the hierarchies (1.85) do not hold among the slow–roll parameters[13], and we find the following inflation parameters

$$\begin{aligned}
n_S - 1 &= -\left(\frac{M_{\rm P}}{f}\right)^2 \frac{3-\cos(\phi/f)}{1+\cos(\phi/f)} , \\
\alpha_S &= -4\left(\frac{M_{\rm P}}{f}\right)^4 \frac{1-\cos(\phi/f)}{[1+\cos(\phi/f)]^2} , \\
\beta_S &= -4\left(\frac{M_{\rm P}}{f}\right)^6 \frac{[1-\cos(\phi/f)]\,[3-\cos(\phi/f)]}{[1+\cos(\phi/f)]^3} , \\
r &= 7\left(\frac{M_{\rm P}}{f}\right)^2 \frac{1-\cos(\phi/f)}{1+\cos(\phi/f)} .
\end{aligned} \tag{3.57}$$

Inflation ends at $|\eta| = 1$ and the relation between the inflaton field and the number of e–folds is given by

$$\cos\left(\frac{\phi}{f}\right) = 1 - y , \tag{3.58}$$

[13]The first strong inequality in (1.85) does hold for $\phi \ll f$, but the second one does not even hold in this limit.

where $y \equiv \dfrac{x^2+2}{x^2+1}\, e^{-Nx^2}$, $x \equiv \dfrac{M_{\rm P}}{f}$. Inserting eq. (3.58) into (3.57) yields

$$\begin{aligned} n_S - 1 &= -x^2\, \frac{2+y}{2-y}\,, \\ \alpha_S &= -4x^4\, \frac{y}{(2-y)^2}\,, \\ \beta_S &= -4x^6\, \frac{y(2+y)}{(2-y)^3}\,, \\ r &= 7x^2\, \frac{y}{2-y}\,. \end{aligned} \tag{3.59}$$

In the course of inflation y increases from a rather small value to $y_{\rm end} = \dfrac{2+x^2}{1+x^2}$ at the end of inflation ($N = 0$). Eqs. (3.59) show that $n_S - 1$, α_S and β_S become more negative as y increases, indicating that the power is reduced at smaller scales. This can also be seen from the exact expression (1.75) which gives

$$\mathcal{P}_{\mathcal{R}_c} = \frac{\Lambda^4 f^2}{12\pi^2\, M_{\rm P}^6} \frac{(2-y)^2}{y}\,, \tag{3.60}$$

which decreases with increasing $y \in [0, 2]$. PBH formation is therefore not possible in this model.

For fixed N, the spectral parameters are determined by x. $|n_S - 1|$ can clearly be made as large as desired (with $n_S < 1$) by choosing a large value of x, *i.e.* a small value of f. On the other hand, $|\alpha_S|$ reaches a maximum at $x^2 \simeq 2/N$ for $y \ll 1$; note that y decreases with increasing x^2. This gives $\alpha_S \gtrsim -1.5/N^2$, *i.e.* $|\alpha_S|$ at the pivot scale cannot be larger than 10^{-3} in this model, well below the current central value.

3.2.5 Arctan inflation

Another inflation model which we are interested to study has been introduced in [107]

$$V(\phi) = V_0 \left[1 + \frac{2}{\pi}\, \arctan\left(\frac{\phi}{\mu}\right)\right]\,. \tag{3.61}$$

This model allows inflation with $n_S \simeq 1$ if $\mu \gg M_{\rm P}$ or $\phi \gg \mu$. However, inflation can be ended by the potential (3.61) only if $\mu \lesssim 0.8\, M_{\rm P}$, since otherwise $\epsilon, |\eta| < 1 \quad \forall\, \phi$. A finite period of inflation thus requires that $\phi \gg \mu$ initially; at the end of inflation, $\phi \to -\infty$, *i.e.* $V \to 0$. During the slow–roll phase the hierarchies (1.85) between the

slow–roll parameters hold, and we find

$$\begin{aligned} n_S - 1 &\simeq -\frac{4}{\pi}\left(\frac{M_{\rm P}}{\phi}\right)^2 \frac{\mu}{\phi}\,, \\ \alpha_S &\simeq -\frac{12}{\pi^2}\left(\frac{M_{\rm P}}{\phi}\right)^4 \left(\frac{\mu}{\phi}\right)^2 = -\frac{3}{4}(n_S-1)^2\,, \\ \beta_S &\simeq -\frac{72}{\pi^3}\left(\frac{M_{\rm P}}{\phi}\right)^6 \left(\frac{\mu}{\phi}\right)^3 = \frac{9}{8}(n_S-1)^3\,, \\ r &\simeq \frac{7}{\pi^2}\left(\frac{M_{\rm P}}{\phi}\right)^2 \left(\frac{\mu}{\phi}\right)^2\,, \end{aligned} \tag{3.62}$$

where we have approximated the denominators of eqs. (1.48) and (1.52) by $2V_0$, as appropriate for the slow–roll phase where $\phi \gg \mu$. In terms of the number N of e–folds of inflation that occurred after the inflaton field reached the value ϕ, we find

$$n_S - 1 \simeq -\frac{4}{3N+\pi}\,, \tag{3.63}$$

where we have used the fact that inflation ends at $\phi_{\rm end} \simeq (M_{\rm P}^2\,\mu)^{1/3}$. This agrees with the currently allowed range for $38 \leq N \leq 95$. However, while α_S is negative, its absolute value is only of order 10^{-3} for allowed values of n_S; moreover, since β_S is also negative, PBH formation is not possible. Indeed, one can see from the exact expression (1.75) that the power decreases steadily during inflation

$$\mathcal{P}_{\mathcal{R}_c} = \frac{V_0}{12\pi^2\,M_{\rm P}^6}\left[1 + \frac{2}{\phi}\,\arctan\left(\frac{\phi}{\mu}\right)\right]^3 \left(1 + \frac{\phi^2}{\mu^2}\right)\,. \tag{3.64}$$

This decreases with decreasing ϕ for $\phi_{\rm end} \leq \phi < \infty$.

4 Conclusion

In this thesis we have investigated the formation of Primordial Black Holes (PBHs) in the radiation dominated era just after inflation. We have focused on density perturbations originating from the slow–roll phase of inflation.

In chapter 2 we reviewed the Press–Schechter type formalism for PBH formation. We have assumed that the mass of the collapsed region to form long–lived PBH is only 20% of the entire energy density inside the particle horizon. We found that for the formation of PBHs with mass larger than 10^{15} g, which could form (part of) the cold dark matter in the Universe, the spectral index at scale $k_{\rm PBH}$ should be at least 1.37, even for the lower value of 1/3 for the threshold $\delta_{\rm th}$. We also showed that PBHs abundance is sensitive to the value of $\delta_{\rm th}$.

This spectral index is much above the value measured at much larger length scales in the CMB. PBH formation therefore requires significant positive running of the spectral index when k is increased. We compared this with the values of the spectral index and its running derived from current data on large scale structure. These include analyses of CMB anisotropies from the WMAP (7 year) and SPT collaborations, as well as data on BAO and on the abundance of *clusters*, and direct measurements of the Hubble constant H_0. At the pivot scale of this data set one finds $n_S(k_{\rm pivot}) = 0.9751$ as central value. The first derivative $\alpha_S(k_0)$ would then need to exceed 0.020 if it alone were responsible for the required increase of the spectral index; this is more than $3\,\sigma$ above the current central value of this quantity ($\alpha_S(k_{\rm pivot}) = -0.017$). However, the second derivative (the "running of the running") of the spectral index β_S is currently only very weakly constrained. We showed in a model–independent analysis that this easily allows values of $n(k_{\rm PBH})$ large enough for PBH formation, even if the first derivative of the spectral index is negative at CMB scales. By mentioned data we also found that values of β_S up to 0.017 are allowed.

In chapter 3 we applied this formalism to a wide class of inflationary models, under the constraints imposed by the data mentioned above. We classified the inflation models in small–field and large–field models. We have shown that only one small–field model,

the running–mass model, allows sizable positive running of running of the spectral index, and is thus a good candidate for long–lived PBHs formation, albeit only in a narrow range of parameter space. In contrast, all the large–field models we studied predict small or negative values for the second derivative of the spectral index, and thus predict negligible PBH formation due to the collapse of overdense regions seeded during inflation.

As a by–product of our analysis, we found that most of the models we studied either predict $n_S < 1$, as indicated by present data, or can at least accommodate it, the single exception being inverse power law inflation (a large–field model). In contrast, *none* of the models we analyzed allows to reproduce a large negative value of α_S, as preferred by current data. If future data *e.g.* Planck [108] confirm with high precision that $\alpha_S \lesssim -0.01$, all simple single–field models of inflation would be excluded. Similarly, proving conclusively that the second derivative of the spectral index is positive would exclude all the large–field models we investigated. Future analyses of the spectrum of primordial density perturbations thus hold great promise to discriminate between inflationary scenarios, or even to challenge the paradigm of single–field inflation.

A Relation between M and R

We assume that the standard ΛCDM model applies, with the age of the Universe being $t_0 = 13.7$ Gy, the Hubble parameter being $h = 0.738 \pm 0.024$ [5]. The Friedmann equation in the radiation era is

$$H^2 = \frac{8\pi\, G}{3}\rho = \frac{4\pi^3\, G}{45} g_* T^4\,, \tag{A.1}$$

where g_* counts the number of the relativistic degrees of freedom and we used the radiation density, $\rho = \dfrac{\pi^2}{30} g_* T^4$. This can be integrated to give

$$t \simeq 0.738 \left(\frac{g_*}{10.75}\right)^{-1/2} \left(\frac{T}{1\,\mathrm{MeV}}\right)^{-2} \mathrm{s}\,, \tag{A.2}$$

where $g_* (\simeq 10.75)$ and $T (\simeq 1$ MeV) are normalized to their values at the start of the BBN epoch. Since we are only considering PBHs which form during the radiation era, the initial PBH mass M is related to the particle horizon mass $M_{\rm PH}$ (which is the particle horizon in the inflationary case) by

$$M_{\rm PBH} = \gamma\, M_{\rm PH} = \frac{4\pi}{3}\gamma\, \rho\, H^{-3} \simeq 2.03 \times 10^5\, \gamma \left(\frac{t}{1\,\mathrm{s}}\right) M_\odot\,. \tag{A.3}$$

Here γ is a numerical factor which depends on the details of gravitational collapse. A simple analytical calculation suggests that it is around $\gamma \simeq w^{3/2} = (1/\sqrt{3})^3 \simeq 0.2$ during the radiation era[1] [31].

During radiation domination $aH \propto a^{-1}$, and expansion at constant entropy gives $\rho \propto g_*^{-1/3} a^{-4}$ [23] (where we have approximated the temperature and entropy degrees of freedom as equal). This implies that

$$M_{\rm PBH} = \gamma M_{\rm eq} (k_{\rm eq} R)^2 \left(\frac{g_{*,\,\rm eq}}{g_*}\right)^{1/3}\,, \tag{A.4}$$

[1] Throughout we assume for simplicity that the PBH mass is a fixed fraction γ of the horizon mass corresponding to the smoothing scale. This is not strictly true. In general the mass of PBHs is expected to depend on the amplitude, size and shape of the perturbations [86, 109].

where the subscript "eq" refers to quantities evaluated at matter–radiation equality. In the early Universe, the effective relativistic degree of freedom g_* is expected to be of order 100, while $g_{*,\,\mathrm{eq}} = 3.36$ and $k_{\mathrm{eq}} = 0.07\,\Omega_{\mathrm{m}} h^2\,\mathrm{Mpc}^{-1}$ ($\Omega_{\mathrm{m}} h^2 = 0.1334$ [4]). The horizon mass at matter–radiation equality is given by

$$M_{\mathrm{eq}} = \frac{4\pi}{3}\rho_{\mathrm{rad},\,\mathrm{eq}}\, H_{\mathrm{eq}}^{-3} = \frac{4\pi}{3}\frac{\rho_{\mathrm{rad},\,0}}{k_{\mathrm{eq}}^3\, a_{\mathrm{eq}}}\,, \tag{A.5}$$

where $a_{\mathrm{eq}}^{-1} = (1 + z_{\mathrm{eq}}) = 3146$ and (assuming three species of massless neutrinos) $\Omega_{\mathrm{rad},\,0} h^2 = 4.17 \times 10^{-5}$. Then it is straightforward to show that

$$\frac{R}{1\,\mathrm{Mpc}} = 5.54 \times 10^{-24}\,\gamma^{-\frac{1}{2}} \left(\frac{M_{\mathrm{PBH}}}{1\,\mathrm{g}}\right)^{1/2} \left(\frac{g_*}{3.36}\right)^{1/6}. \tag{A.6}$$

Assuming adiabatic expansion after PBH formation, the ratio of the PBH number density to the entropy density, n_{PBH}/s, is conserved. Using the relation $\rho = 3\,s\,T/4$, the fraction of the Universe's mass in PBHs at their formation time is then related to their number density $n_{\mathrm{PBH}}(t)$ during the radiation era by

$$\begin{aligned} \beta(M) &\equiv \frac{\rho_{\mathrm{PBH}}(t_{\mathrm{i}})}{\rho(t_{\mathrm{i}})} = \frac{M\, n_{\mathrm{PBH}}(t_{\mathrm{i}})}{\rho(t_{\mathrm{i}})} = \frac{4}{3}\frac{M}{T_{\mathrm{i}}}\frac{n_{\mathrm{PBH}}(t)}{s(t)} \\ &\simeq 7.99 \times 10^{-29}\,\gamma^{-1/2} \left(\frac{g_{*\mathrm{i}}}{106.75}\right)^{1/4} \left(\frac{M}{M_\odot}\right)^{3/2} \left(\frac{n_{\mathrm{PBH}}(t_0)}{1\,\mathrm{Gpc}^{-3}}\right), \end{aligned} \tag{A.7}$$

where the subscript "i" indicates values at the epoch of PBH formation and we have assumed $s = 8.54 \times 10^{85}\,\mathrm{Gpc}^{-3}$ today. $g_{*\mathrm{i}}$ is now normaliazed to the value g_* at around 10^{-5} s since it does not increase much before that in the SM and most PBHs are likely to form before then. The current density parameter for PBHs which have not yet evaporated is given by

$$\Omega_{\mathrm{PBH}} = \frac{M\, n_{\mathrm{PBH}}(t_0)}{\rho_c} \simeq \left(\frac{\beta(M)}{1.15 \times 10^{-8}}\right) \gamma^{1/2} \left(\frac{g_{*\mathrm{i}}}{106.75}\right)^{-1/4} \left(\frac{M}{M_\odot}\right)^{-1/2}, \tag{A.8}$$

which is more precise from eq. (1.10). There is also an implicit dependence on the Hubble parameter here (since factor of Ω always appear with h^2). An immediate constraint on $\beta(M)$ comes from the limit on the CDM density parameter, $\Omega_{\mathrm{CDM}}\, h^2 = 0.111 \pm 0.002$ [1], requires $\Omega_{\mathrm{PBH}} < 0.20$. This implies

$$\beta(M) < 2.03 \times 10^{-18}\,\gamma^{-1/2} \left(\frac{g_{*\mathrm{i}}}{106.75}\right)^{1/4} \left(\frac{M}{10^{15}\,\mathrm{g}}\right)^{1/2} \quad (M \gtrsim 10^{15}\,\mathrm{g})\,. \tag{A.9}$$

This constraint applies only for PBHs which have not evaporated yet. Note that the dependences on γ and g_* in eq. (A.7) and subsequent equations arise through relationship between M and T_{i}. Since β always appears in combination with $\gamma^{1/2}\, g_*^{-1/4}$, it is

convenient to define a new parameter

$$\beta'(M) \equiv \gamma^{1/2} \left(\frac{g_{*\mathrm{i}}}{106.75}\right)^{-1/4} \beta(M)\,. \tag{A.10}$$

This parameter is the one that appears in Table 1.2 and figure 1.1 in this thesis.

B Power spectrum

The power spectrum is a useful quantity to characterize the properties of the perturbations. For a generic quantity $g(\mathbf{x}, t)$, which can expanded in Fourier space as [92]

$$g(\mathbf{x}, t) = \int \frac{d^3\mathbf{k}}{(2\pi)^{3/2}} e^{i\mathbf{k}.\mathbf{x}} g_{\mathbf{k}}(t)\,, \tag{B.1}$$

the power spectrum is the Fourier transform of the two-point correlation function which can be defined as

$$\left\langle g^*_{\mathbf{k_1}} g_{\mathbf{k_2}} \right\rangle \equiv \delta^3(\mathbf{k}_1 - \mathbf{k}_2) \frac{2\pi^2}{k^3} \mathcal{P}_g(k)\,. \tag{B.2}$$

This definition leads to the usual relation

$$\left\langle g^2(\mathbf{x},\, t) \right\rangle = \int \frac{dk}{k} \mathcal{P}_g(k)\,. \tag{B.3}$$

Armed with these definitions, we can compute the variance of the perturbations of the generic field χ

$$\begin{aligned} \left\langle (\delta\chi(\mathbf{x},\, t))^2 \right\rangle &= \int \frac{d^3\mathbf{k}}{(2\pi)^{3/2}} \left|\delta\chi_{\mathbf{k}}\right|^2 \\ &= \int \frac{dk}{k} \frac{k^3}{2\pi^2} \left|\delta\chi_{\mathbf{k}}\right|^2 \\ &= \int \frac{dk}{k} \mathcal{P}_{\delta\chi}(k)\,, \end{aligned} \tag{B.4}$$

which defines the power spectrum of the fluctuations of the scalar field χ

$$\mathcal{P}_{\delta\chi}(k) = \frac{k^3}{2\pi^2} \left|\delta\chi_{\mathbf{k}}\right|^2\,. \tag{B.5}$$

For a massless scalar field, by using eq. (1.64) we obtain

$$\mathcal{P}_{\delta\chi}(k) = \left(\frac{H}{2\pi}\right)^2\,. \tag{B.6}$$

So the power spectrum of fluctuations of the scalar field χ on superhorizon scales is independent of the wavelength, *i.e.* is scale invariant. Since the inflaton is massive scalar field, this is not exactly true for the case of the inflaton, so we also define the *spectral index* $n_{\delta\chi}$ of the fluctuations as

$$n_{\delta\chi} - 1 = \frac{d \ln \mathcal{P}_{\delta\chi}}{d \ln k} \,. \tag{B.7}$$

Bibliography

[1] R. Keisler, C. L. Reichardt, K. A. Aird, B. A. Benson, L. E. Bleem, J. E. Carlstrom, C. L. Chang and H. M. Cho *et al.*, Astrophys. J. **743**, 28 (2011) [arXiv:1105.3182 [astro-ph.CO]].

[2] http://pole.uchicago.edu/

[3] W. J. Percival *et al.* [SDSS Collaboration], Mon. Not. Roy. Astron. Soc. **401**, 2148 (2010) [arXiv:0907.1660 [astro-ph.CO]].

[4] http://map.gsfc.nasa.gov/;

E. Komatsu *et al.* [WMAP Collaboration], Astrophys. J. Suppl. **192**, 18 (2011) [arXiv:1001.4538 [astro-ph.CO]].

[5] A. G. Riess, L. Macri, S. Casertano, H. Lampeitl, H. C. Ferguson, A. V. Filippenko, S. W. Jha and W. Li *et al.*, Astrophys. J. **730**, 119 (2011) [Erratum-ibid. **732**, 129 (2011)] [arXiv:1103.2976 [astro-ph.CO]].

[6] R. D. Peccei and H. R. Quinn, Phys. Rev. Lett. **38**, 1440 (1977).

[7] A. Kusenko, Phys. Rept. **481**, 1 (2009) [arXiv:0906.2968 [hep-ph]].

[8] H. E. Haber and G. L. Kane, Phys. Rept. **117**, 75 (1985);

H. P. Nilles, Phys. Rept. **110**, 1 (1984).

[9] http://lhc.web.cern.ch/lhc/

[10] http://cogent.pnnl.gov/

[11] E. Aprile *et al.* [XENON100 Collaboration], Phys. Rev. Lett. **105**, 131302 (2010) [arXiv:1005.0380 [astro-ph.CO]].

[12] R. Bernabei *et al.* [DAMA and LIBRA Collaborations], Eur. Phys. J. C **67**, 39 (2010) [arXiv:1002.1028 [astro-ph.GA]].

[13] Z. Ahmed *et al.* [CDMS-II Collaboration], Phys. Rev. Lett. **106**, 131302 (2011) [arXiv:1011.2482 [astro-ph.CO]].

[14] T. Tanaka *et al.* [Super-Kamiokande Collaboration], Astrophys. J. **742**, 78 (2011) [arXiv:1108.3384 [astro-ph.HE]].

[15] J. D. Zornoza, arXiv:1204.5066 [astro-ph.HE].

[16] R. Abbasi *et al.* [IceCube Collaboration], Phys. Rev. D **85**, 042002 (2012) [arXiv:1112.1840 [astro-ph.HE]].

[17] http://www.ams02.org/

[18] M. Ackermann *et al.* [LAT Collaboration], arXiv:1205.2739 [astro-ph.HE].

[19] S. W. Hawking, Commun. Math. Phys. **43** (1975) 199 [Erratum-ibid. **46** (1976) 206].

[20] S. Hawking, Mon. Not. Roy. Astron. Soc. **152** (1971) 75.

[21] Ya. B. Zel'dovich and I. D. Novikov, Sov. Astron. A. J. **10** (1967) 602.

[22] B. J. Carr and S. W. Hawking, Mon. Not. Roy. Astron. Soc. **168** (1974) 399.

[23] E. W. Kolb and M. S. Turner, *The Early Universe*, Addison-Wesley, Redwood City, 1990.

[24] S. W. Hawking, Nature **248**, 30 (1974).

[25] D. N. Page, Phys. Rev. D **16**, 2402 (1977).

[26] J. H. MacGibbon, Phys. Rev. D **44**, 376 (1991).

[27] B. J. Carr, K. Kohri, Y. Sendouda and J. 'i. Yokoyama, Phys. Rev. D **81**, 104019 (2010) [arXiv:0912.5297 [astro-ph.CO]].

[28] D. N. Page and S. W. Hawking, Astrophys. J. **206**, 1 (1976).

[29] N. A. Porter and T. C. Weekes, Nature **277** (1979) 199.

[30] B. J. Carr, Astrophys. J. **206**, 8 (1976).

[31] B. J. Carr, Astrophys. J. **201**, 1 (1975).

[32] M. Y. Khlopov and A. G. Polnarev, Phys. Lett. B **97**, 383 (1980).

[33] P. Widerin and C. Schmid, astro-ph/9808142.

[34] K. Jedamzik, Phys. Rev. D **55**, 5871 (1997) [astro-ph/9605152].

[35] M. Khlopov, B. A. Malomed and I. B. Zeldovich, Mon. Not. Roy. Astron. Soc. **215**, 575 (1985).

[36] B. J. Carr, J. H. Gilbert and J. E. Lidsey, Phys. Rev. D **50**, 4853 (1994) [astro-ph/9405027].

[37] M. Crawford and D. N. Schramm, Nature **298**, 538 (1982);

S. W. Hawking, I. G. Moss and J. M. Stewart, Phys. Rev. D **26**, 2681 (1982);

M. Sasaki, H. Kodama and K. Sato, Prog. Theor. Phys. **68**, 1561 (1982);

D. La and P. J. Steinhardt, Phys. Lett. B **220**, 375 (1989);

M. Y. Khlopov, R. V. Konoplich, S. G. Rubin and A. S. Sakharov, hep-ph/9807343;

R. V. Konoplich, S. G. Rubin, A. S. Sakharov and M. Y. Khlopov, Phys. Atom. Nucl. **62**, 1593 (1999) [Yad. Fiz. **62**, 1705 (1999)].

[38] A. Polnarev and R. Zembowicz, Phys. Rev. D **43**, 1106 (1991);

S. W. Hawking, Phys. Lett. B **231**, 237 (1989);

J. Garriga and M. Sakellariadou, Phys. Rev. D **48**, 2502 (1993) [hep-th/9303024];

R. R. Caldwell and P. Casper, Phys. Rev. D **53**, 3002 (1996) [gr-qc/9509012];

J. H. MacGibbon, R. H. Brandenberger and U. F. Wichoski, Phys. Rev. D **57**, 2158 (1998) [astro-ph/9707146];

M. Nagasawa, Gen. Rel. Grav. **37**, 1635 (2005).

[39] R. R. Caldwell, A. Chamblin and G. W. Gibbons, Phys. Rev. D **53**, 7103 (1996) [hep-th/9602126];

S. G. Rubin, A. S. Sakharov and M. Y. Khlopov, J. Exp. Theor. Phys. **91**, 921 (2001) [hep-ph/0106187];

V. Dokuchaev, Y. Eroshenko and S. Rubin, Grav. Cosmol. **11**, 99 (2005) [astro-ph/0412418].

[40] B. J. Carr and J. E. Lidsey, Phys. Rev. D **48**, 543 (1993).

[41] B. A. Bassett and S. Tsujikawa, Phys. Rev. D **63**, 123503 (2001) [hep-ph/0008328];

R. Easther and M. Parry, Phys. Rev. D **62**, 103503 (2000) [hep-ph/9910441];

A. M. Green and K. A. Malik, Phys. Rev. D **64**, 021301 (2001) [hep-ph/0008113].

[42] J. Yokoyama, Astron. Astrophys. **318**, 673 (1997) [astro-ph/9509027];

J. Garcia-Bellido, A. D. Linde and D. Wands, Phys. Rev. D **54**, 6040 (1996) [astro-ph/9605094];

J. E. Lidsey, T. Matos and L. A. Urena-Lopez, Phys. Rev. D **66**, 023514 (2002) [astro-ph/0111292];

S. Chongchitnan and G. Efstathiou, JCAP **0701**, 011 (2007) [astro-ph/0611818];

K. Kohri, C. -M. Lin and D. H. Lyth, JCAP **0712**, 004 (2007) [arXiv:0707.3826 [hep-ph]].

[43] P. Ivanov, P. Naselsky and I. Novikov, Phys. Rev. D **50**, 7173 (1994);

A. M. Green and A. R. Liddle, Phys. Rev. D **60**, 063509 (1999) [astro-ph/9901268];

J. 'i. Yokoyama, Phys. Rev. D **58**, 107502 (1998) [gr-qc/9804041].

[44] M. Drees and E. Erfani, JCAP **1201**, 035 (2012) [arXiv:1110.6052 [astro-ph.CO]].

[45] M. Drees and E. Erfani, JCAP **1104**, 005 (2011) [arXiv:1102.2340 [hep-ph]].

[46] S. M. Leach, I. J. Grivell and A. R. Liddle, Phys. Rev. D **62**, 043516 (2000) [astro-ph/0004296];

K. Kohri, D. H. Lyth and A. Melchiorri, JCAP **0804**, 038 (2008) [arXiv:0711.5006 [hep-ph]];

A. S. Josan and A. M. Green, Phys. Rev. D **82**, 047303 (2010) [arXiv:1004.5347 [hep-ph]];

W. H. Kinney, Phys. Rev. D **66**, 083508 (2002) [astro-ph/0206032];

L. Alabidi and K. Kohri, Phys. Rev. D **80**, 063511 (2009) [arXiv:0906.1398 [astro-ph.CO]].

[47] Y. B. Zel'dovich and A. A. Starobinsky. Sov. J. Exp. Theor. Lett. **24** (1976) 571.

[48] M. S. Turner, Phys. Lett. B **89**, 155 (1979);

J. D. Barrow, E. J. Copeland, E. W. Kolb and A. R. Liddle, Phys. Rev. D **43**, 984 (1991);

N. Upadhyay, P. Das Gupta and R. P. Saxena, Phys. Rev. D **60**, 063513 (1999) [astro-ph/9903253];

A. D. Dolgov, P. D. Naselsky and I. D. Novikov, [astro-ph/0009407].

[49] K. Kohri and J. Yokoyama, Phys. Rev. D **61**, 023501 (2000) [astro-ph/9908160];

S. Miyama and K. Sato, Prog. Theor. Phys. **59**, 1012 (1978).

[50] E. Bugaev and P. Klimai, Phys. Rev. D **79**, 103511 (2009) [arXiv:0812.4247 [astro-ph]];

E. V. Bugaev and K. V. Konishchev, Phys. Rev. D **66**, 084004 (2002) [astro-ph/0206082].

[51] M. Y. Khlopov, A. Barrau and J. Grain, Class. Quant. Grav. **23**, 1875 (2006) [astro-ph/0406621].

[52] A. M. Green, Phys. Rev. D **60**, 063516 (1999) [astro-ph/9903484].

[53] P. He and L. -Z. Fang, Astrophys. J. **568**, L1 (2002) [astro-ph/0202218].

[54] K. J. Mack and D. H. Wesley, arXiv:0805.1531 [astro-ph].

[55] C. Alcock *et al.* [MACHO Collaboration], Astrophys. J. **542**, 281 (2000) [astro-ph/0001272].

[56] T. Kanazawa, M. Kawasaki and T. Yanagida, Phys. Lett. B **482**, 174 (2000) [hep-ph/0002236].

[57] D. Blais, T. Bringmann, C. Kiefer and D. Polarski, Phys. Rev. D **67**, 024024 (2003) [astro-ph/0206262].

[58] D. Blais, C. Kiefer and D. Polarski, Phys. Lett. B **535**, 11 (2002) [astro-ph/0203520].

[59] R. Saito, J. 'i. Yokoyama and R. Nagata, JCAP **0806**, 024 (2008) [arXiv:0804.3470 [astro-ph]];

K. J. Mack, J. P. Ostriker and M. Ricotti, Astrophys. J. **665**, 1277 (2007) [astro-ph/0608642].

[60] P. Meszaros, Astron. Astrophys. **38**, 5 (1975);

N. Afshordi, P. McDonald and D. N. Spergel, Astrophys. J. **594**, L71 (2003) [astro-ph/0302035].

[61] N. Duechting, Phys. Rev. D **70**, 064015 (2004) [astro-ph/0406260];

M. Y. Khlopov, S. G. Rubin and A. S. Sakharov, astro-ph/0401532;

R. Bean and J. Magueijo, Phys. Rev. D **66**, 063505 (2002) [astro-ph/0204486].

[62] T. Nakamura, M. Sasaki, T. Tanaka and K. S. Thorne, Astrophys. J. **487**, L139 (1997) [astro-ph/9708060];

K. Ioka, T. Tanaka and T. Nakamura, Phys. Rev. D **60**, 083512 (1999) [astro-ph/9809395];

K. T. Inoue and T. Tanaka, Phys. Rev. Lett. **91**, 021101 (2003) [gr-qc/0303058].

[63] F. Halzen, E. Zas, J. H. MacGibbon and T. C. Weekes, Nature **353**, 807 (1991).

[64] E. L. Wright, astro-ph/9509074;

R. Lehoucq, M. Casse, J. -M. Casandjian and I. Grenier, arXiv:0906.1648 [astro-ph.HE].

[65] M. S. Turner, Nature **297**, 379 (1982);

P. Kiraly, J. Szabelski, J. Wdowczyk and A. W. Wolfendale, Nature **293**, 120 (1981);

A. Barrau, G. Boudoul, F. Donato, D. Maurin, P. Salati and R. Taillet, Astron. Astrophys. **388**, 676 (2002) [astro-ph/0112486].

[66] D. B. Cline and W. -p. Hong, Astrophys. J. **401**, L57 (1992);

A. Barnacka, J. -F. Glicenstein and R. Moderski, arXiv:1204.2056 [astro-ph.CO].

[67] J. H. MacGibbon, Nature **329**, 308 (1987);

J. D. Barrow, E. J. Copeland and A. R. Liddle, Phys. Rev. D **46**, 645 (1992);

S. Alexeyev, A. Barrau, G. Boudoul, O. Khovanskaya and M. Sazhin, Class. Quant. Grav. **19**, 4431 (2002) [gr-qc/0201069];

P. Chen and R. J. Adler, Nucl. Phys. Proc. Suppl. **124**, 103 (2003) [gr-qc/0205106];

P. Chen, New Astron. Rev. **49**, 233 (2005) [astro-ph/0406514];

A. Barrau, D. Blais, G. Boudoul and D. Polarski, Annalen Phys. **13**, 115 (2004) [astro-ph/0303330];

K. Nozari and S. H. Mehdipour, Mod. Phys. Lett. A **20**, 2937 (2005) [arXiv:0809.3144 [gr-qc]];

S. Alexander and P. Meszaros, hep-th/0703070 [hep-th].

[68] S. B. Giddings and M. L. Mangano, Phys. Rev. D **78**, 035009 (2008) [arXiv:0806.3381 [hep-ph]].

[69] L. A. Anchordoqui, J. L. Feng, H. Goldberg and A. D. Shapere, Phys. Rev. D **65**, 124027 (2002) [hep-ph/0112247].

[70] A. M. Green and A. R. Liddle, Phys. Rev. D **56**, 6166 (1997) [astro-ph/9704251].

[71] A. S. Josan, A. M. Green and K. A. Malik, Phys. Rev. D **79**, 103520 (2009) [arXiv:0903.3184 [astro-ph.CO]].

[72] J. S. Bullock and J. R. Primack, Phys. Rev. D **55**, 7423 (1997) [astro-ph/9611106];

P. Ivanov, Phys. Rev. D **57** (1998) 7145 [astro-ph/9708224];

J. C. Hidalgo, arXiv:0708.3875 [astro-ph];

J. C. Hidalgo, arXiv:0910.1876 [astro-ph.CO];

P. Pina Avelino, Phys. Rev. D **72**, 124004 (2005) [astro-ph/0510052].

[73] H. I. Kim, C. H. Lee and J. H. MacGibbon, Phys. Rev. D **59**, 063004 (1999) [astro-ph/9901030];

D. Polarski, Phys. Lett. B **528**, 193 (2002) [astro-ph/0112328];

J. E. Lidsey, B. J. Carr and J. H. Gilbert, Nucl. Phys. Proc. Suppl. **43**, 75 (1995);

H. I. Kim and C. H. Lee, Phys. Rev. D **54**, 6001 (1996).

[74] E. Erfani, *The Standard Model Higgs as the Inflaton?*, High Energy Physics Diploma Dissertation, ICTP, Trieste, 2008;

V. Mukhanov, *Physical foundations of Cosmology*, Cambridge University Press, 2005.

[75] A. H. Guth, Phys. Rev. D **23**, 347 (1981).

[76] A. R. Liddle and D. H. Lyth, Phys. Lett. B **291**, 391 (1992) [astro-ph/9208007].

[77] A. D. Linde, Phys. Rev. D **49**, 748 (1994) [astro-ph/9307002].

[78] A. R. Liddle and S. M. Leach, Phys. Rev. D **68**, 103503 (2003) [astro-ph/0305263].

[79] A. D. Linde, Phys. Lett. B **175**, 395 (1986).

A. D. Linde, D. A. Linde and A. Mezhlumian, Phys. Rev. D **49**, 1783 (1994) [gr-qc/9306035].

[80] A. R. Liddle and D. H. Lyth, *Cosmological Inflation and Large-Scale Structure*, Cambridge University Press, 2000;

D. H. Lyth and A. R. Liddle, *The Primordial Density Perturbation*, Cambridge University Press, 2009.

[81] A. Kosowsky and M. S. Turner, Phys. Rev. D **52**, 1739 (1995) [astro-ph/9504071].

[82] Q. -G. Huang, JCAP **0611**, 004 (2006) [astro-ph/0610389].

[83] M. Cortes, A. R. Liddle and P. Mukherjee, Phys. Rev. D **75**, 083520 (2007) [astro-ph/0702170].

[84] S. Hannestad, S. H. Hansen and F. L. Villante, Astropart. Phys. **16**, 137 (2001) [astro-ph/0012009];

E. J. Copeland, I. J. Grivell and A. R. Liddle, Mon. Not. Roy. Astron. Soc. **298**, 1233 (1998) [astro-ph/9712028].

[85] W. H. Press and P. Schechter, Astrophys. J. **187**, 425 (1974).

[86] K. Jedamzik and J. C. Niemeyer, Phys. Rev. D **59**, 124014 (1999) [astro-ph/9901293];

J. C. Niemeyer and K. Jedamzik, Phys. Rev. Lett. **80**, 5481 (1998) [astro-ph/9709072].

[87] E. J. Copeland, A. R. Liddle, J. E. Lidsey and D. Wands, Phys. Rev. D **58**, 063508 (1998) [gr-qc/9803070].

[88] T. Bringmann, C. Kiefer and D. Polarski, Phys. Rev. D **65**, 024008 (2002) [astro-ph/0109404].

[89] D. H. Lyth, K. A. Malik, M. Sasaki and I. Zaballa, JCAP **0601**, 011 (2006) [astro-ph/0510647];

I. Zaballa, A. M. Green, K. A. Malik and M. Sasaki, JCAP **0703**, 010 (2007) [astro-ph/0612379].

[90] D. H. Lyth, JCAP **1107**, 035 (2011) [arXiv:1012.4617 [astro-ph.CO]].

[91] J. Garcia-Bellido, A. D. Linde and D. Wands, Phys. Rev. D **54**, 6040 (1996) [astro-ph/9605094];

T. Kawaguchi, M. Kawasaki, T. Takayama, M. Yamaguchi and J. 'i. Yokoyama, Mon. Not. Roy. Astron. Soc. **388**, 1426 (2008) [arXiv:0711.3886 [astro-ph]];

M. Kawasaki, T. Takayama, M. Yamaguchi and J. 'i. Yokoyama, Phys. Rev. D **74**, 043525 (2006) [hep-ph/0605271];

M. Kawasaki, M. Yamaguchi and J. 'i. Yokoyama, Phys. Rev. D **68**, 023508 (2003) [hep-ph/0304161];

L. Randall, M. Soljacic and A. H. Guth, Nucl. Phys. B **472**, 377 (1996) [hep-ph/9512439];

M. Kawasaki and T. Yanagida Phys. Rev. D **59**, 043512 (1999) [hep-ph/9807544];

M. Kawasaki, N. Sugiyama and T. Yanagida, Phys. Rev. D **57**, 6050 (1998) [hep-ph/9710259];

M. Yamaguchi and J. 'i. Yokoyama, Phys. Rev. D **70**, 023513 (2004) [hep-ph/0402282];

J. 'i. Yokoyama, Phys. Rept. **307**, 133 (1998);

J. Yokoyama, Prog. Theor. Phys. Suppl. **136**, 338 (1999);

M. Yamaguchi, Phys. Rev. D **64**, 063503 (2001) [hep-ph/0105001].

[92] D. H. Lyth and A. Riotto, Phys. Rept. **314**, 1 (1999) [hep-ph/9807278];

A. Mazumdar and J. Rocher, Phys. Rept. **497**, 85 (2011) [arXiv:1001.0993 [hep-ph]].

[93] P. Adshead, R. Easther, J. Pritchard and A. Loeb, JCAP **1102**, 021 (2011) [arXiv:1007.3748 [astro-ph.CO]].

[94] E. D. Stewart, Phys. Lett. B **391**, 34 (1997) [hep-ph/9606241];

E. D. Stewart, Phys. Rev. D **56**, 2019 (1997) [arXiv:hep-ph/9703232].

[95] L. Covi and D. H. Lyth, Phys. Rev. D **59**, 063515 (1999) [hep-ph/9809562].

[96] L. Covi, Phys. Rev. D **60**, 023513 (1999) [hep-ph/9812232].

[97] L. Covi, D. H. Lyth, A. Melchiorri and C. J. Odman, Phys. Rev. D **70**, 123521 (2004) [astro-ph/0408129].

[98] L. Covi, D. H. Lyth and L. Roszkowski, Phys. Rev. D **60**, 023509 (1999) [hep-ph/9809310];

L. Covi and D. H. Lyth, Phys. Rev. D **59**, 063515 (1999) [hep-ph/9809562];

L. Covi and D. H. Lyth, Mon. Not. Roy. Astron. Soc. **326**, 885 (2001) [astro-ph/0008165];

D. H. Lyth and L. Covi, Phys. Rev. D **62**, 103504 (2000) [astro-ph/0002397];

L. Covi, D. H. Lyth and A. Melchiorri, Phys. Rev. D **67**, 043507 (2003) [hep-ph/0210395].

[99] W. H. Kinney, E. W. Kolb, A. Melchiorri and A. Riotto, Phys. Rev. D **69**, 103516 (2004) [hep-ph/0305130];

R. Easther and H. Peiris, JCAP **0609**, 010 (2006) [astro-ph/0604214];

H. Peiris and R. Easther, JCAP **0610**, 017 (2006) [astro-ph/0609003].

[100] G. F. Giudice and R. Rattazzi, Phys. Rept. **322**, 419 (1999) [hep-ph/9801271].

[101] D. H. Lyth, Phys. Rev. Lett. **78**, 1861 (1997) [hep-ph/9606387].

[102] A. D. Linde, Phys. Lett. B **129**, 177 (1983).

[103] F. L. Bezrukov and M. Shaposhnikov, Phys. Lett. B **659**, 703 (2008) [arXiv:0710.3755 [hep-th]].

[104] C. P. Burgess, H. M. Lee and M. Trott, JHEP **0909**, 103 (2009) [arXiv:0902.4465 [hep-ph]];

C. P. Burgess, H. M. Lee and M. Trott, JHEP **1007**, 007 (2010) [arXiv:1002.2730 [hep-ph]].

[105] F. Bezrukov, A. Magnin, M. Shaposhnikov and S. Sibiryakov, JHEP **1101**, 016 (2011) [arXiv:1008.5157 [hep-ph]].

[106] K. Freese, J. A. Frieman and A. V. Olinto, Phys. Rev. Lett. **65**, 3233 (1990).

[107] S. M. Leach, A. R. Liddle, J. Martin and D. J. Schwarz, Phys. Rev. D **66**, 023515 (2002) [astro-ph/0202094].

[108] http://www.rssd.esa.int/index.php?project=PLANCK

[109] M. Shibata and M. Sasaki, Phys. Rev. D **60**, 084002 (1999) [gr-qc/9905064];

J. C. Hidalgo and A. G. Polnarev, Phys. Rev. D **79**, 044006 (2009) [arXiv:0806.2752 [astro-ph]].